REGULATION OF DEVELOPMENTAL CHANGES IN HEMATOPOETIC STEM CELL SELF-RENEWAL

by

Michael Rebin Copley

B.Sc. (Honours), The University of Victoria, 2006

A THESIS SUBMITTED IN PARTIAL FULFILLMENT OF

THE REQUIREMENTS FOR THE DEGREE OF

DOCTOR OF PHILOSOPHY

in

THE FACULTY OF GRADUATE STUDIES

(Experimental Medicine)

THE UNIVERSITY OF BRITISH COLUMBIA

(Vancouver)

August 2013

Abstract

Mouse hematopoietic stem cells (HSCs) undergo a post-natal transition in several properties, including a marked reduction in their self-renewal activity. To investigate the molecular basis of this difference, we devised a single strategy to isolate fetal and adult HSCs at similarly high frequencies. This strategy, involving fluorescence-activated cell sorting of cells with a $CD45^{+}EPCR^{+}CD48^{-}CD150^{+}$ (ESLAM) phenotype, allows isolation of HSCs at a frequency of ~1 in 2 from all developmental time points tested (mouse embryonic day (E) 14.5 to adult). Comparison of differentially expressed genes in primitive populations of fetal and adult hematopoietic cells showed that heightened expression of *Hmga2* was a feature of fetal as compared to adult HSCs. We also identified let-7 microRNAs (miRNAs) and a negative regulator of their biogenesis, *Lin28b*, to be expressed in an opposite and similar pattern to *Hmga2*, respectively. Since *Hmga2* is a well-established target of let-7 miRNAs, we hypothesized that the Lin28b-let-7-Hmga2 axis plays a central role in the determination of fetal versus adult HSC self-renewal identity. We also found that Lin28 overexpression in adult HSCs restores a higher, fetal-like, self-renewal potential in them, and this effect is phenocopied by direct overexpression of Hmga2. Conversely, HSCs from fetal $Hmga2^{-/-}$ mice display a prematurely acquired adult-like self-renewal activity. Importantly, we show that Lin28-mediated activation of Hmga2 expression, which is responsible for the activation of a fetal-like self-renewal potential in adult HSCs, is *not* the mechanism by which Lin28 reprograms adult HSCs to undergo fetal-like B-cell differentiation. Together, these findings suggest a model of development in which Lin28b acts as a master regulator and Hmga2 serves as a more specific downstream modulator of HSC self-renewal. These findings may help inform strategies to improve the therapeutic use of HSCs. Furthermore, since *Lin28b* and *Hmga2* are oncogenes, we

speculate that the fetal/neonatal specific pattern of expression of these genes may contribute to the pathogenesis of pediatric leukemias.

Preface

A portion of Chapter 1 has been published in a review in Cell Stem Cell entitled "Hematopoietic stem cell heterogeneity takes center stage" (Cell Stem Cell 2012) (1), which was written by myself, Philip Beer (PB) and my supervisor, Connie J. Eaves (CJE).

Chapter 2 represents my contributions to manuscripts co-authored with other members of the Eaves' lab: Claudia Benz (CB), David Kent (DK) and Michelle Bowie (MB). Figure 2.1 is unpublished data. Figures 2.2 and 2.3 have been published in the manuscript "Hematopoietic Stem Cell Subtypes Expand Differentially during Development and Display Distinct Lymphopoietic Programs" by CB et al. in Cell Stem Cell (2). For this study I performed the majority of the single-cell transplants for the 3- and 4-week-old donor mice. I also provided a significant contribution to the interpretation of the data and the preparation and writing of the manuscript as a whole. A version of Figure 2.4 was published in "Steel factor responsiveness regulates the high self-renewal phenotype of fetal hematopoietic stem cells" by MB et al. in Blood (3). For this study, I helped to design the experiment and worked with DK to perform the cell isolation, culturing and transcript measurements. Figure 2.5 represents a subset of the data that were published in DK's Blood manuscript entitled "Prospective isolation and molecular characterization of hematopoietic stem cells with durable self-renewal potential" (4). For this study I worked with DK to isolate RNA from highly purified fetal and adult HSCs and performed transcript measurements on these cells. The data in Figures 2.6 and 2.7 have not been published but are included in our submitted manuscript entitled "The Lin28b-let-7-Hmga2 axis determines the higher self-renewal potential of fetal hematopoietic stem cells". For this study, I designed all experiments with input from CJE, CB and SB. I performed all experiments with assistance from SB for transcript analyses and Hmga2 protein measurements.

The results presented in Chapter 3 have been submitted for publication in a manuscript entitled "The Lin28b-let-7-Hmga2 axis determines the higher self-renewal potential of fetal haematopoietic stem cells". I performed all of the experiments with assistance from SB for qRT-PCR, intracellular flow cytometry, peritoneal cavity cell analyses and Ki-67/Annexin V staining. Florian Kuchenbauer and SB assisted with let-7 measurements. Affymetrix array hybridizations were performed by Sarah Padilla at the Centre for Translational and Applied Genomics (CTAG; Vancouver, BC, Canada) and data analyses were performed by David Knapp. Concentrated lentivirus was prepared by Glenn Edin. David Treloar (DT) collected ESLAM HSCs from E14.5 fetal livers for qRT-PCR analyses. Heidi Mader, Keegan Rowe, Chris Day and DQT performed the analyses of transplanted mice under my direction. I worked with CJE to design and interpret all experiments with input from C.B., D.K., Stefan Woehrer and Richard Keith Humphries. I wrote the manuscript with CJE and received significant input from SB, CB and PB.

Table of Contents

List of Tables

List of Figures

List of Abbreviations

2-ME	2-beta-mercaptoethanol
ALL	Acute lymphoblastic leukemia
AGM	Aorta-gonado-mesonephros
BFU-E	Burst forming unit-erythroid
BIT	BSA, insulin and transferrin
B6	C57Bl/6J-Ly5.2
BM	Bone marrow
BSA	Bovine serum albumin
C.I.	Confidence interval
CAFC	Cobblestone area forming cell
CB	Cord blood
CFC	Colony-forming cell
CFU-E	Colony-forming unit erythroid
CFU-GEMM	Colony-forming unit-granulocyte erythrocyte macrophage megakaryoctye
CFU-GM	Colony-forming unit-granulocyte macrophage
CFU-S	Colony-forming unit spleen
cGy	CentiGray
CRU	Competitive repopulating unit
DAB	Data above background
DAPI	4',6-diamidino-2-phenylindole
E	Embryonic day
EPCR	Endothelial protein C receptor
Epo	Erythropoietin
FACS	Fluorescence-activated cell sorting
FBS	Fetal bovine serum
FDR	False discovery rate
FL	Fetal liver
FoB	Follicular zone B-cell
GEO	Gene Expression Omnibus

GM	Granulocyte/monocyte
GVHD	Graft-versus-host disease
HBSS	Hank's balanced salt solution
HF	HBSS + 2% fetal bovine serum
HLA	Human leukocyte antigen
HSC	Hematopoietic stem cell
Hst	Hoechst 33342
IGF-2	Insulin-like growth factor 2
IL	Interleukin
IMDM	Iscove's modified Dulbecco's medium
KO	Knockout
LDA	Limiting dilution assay
Lin	Lineage
LNA	Locked nucleic acid
LTC-IC	Long-term culture-initiating cell
LV	Lentivirus
miRNA	microRNA
MzB	Marginal zone B-cell
NH_4Cl	Ammonium chloride lysis solution
PB	Peripheral blood
PBS	Phosphate-buffered saline
Pep3b	C57Bl/6J:Pep3b-Ly5.1
PI	Propidium iodide
qRT-PCR	Quantitative reverse-transcription PCR
Rho	Rhodamine-123
S.E.M.	Standard error of the mean
SAGE	Serial analysis of gene expression
SF	Steel factor
SFM	Serum-free medium
SP	Side population
TCR	T-cell receptor

W41	C57Bl/6J W^{41}/W^{41}
WBC	White blood cell
WT	Wild-type
YFP	Enhanced yellow fluorescent protein

Acknowledgements

To Connie, thank you for so many things. For always having an open door, for never letting me do less than my best, for teaching me to question everything and for inspiring me every step of the way. The scientific community that you have created in the lab is something very special and I feel so privileged to have been a part of it.

To past and present members of my supervisory committee, Keith, Aly, Pamela and Clay. Your scientific and strategic advice along the way has been invaluable.

To all the members of the Eaves' lab. You are the best group of friends and colleagues that I have ever had the pleasure to work alongside. In particular, to Michelle Bowie, for your trailblazing work. To David K. and Brad, for showing me the ropes and putting up with me during my formative years. To past, present and future members of the "the team", Claudia, Stefan and Sonja, for the fruitful discussions, camaraderie and collaborative efforts. Maisam and Mel, for always being there to scrutinize my work and keep me out of trouble. Dr. Beer, thanks for the refreshments and refreshing scientific deliberations. To the many students that have slaved away with me, Elaine Ma, Jay Cheyne, Heidi Mader, Keegan Rowe, Chris Day and David Treloar, I could not have done it (quite literally) without you. Finally, to Margaret, Glenn and Darcy, thanks for all of your hard work. Also to Carl Hansen, Jamie Piret, Oleh Petriv and Veronique Lecault for many exciting collaborations and discussions.

To the UBC MD/PhD program, Lynn Raymond, Torsten Nielsen and Jane Lee, thank you for accepting me into, and supporting me throughout this remarkable program. To the Genetics Graduate Program and Hugh Brock. To Experimental Medicine and Vince Duronio. Also, to Sharon Salloum, for being there for me and the many other students you have supported. To the University of British Columbia, Michael Smith Foundation for Health Research, the Canadian Institutes of Health Research and the Vanier Canada Graduate Scholarship for generous financial support.

To TFL support staff, in particular Alice Chau, Amanda Kotzer and Cynthia Wong. ARC staff and management including Tina Nolan, Gayle Paquette, Jane, Elaine, Tara, Melissa, and Vincent. To the staff of the TFL flow cytometry core, David Ko, Gayle Thornbury, Wenbo Xu.

To my UVic professors Terry Pearson, for introducing me to hematopoiesis and hematopoietic stem cells, and David Levin, for turning me onto research.

To my Grandpa Paul, Grandpa Doug and Nana Helen, for your unwavering love and support, whatever my pursuit. To Jeanette, for being the best mother-in-law in the world. To my sisters, Anna and Alex, I am incredibly proud of you. Thanks you for always believing in me. Mom and Dad, you are and continue to be an inspiration, both professionally and personally.

To Jenn. The love of my life. The smile at the end of the day that keeps me going, even when the data has gotten me down. Your belief in me is the reason I believe in myself. I could not have done any of this without you.

Dedication

To my little family, Jenn and Jack.
Like all I do, this is for you.

Chapter 1 Introduction

1.1 Development of hematopoiesis and hematopoietic stem cells (HSCs)

The mammalian blood system produces a collection of morphologically and functionally diverse mature cells (erythrocytes, platelets, neutrophils, eosinophils, basophils, mast cells, macrophages, dendritic cells, T-cells, NK-cells and B-cells), which cooperatively orchestrate key physiological processes. These include solute and O_2 transport, immunity and hemostasis. All of these mature blood cell types are ultimately derived, through a process of blood formation known as hematopoiesis, from rare bone marrow (BM) cells called hematopoietic stem cells (HSCs) (~1 per 20,000 in the adult mouse) (5). Although much progress has been made in identifying genes whose expression appears related to the possession of HSC functionality, a molecular signature that specifically identifies HSCs has not yet been elucidated. Therefore, the definition of HSCs continues to rely on functional (retrospective) tracking of their activities at a single-cell level. Accordingly, in the following sections, I will review the evolution that has occurred in defining HSCs based on bioassays of their functional properties, followed by a discussion of molecular insights gained that relate to their various specific properties.

During mouse development, the first hematopoietic cells to become detectable are nucleated erythrocytes that appear within the extra-embryonic blood islands of the yolk sac between embryonic day (E) 7-7.5 (6). Interestingly, this occurs 2 days before cells with transplantable HSC activity can be detected (i.e. cells able to regenerate stable, long-term production of blood cells in irradiated mice). HSCs first become detectable in the aorta-gonado-mesonephros (AGM) region of the embryo proper on E10.5 (7-10). Soon after, HSCs can also be found in other tissues including the placenta (11, 12), yolk sac and fetal liver (FL) (13). Although HSCs in the FL are thought to be derived entirely from colonizing cells arising first in other

tissues (14, 15), there is evidence that some HSCs in the yolk sac (16) and placenta (12) are generated *in situ* de novo. Around E11, the FL becomes the major site of hematopoiesis until birth (8, 17-19). Colonization of the BM begins on E17 after which the BM becomes the major hematopoietic organ throughout adulthood (20) (Figure 1.1).

1.2 Quantification of HSCs

Most mature blood cells are easily identified using a microscope by their unique morphological features seen in stained preparations, whereas most primitive hematopoietic cells all appear morphologically as blasts and have no phenotypic features that allow the discrimination of subsets with distinct biologic potentials. Recognition of this inability to uniquely identify HSCs and downstream progenitor cells directly, coupled with the discovery in the 1950's that the lethal effects of ionizing radiation on the blood-forming system could be averted by transplants of histocompatible bone marrow cells (21, 22), led to the concept of functional transplant-based methods to detect their presence by the extent and duration of their mature blood cell-generating capacity.

Functional assays to measure HSCs rely on detecting the ability of an individual cell to display a combination of cellular properties that historically have been considered to uniquely define this cell type: i.e. multi-potent differentiation and *long-term* production of many generations of daughter cells, which are characterized by the same undifferentiated state but differentiation potential. Importantly, we now appreciate that a more stringently defined combination of these properties is necessary for the specificity required to detect HSCs exclusively. This is needed because other cell types may share one or more of the properties originally attributed exclusively to HSCs. For example, some progenitor cells can produce most

if not all lineages but cannot self-renew for as long as HSCs (23). Also, mature B- and T-cells can self-renew for very prolonged periods but are highly restricted in their differentiation potential. Furthermore, it is now clear that there are subsets of HSCs that when serially-transplanted maintain their "subset" properties: e.g. they may possess robust self-renewal activity, but produce no or very few lymphoid cells (24). Such cells would therefore not be identified by classical, historically imposed, criteria that require both lymphoid and myeloid cell outputs to be revealed.

1.2.1 Colony-forming unit-spleen assay

The first quantitative HSC assay, and concomitant direct demonstration of a multi-potent hematopoietic cell with self-renewal activity, was described by Till and McCulloch in 1961 (25). These researchers made the seminal observation that the spleens of irradiated mice transplanted with different doses of BM cells, contained different numbers of surface nodules, the numbers of which were linearly related to the transplant dose (25). In follow-up work, it was confirmed that these nodules are clones (i.e. derived from a single cell) (26) and contained progeny that could produce new nodules/clones in the spleens of transplanted secondary irradiated mice, a phenomenon they named self-renewal (27). Subsequent studies have shown that the majority of these colony-forming units-spleen (CFU-S) are myelo-erythroid restricted progenitor cells (28, 29). Nonetheless, this first functional HSC assay established the basic principles underlying most current quantitative HSC assays.

1.2.2 Long-term culture-initiating cell (LTC-IC) and cobblestone area forming cell (CAFC) assays

The LTC-IC assay is an *in vitro* method that detects cells that can produce CFCs and are being generated after 4-6 weeks of co-culture of the test cells with stromal cells. LTC-IC

frequencies are determined by performing the initial cultures at limiting dilution and then calculating the frequency of cells that could generate CFCs detectable at the end of the culture period, as the proportion of wells which are ultimately positive (or negative) for this endpoint (30). Alternatively, a relative measure of the number of LTC-ICs initially present can be determined from the total yield of CFCs generated in "bulk" long-term cultures performed under conditions where CFC output is a linear function of the LTC-IC input and the average output of CFCs per LTIC-IC remains constant (31, 32).

The CAFC assay is a variant of the LTC-IC assay in which the endpoint of hematopoietic activity is the detection of discrete areas of hematopoietic cells growing within the stromal layer (30). Both the CAFC and LTC-IC assays are thought to detect some HSCs as long as the duration of the culture is at least 4 weeks, although they likely also detect cells that are more mature than HSCs (30, 33).

1.2.3 Competitive repopulation assays

The most commonly used method to detect and compare different test sources of HSCs is known as the competitive repopulation assay. This assay measures the ability of the test cells to compete with a source of HSC-containing control cells to produce mature blood cells in co-transplanted congenic recipients (34). The initial version of this assay used lethally irradiated mice to eliminate regeneration of host cells, and distinguished the two sources of co-injected cells by following the different hemoglobin types present in the erythrocytes produced by cells from congenic donors (34). For these experiments to yield consistent data, large input numbers of HSCs in the control population are required to minimize the heterogeneity in HSC outputs seen when these are transplanted in low numbers. Subsequently, this approach was modified to use leukocyte chimerism as the endpoint which was made possible by the advent of other

congenic markers (35). However, this strategy does not allow HSCs to be individually quantified since the endpoint can be affected both by differences in HSC quality (i.e. mature cell output per HSC) and quantity (i.e. frequency of HSCs in a test source).

To enable HSC quantification, independent of differences in the output per individual HSC, the competitive repopulating system was combined with a LDA strategy and a minimal competitive dose of cells. This dose was just sufficient to enable maximum sensitivity to be achieved, without losing recipients due to hematopoietic failure. The cells thus quantified are then referred to as competitive repopulating units (CRUs) (36). The CRU assay involves the injection of serial dilutions of test cells into congenic hosts, followed by the measurement of the proportion of recipients in each group whose blood cells are not repopulated by the test cells. Although this assay has also evolved, for the last decade it has been generally agreed that any mice that did not have detectable test-cell-derived B-cells, T-cells and myeloid cells for at least 16 weeks, were negative for the purposes of calculating CRU frequencies. This endpoint was defined on the assumption that all HSCs can sustain the output of cells of all 3 of these hematopoietic lineages for at least 16 weeks (Figure 1.2). However, we have more recently adopted an endpoint that does not require evidence of lymphoid cell production since some cells able to reconstitute secondary and even tertiary recipients (i.e. have robust self-renewal activity), do not produce lymphoid cells (24). The 16-week time interval is considered long enough to minimize the possibility that cells with limited self-renewal capacity (referred to as progenitor cells) will be detected as HSCs (37). This system is also highly sensitive as demonstrated by single-cell transplantation experiments with purified subsets of cells in which up to one half of the cells show HSC activity (2, 4, 38). In order for test cells to read out they must survive in the bloodstream and home to a supportive microenvironment. Thus it remains unresolved as to

whether the current inability to attain 100% pure populations of HSCs reflects a true impurity of HSCs or an inadequacy of current methods to detect cells with similar biological potentials.

1.2.4 Single-cell transplantation assays

With the advent of reagents and methods to reliably enrich HSCs to purities of greater than 1 in 4 (4, 38-40), it has become feasible to measure HSC frequencies directly by assessing the outcomes of single-cell transplants, thus bypassing the need for LDA approaches. Instead, HSC frequencies in such HSC-enriched populations are simply calculated as the proportion of irradiated recipient mice that are found to meet a set of reconstitution criteria.

Single-cell transplantation studies have revealed the existence of distinct subsets of mouse HSCs with unique differentiation patterns (2, 24). Although such approaches have proven very powerful, the relevance of the findings generated with this technique involve a number of assumptions to be made. One is that the self-renewal and differentiation potential of HSCs is meaningfully assessed when their activity is measured at a clonal level in the presence of very few other HSCs. Another is that the prospectively isolated HSCs are representative of the bulk of HSCs in mice and not a particular subset enriched by the markers used to obtain them. Recent work using approaches that do not rely on such assumptions have yielded similar findings of heterogeneity in HSC differentiation potential and therefore support this finding (41).

1.2.5 Phenotyping

No single cell surface marker or even combination of markers identified to date has been found to enable all cells with HSC activity (as defined above) to be isolated at 100% purity. Nevertheless, recent marker combinations have been found to enable a high degree of enrichment to be obtained from various sources (42). An additional issue is the variable loss or gain of marker expression that occurs according to the activation/proliferative state of HSCs

(Tables 1.1 and 1.2). The use of phenotypes for quantification and identification of HSCs has therefore to be used with caution and cannot be applied to irrefutably define HSCs unless validated for the particular population being assessed. Nonetheless, with appropriate attention to these caveats, direct identification of HSCs based on their phenotype has been useful for determining locations of HSCs in situ (43), molecular analyses of their properties (44, 45), and as a rapid surrogate in screening experiments (46).

1.2.6 Molecular strategies to track individual HSC-derived clones

Viral vectors introduced into HSCs allow clonal tracking of their progeny without the need for initial purification of the starting cells or their assessment by LDA or single cells transplants. This is accomplished either by sequencing the genomic location of retroviral or lentiviral vectors that insert semi-randomly into the DNA of transduced cells (47), by transducing cells with vectors that each carry a unique sequence (referred to as a barcode) and ensuring that each test cell is transduced by only one virus (48), or by lentiviral transduction of cells with vectors expressing red, green or blue fluorescent proteins, a strategy known as red-green-blue marking{Weber, 2011 #420}. The first of these approaches was introduced in the 1980's and enabled the diversity and longevity of HSC clones to first be documented on a large scale (37). This strategy has also been applied to characterize human HSCs transplanted into both immunodeficient mice (49) and patients receiving genetically modified cells for therapeutic purposes (50, 51). Barcoding HSCs to assess their behavior in mice transplanted with large numbers of HSCs has been introduced and exploited more recently (41). Interestingly, initial studies suggest that the clonal patterns of long-term differentiation obtained in mice transplanted with barcoded HSCs are similar to those previously obtained using single-cell transplants (24, 41).

However, tracking vector marked HSCs by either method, also has caveats. The transduction of HSCs with a viral vector requires that the HSCs be cultured for sufficient time to achieve the efficiency desired and this frequently causes the properties of the HSCs being transduced to be altered. For example, transduction of quiescent adult BM HSCs is poor, particularly when retroviral vectors are used, unless the cells are first stimulated with growth factors that poorly preserve their stem cell status. The site where a viral sequence inserts can also be mutagenic, or at least have functional consequences that may affect the biology of the cell transduced and/or its progeny (51, 52). Other caveats include the dependence on statistical assumptions in deriving clone size information from sequencing barcoded DNA (Nguyen et al, Unpublished).

1.3 Prospective enrichment of HSCs

The ability to prospectively isolate murine HSCs is critical for their study since functional assays used to detect their prior existence necessarily preclude their direct study. The isolation of viable HSCs, which are typically rare members of any hematopoietic tissue, is made possible by staining with antibodies that react with the cell surface and/or fluorescent dyes coupled with multi-parameter FACS. This strategy now allows HSCs to be separated at high yields and purities (25-50%) from all terminally differentiated blood cells and most intermediate "progenitors" including those that can repopulate mice for extensive periods, but not beyond a 4-month secondary transplant (4, 53).

The first FACS-based enrichment scheme for murine adult BM HSCs involved the isolation of Thy-1^{lo} lineage marker-negative (Lin^-) $Sca1^+$ cells (54). This strategy was later replaced by the widely-applied $Lin^-Sca1^+c\text{-}Kit^+$ (LSK) population which is highly HSC-enriched, but most certainly not pure (HSC frequency ~1/30 vs 1/20,000 in unseparated adult BM) (55).

Subsequent studies have now shown that the relatively low purities of HSCs in the LSK population were not attributable to a poor detection efficiency of the functional transplantation assay used for HSC quantification, but rather to an intrinsic biologic heterogeneity of the LSK population. Thus, it later became possible, using markers that are expressed by only a portion of this population to obtain much higher HSC purities (38, 39, 56-61).

The most HSC-enriched population of adult BM HSCs first isolated and used by our group was obtained by FACS isolation of the $Lin^{-}CD45^{mid}Rhodamine123^{-}$ (Rho^{-}) side population (SP) subset (HSC frequency ~1/3) (40). The Rho^{-} and SP parameters of this phenotype represent a unique ability of steady-state murine adult BM HSCs to selectively efflux certain compounds including the mitochondrial dye Rho and the DNA-binding dye Hoechst 33342 (Hst) (62, 63). The efflux of Rho and Hst have been functionally attributed to expression of P-glycoprotein and ABCG2, respectively (64-66). Subsequently it was found that expression of the endothelial protein C receptor (EPCR, CD201) was also a restricted marker on adult BM HSCs (67) and when used in combination with the SP population allowed similarly high HSC purities to be achieved (68).

A confounding feature of many HSC cell-surface markers is the variability of expression they exhibit throughout development and when stimulated to proliferate (activated). Table 1.1 and 1.2 summarize cell-surface marker and dye-efflux phenotypes for adult BM, FL and activated adult BM HSCs. Until very recently the number of HSC markers with expression patterns that reliably correlate with HSC functionality regardless of developmental or activation state (Table 1.2) was extremely limited (i.e. only c-Kit, Sca1, CD43 and all Lin markers except Mac1). This therefore necessitated the development of different methods for achievement of high

enrichments of E14.5 FL HSCs that are cycling (69) and therefore cannot be purified using markers that are "unstable" on activated or dividing HSCs (Table 1.1).

Previous studies in our lab have determined that the Lin^-(w/o Mac1) $Sca1^+CD43^+Mac1^+$ subset of E14.5 FL HSCs contains ~20% HSC (69). The prospective isolation of HSC-enriched populations from fetal and adult tissues using different isolation strategies has enabled critical findings about the developmentally-regulated properties of HSCs (3, 24, 38, 69-71); however, comparison of data obtained from HSCs purified using these different approaches, and to different degrees, is complicated by these factors. This highlighted the importance of developing an HSC-enrichment strategy that would be applicable to both fetal and adult HSCs.

The discovery that the signaling lymphocyte activating molecule (SLAM) family of markers (CD48, CD150 and CD244) have similar expression patterns on steady-state as well as activated adult BM and FL HSCs offered such an opportunity. However, the SLAM markers were found to yield high HSC purities only when combined with "unstable" markers (38, 58, 72, 73). Subsequent studies from our group showed that EPCR staining could be readily combined with the SLAM markers to enable highly purified mouse HSCs (~1/2.5) to be isolated from FL as well as adult BM (2, 4).

1.4 Heterogeneity of HSCs

A key observation that emerged from the study of CFU-S was the high-degree of variability in the numbers and types of daughter cells produced in individual clones (27, 74). This finding was later strengthened by analyses of multi-lineage colonies generated *in vitro*, where external stimuli can be kept the same (75-77). Further reinforcement of this heterogeneous behaviour of individual HSCs was provided by experiments that used retroviral marking to track

clones generated *in vivo* over more prolonged periods (i.e. months to years) (78, 79). These findings stimulated subsequent efforts to elucidate both the local external regulators ("niche" control) of HSC behavior as well as the internal regulators of their various fate choices (i.e. their viability, proliferative state, self-renewal probability, and differentiation lineage options).

Over the past 50 years, most experiments aimed at understanding mechanisms regulating HSC functionality have been designed and the results interpreted based on the assumption that HSCs can be quantified and characterized using a singular measurement of their continuing production at a clonal level of lymphoid and myeloid cells for at least 16 weeks in suitably compromised hosts (80). This assumption is based on the concept that the self-renewal potential and differentiation (lineage) potential of HSCs are largely controlled by a common network of intrinsically specified mechanisms that establish a common ground state in these cells. This is not to be confused with the extent to which these potentialities are expressed, as these are known to be subject to microenvironmental cues. Recent work has now thrown new light on these issues and suggests a greater level of heterogeneity in HSC populations than previously envisaged.

1.4.1 Heterogeneity of HSC differentiation programs

As discussed above, a major technological development in the last decade has been the introduction of methods for purifying to near homogeneity mouse HSCs defined by their ability to produce mature blood cells for at least 16 weeks (38, 39). This made it feasible to examine the *in vivo* clonal outputs of such cells with certainty that the activity being observed could be attributed to one as opposed to several cells—another potential caveat inherent in limiting dilution methods. The mature cell outputs of hundreds of single HSC transplants have now been analyzed, and for many of these, serial transplants have established that the primary patterns observed are stably transmitted over many self-renewal divisions (2, 24). The results have

cemented the controversial idea that some differences in HSC behavior are due to their possession of different differentiation potentialities, as first proposed by Muller-Sieburg and co-workers from serial LDA HSC transplants analyses (81).

Different HSCs subtypes have since been defined using a variety of criteria to distinguish their mature blood cell outputs. The Muller-Sieburg group has defined different HSC subsets as "myeloid-biased" (My-bi), "lymphoid-biased" (Ly-bi), or "balanced" (Bala), based on a measurement of the predominant lineages within the total output of donor-derived blood cells (i.e. exclusive of the recipient's contribution to, or the total number of mature blood cells) (82). Alternatively, our group has distinguished the different differentiation behaviors of individual HSCs by measuring the relative contributions of individual HSC outputs to the total circulating myeloid and lymphoid cell numbers (i.e. those derived from both donor and recipient HSCs). This different method distinguishes HSCs subtypes as "lymphoid-deficient" (α), "balanced" (β), or "myeloid-deficient" (γ and δ). Importantly, both α- and β-HSCs are found to contribute similarly to the circulating pool of myeloid cells (24), which is why we have suggested that lymphoid-deficient rather than myeloid-biased is a more accurate descriptor.

Serial transplantation experiments have been important in establishing the concept that the different clonal patterns of differentiation represent intrinsically stable HSC "programs", as opposed to niche-determined, temporally, or stochastically variable states. Such experiments have shown that only α- and β-HSCs can be serially transplanted, and their unique differentiation behaviors are usually stably maintained over periods of years in primary transplant recipients (2, 24). Likewise, the initial pattern of differentiation by which α- and β-HSCs are defined, is frequently expressed by their clonally generated daughter HSCs when these are transplanted into secondary mice (2, 24, 81-83). However, it is also apparent that the original

HSC program is not always maintained with complete fidelity, as demonstrated by the generation of secondary β clones from primary α clones, and vice versa (2).

The mechanisms determining the lineage outputs that distinguish different HSC subtypes are complex. For example, HSCs with different lymphoid outputs appear to produce lymphoid precursors that display differences in their IL-7 responsiveness (84). In addition, our group (2) has found that the reduced production of lymphoid cells that is characteristic of α-HSCs is due to a deficiency that operates at multiple levels as their progeny attempt to move down the lymphoid pathway (Figure 1.3).

At present, methods to prospectively separate different HSC subtypes are not sufficiently discriminating to enable their differences to be examined at a molecular level. However, microfluidics-based analyses of the transcriptomes of individual cells in a highly purified HSC population have suggested that additional subsets may exist based on their nonrandom pattern of expression of certain genes (85). In addition, several other potential clues have been uncovered. One is the finding that TGF-β may influence HSC subtypes differently (86). A second is the finding that the microenvironment of the BM is a preferential site of enrichment for α- versus β-HSCs (2). A third is the recent observation that *BTAF*, a gene found to regulate DNA damage responses, may differentially influence the maintenance of the α- versus β-HSC states (87).

Taken together, these findings suggest that differences will be found in the molecular machinery that determines the differentiation *potential* of individual HSCs, and that such differences will be maintained in the clonally-derived daughter HSCs produced in consecutive self-renewal divisions. The impressive stability of the differentiation behavior that these HSCs and their progeny HSCs display is consistent with an underlying epigenetic mechanism. The recent observation of perturbations in both human and mouse blood cell lineage outputs

associated with alterations in the DNA methylation machinery provides further support for this idea (88-92).

The clones produced by individual HSCs in irradiated mice display a large range of different lymphoid and myeloid cell outputs. However, this heterogeneity in differentiation behavior is not the exclusive result of random fluctuations in the expression of a multi-lineage program. Rather, this heterogeneity appears to reflect the operation of an intrinsically determined control mechanism that establishes a unique program in each HSC. Although little is known about this mechanism, it is clear that it can be perpetuated through many HSC self-renewal divisions with relatively high, but not rigidly fixed, fidelity, and that it targets multiple downstream stages of the lymphoid commitment and differentiation process.

1.4.2 Heterogeneity of HSC proliferative state regulation

In adult mice and humans, most of the HSCs are in a proliferatively inactive (quiescent, G_0) state. The most recent studies of the HSC compartment in adult mice indicate that it is composed of 2 kinetically distinct subpopulations, with turnover rates of 5 weeks and 21 weeks (termed activated and dormant HSC, respectively) (93). This contrasts with earlier reports which suggested turnover rates of 4-5 weeks (94, 95), although these latter rates were based on analyses of a phenotypically defined compartment that we now understand is predominantly composed of cells that do not have durable self-renewal activity. Similar information is not available for human HSCs, but a prolonged HSC turnover rate (40 weeks) has also been suggested (96). These observations raise a number of questions regarding the differences between activated and dormant HSCs, including their mechanisms of regulation, whether they are hierarchically structured or correlate with different lineage programs, and how their numbers change during ontogeny and aging.

TGF-β is well known for its ability to arrest the cycling of primitive hematopoietic cells, but evidence that this contributes to the homeostatic regulation of HSCs *in vivo* has been inconclusive. In a recent series of experiments, freshly isolated HSCs were found to display active TGF-β signaling (97), indicating a role for this pathway *in vivo*. Further corroboration comes from studies in which HSCs unable to express a TGF-β receptor demonstrated impaired long-term hematopoiesis and heightened proliferative activity in transplanted recipients (98). The same group also identified non-myelinating Schwann cells as the cells responsible for the activation of TGF- β in the BM, thereby uncovering a potential novel activity of this cell type as an upstream regulator of TGF-β-mediated control of HSC quiescence (98).

The signaling components responsible for HSC responses to both proliferative and anti-proliferative signals have recently been further elucidated. Once of these is Foxo3a, which has been shown to act as a HSC dormancy factor via its ability to regulate p27 and p57 (99). This effect is likely facilitated by a p27/p57-mediated blockade of the nuclear transport of Hsc70/cyclin D1, since a knockout of both of these genes leads to increased cycling and an associated nuclear import of this complex (100). Changes in the levels of reactive oxygen species in HSCs and alterations in oxygen sensing molecules also appear to be associated with changes in HSC turnover rates (99, 101). However, it remains unclear whether these are a cause or consequence of changes in HSC cycling. Finally, the tumor suppressor *Lkb1* was recently found to be important for the maintenance of HSC quiescence as its conditional deletion leads to loss of quiescence followed by rapid HSC depletion and pancytopenia (102).

1.4.3 Heterogeneity of HSC self-renewal activity

The concept of distinct subsets of repopulating cells dates back several decades (103), and the fact that they can be prospectively isolated as phenotypically separable subsets has been

recognized for over a decade (80). However, evidence of different subsets of HSCs with more prolonged self-renewal abilities has only recently been obtained (24, 53, 83, 104-106). This evidence is based on two types of measurements. One is the lifetime of individual HSC-derived clones of mature blood cells produced in transplanted mice, which are observed to range from a minimum of 4 months (by definition) to >2 years. The second more stringent endpoint is the detection of clonally perpetuated blood cell production that is sustained through at least 3 serial transplants (i.e. beyond the lifetime of a normal mouse). The prolonged maintenance of daughter HSC activity for at least 6 months following secondary transplantation appears to be associated with the maintenance of robust myeloid differentiation activity that is shared by α- and β-HSCs. In contrast, in HSCs that have more time-restricted myeloid outputs (intermediate HSCs) and/or have become largely restricted to producing lymphoid cells (γ and δ subtypes), self-renewal activity is not usually maintained beyond 4 months after initial transplantation (24). Importantly, mouse HSCs with more limited self-renewal activities can be prospectively distinguished from those that exhibit durable activity, the latter being most enriched within a sub-population that does not express CD49b and shows the highest expression of CD150 (encoded by *Slamf1*) (4, 38, 53, 106).

Steel factor (SF, also known as Kit ligand or Stem Cell Factor (SCF)), has long been known to play a key role in the control and maintenance of primitive hematopoietic cells (107). New insights obtained in the last 5 years include the demonstration that SF can rapidly modulate self-renewal decisions of mouse HSC, even when other variables including cell death and cell cycle progression are kept constant (68). The cellular origins of SF important for HSC regulation *in vivo* have also recently been clarified. This was achieved by generating different types of transgenic mice in which the *Kitl* gene was deleted in a cell type-specific manner, followed by

analysis of HSC activity. These experiments showed that SF produced by endothelial and perivascular stromal cells, but not from osteoblasts, is necessary for mouse HSC regeneration post-transplant (43). These findings reinforce previous studies indicating a role for external signals in regulating the extent to which adult HSCs express their innate self-renewal potential *in vivo* (104).

Over the last 2 decades, the many transcription factors, chromatin modifiers and cell cycle regulators that have been found to affect HSC self-renewal behaviour suggest that a number of different pathways regulate this process. The recently demonstrated role of epigenetic regulators in affecting HSC self-renewal adds another layer of complexity (92). However, whether these factors influence self-renewal independently of cell survival or proliferation, and how their effects are ultimately integrated remain largely obscure.

Our current understanding of mouse HSC self-renewal control suggests that the probability of undergoing a self-renewal division and the durability of this behavior is an intrinsically determined phenomenon that can be modified by the presence or absence of extrinsic factors. Additionally, the durability of this activity appears tightly linked to the maintenance of an active myeloid differentiation program.

1.5 Hematopoietic developmental transitions

As described earlier, a key difference in hematopoiesis in the developing fetus compared to the adult is the major anatomical site where this occurs (i.e. FL versus adult BM). Interestingly, the HSCs, progenitors and differentiated cell types produced within these sites differ in multiple properties that may represent developmentally regulated cell-intrinsic

programs. Recent work suggests that some of these developmental changes may be regulated by one or several common mechanisms.

1.5.1 Developmental effects on progenitors and terminally differentiated subsets

1.5.1.1 Hemoglobin switching

Hemoglobin is a tetrameric metalloprotein produced in erythrocytes that acts to transport O_2 and CO_2. Two developmental switches in the expression of the globin subunits, which make up the haemoglobin molecule, occur during development and serve to alter physiological properties of this protein (108).

As previously mentioned, the first hematopoietic cells produced in the developing mouse embryo are primitive erythrocytes. This transient population is distinguished from definitive erythrocytes by its retention of a nucleus and expression of primitive embryonic globin genes (109). Enucleated definitive erythrocytes, produced by the HSCs that arise a few days later, differ from primitive erythrocytes by their expression of definitive globin genes.

In contrast to this primitive-to-definitive switch that occurs in all mammals, a second type of haemoglobin switching, called the fetal-to-adult switch, only occurs in humans and old world monkeys. This transition, which involves a change from γ- to β-globin expression, is initiated in the mid-gestation fetus and is completed by one year of age. This alteration is thought to facilitate increased oxygen scavenging from maternal blood since the HbF molecule ($\alpha_2\gamma_2$) has a higher oxygen affinity than the adult-type haemoglobin ($\alpha_2\beta_2$).

1.5.1.2 Megakaryocyte maturation

Megakaryocytes in adults are large, polyploid cells that mature in the marrow and give rise to platelets by a process of cytoplasmic budding. In contrast, megakaryocytes from human

umbilical cord blood (CB), which serve the same platelet-producing function, are small cells with a lower ploidy (110-112). These differences seem to represent cell-intrinsic programs based on the finding that cultured CB, when compared to mobilized peripheral blood (PB), gives rise to smaller megakaryocytes with a lower ploidy (113, 114). Interestingly, CB-derived progenitors also give rise to approximately 10-fold more megakaryoctyes under these conditions, suggesting a mechanism involving a reduction in the proportion of mitoses which culminate in cytokinesis (115).

Although differences in the size and ploidy of neonatal versus adult megakaryoctyes has historically been thought to reflect different levels of maturity (i.e. neonatal megakaryocytes are smaller and therefore less mature than adult megakaryocytes), recent work has shown that the smaller neonatal megakaryoctyes are cytoplasmically mature (115). Taken together, these results suggest the existence of a fetal/neonatal-specific pattern of megakaryopoiesis, which is characterized by the production of a larger number of cytoplasmically mature but lower ploidy megakaryocytes.

1.5.1.3 Myeloid progenitors

Some of the earliest studies comparing fetal and adult hematopoietic tissues used the CFU-S assays as an endpoint (described above in Section 1.2.1). Since this assay is now appreciated to capture a heterogeneous population, mostly composed of myelo-erythroid restricted progenitors with HSCs representing a relatively rare component (28, 29), such early findings can now be considered to reflect properties of myeloid progenitors.

One of these properties is the higher rate of turnover of fetal relative to adult CFU-S. This was elegantly demonstrated by measuring the fractional survival of FL or adult BM CFU-S after their exposure to a high specific activity-H^3-thymidine versus and unlabeled control. After only a

20-minute exposure *in vitro*, it was found that 40% of the FL CFU-S were killed as compared to <10% for the adult BM CFU-S (116), suggesting a higher proportion of CFU-S in the fetal population are in the S-phase of the cell cycle.

Differences between fetal and adult erythroid-restricted progenitors (colony-forming unit erythroid; CFU-E) were also noted in early studies. Fetal CFU-E contain a higher proportion of S-phase cells than their adult counterparts and are more sensitive to erythropoietin (Epo) as shown by dose-response analyses of their ability to express their clonogenic potential *in vitro* (117). The change in Epo sensitivity of CFU-E was reported to occur gradually between fetal and adult life (118).

1.5.2 Effects on HSC activities

Like developmental differences in mature hematopoietic cells, the properties of HSCs themselves are also known to change during ontogeny. For the purposes of clarity, these (discussed below) have been separated from the developmental changes that seem to be restricted to more committed progenitors (discussed above). This may, however, represent an oversimplification since most current studies lack the resolution to properly distinguish which properties might be ultimately regulated in part or wholly by molecular events occurring in HSCs.

1.5.2.1 Proliferative activities

Similar to CFU-S (116), fetal-stage HSCs proliferate more rapidly than their adult counterparts (119, 120). These early findings were recently refined by the demonstration that FL HSCs are uniformly cycling whereas only approximately 10% of adult BM HSCs are at any given time (69).

1.5.2.2 HSC regenerative behaviours

The first evidence that FL HSCs have a greater regenerative ability than adult BM HSCs came from an early study showing the ability of marked cells to gain gradual ascendancy when co-transplanted with a graft of adult BM cells containing a greater number of HSCs (18). It has since been demonstrated that fetal HSCs also repopulate irradiated mice more rapidly (120-122). This difference in regenerative ability is now appreciated to be at least partly due to a greater *in vivo* self-renewal of FL HSCs, since they produce significantly more daughter HSCs than adult BM HSCs *in vivo*, regardless of HSC input number (10, 100 or 1000) (123). In 2007, Bowie et al. showed that FL HSCs, when compared to their adult counterparts, amplify their numbers more rapidly following their transplantation into sublethally irradiated hosts. This difference is most pronounced during the second week following transplantation (FL-derived HSCs increase 8-fold whereas adult BM numbers remained largely unchanged) (70).

1.5.2.3 Lineage outputs

HSC differentiation potential has been determined using transplantation of fetal and adult hematopoietic cells into irradiated adult hosts. This approach has revealed differences in the types and relative amounts of mature cell types produced by fetal compared to adult HSCs.

One of these differences is the relative myeloid-output activity of fetal HSCs. This was shown in experiments where FL and adult BM populations containing approximately 10 HSCs were injected into different mice, and the proportion of myeloid cells in donor HSC-derived PB cells measured. The proportion of donor-derived myeloid cells produced from transplanted HSCs was found to be approximately 2-fold higher for mice transplanted with cells from a fetal compared to an adult source (70).

Fetal and adult HSCs also differ with respect to the properties of the lymphoid progenitors and differentiated lymphoid cells they produce. The first indication of this difference came from a seminal study in 1985 in which the authors observed that a subset of B cells, called B2 B cells, can be produced upon transplantation of either neonatal liver or adult BM; however, another subset, called B1 B cells, can only be made efficiently by neonatal liver cells (124). More recently, it was shown that this difference applies specifically to B1a cells and that it is ultimately mediated by differences in HSC potential (125). These authors also found that IL-7 is required for adult but not fetal B-cell development and that the fetal-to-adult switch in IL-7 dependence occurs between 1 and 2 weeks after birth (125).

During mouse development, the first $CD4^-CD8^-$ cells that appear in the thymus express the Vγ3 Vδ1 T cell receptor (TCR), followed by a second wave of TCR Vγ4 Vδ1 cells (126, 127). Like B-1a B cells, the production of these fetal-type T cells is mediated at the HSC level since adult HSCs can only produce adult-type (Vγ2, Vγ5, and TCR αβ) T cells (127).

1.5.2.4 Developmental differences in HSC responsiveness to SF

SF is a transmembrane growth factor that is encoded by the *Sl* locus. SF binds to a type III receptor tyrosine kinase called KIT (CD117) that is encoded by a gene in the *W* locus. Even before the products encoded by the *W* and *Sl* loci were known to represent a receptor-ligand pair mediating HSC responses, studies of the defects caused by mutations at both loci had pointed to their complementary involvement in HSC regulation. For example, both fetal and adult hematopoietic tissues from mice carrying mutations within the kinase domain of *Kit* show reduced CFU-S activity (107). Mice with a W^{41}/W^{41} genotype are of particular interest because they are viable and fertile (in contrast to those with more severe *W*-mutation) (128), but still have significantly reduced HSC numbers (10 to 20-fold). As a result, sublethally irradiated adult

W^{41}/W^{41} mice can be used as hosts to detect transplanted (wild-type) HSCs with the same sensitivity as lethally irradiated wild-type hosts given a minimal radioprotective transplant (129). In contrast, *Sl*-mutant mice, which have deletions in the SF genomic sequence (130), have a microenvironmental niche defect that normally stimulates the regeneration of CFU-S and is required to sustain their numbers throughout adult (but not fetal) life (107).

HSCs from all stages of development express the same levels of KIT receptor on the cell surface regardless of their cycling status or position in the cell cycle (3, 55, 69, 131). However, several lines of evidence point to differences in the requirements and responsiveness of fetal and adult HSCs to SF stimulation. *Sl*/*Sl* mice, which lack expression of both the transmembrane and soluble forms of SF, die at around E15-16, their CFU-S and phenotypically-defined HSCs ($Thy^{lo}Lin^{-}Sca\text{-}1^{+}$) increase 3 to 5-fold between E13-15 thereby implying that at least some fetal HSC self-renewal divisions can occur in the absence of SF (55). *In vitro*, the ability of different concentrations of soluble SF to modulate HSC self-renewal divisions directly has been demonstrated using highly purified starting populations and functional readouts of retained or lost HSC activity (40, 133, 134). These experiments have further demonstrated that the self-renewal responses of fetal and adult HSCs to soluble SF in serum-free suspension cultures are both steeply SF concentration-dependent above and below an optimum level. Nevertheless, their specific sensitivities to SF are markedly different. Fetal HSCs are 6-fold more sensitive to SF than their adult counterparts with maximum maintenance of fetal HSC activity in medium containing 50 ng/ml of SF (only) as compared to the 300 ng/ml of SF (+20 ng/ml IL-11) required to achieve a similar result with adult HSCs (3).

1.5.2.5 Candidate regulators of developmentally distinct HSC programs

Another distinction between fetal and adult HSCs can be made regarding their dependence on gene products. The prototype for such genes is *Bmi1*, a member of the polycomb repressive complex 1 (Prc1), that when deleted allows for the generation of a normal FL HSC compartment, however, BM failure secondary to HSC depletion occurs 1-2 months after birth (135). Similarly, *Gfi*$^{-/-}$ mice develop normally, but when their BM cells are transplanted they have a reduced ability to repopulate irradiated recipients suggesting their adult HSCs are impaired (136). Similarly, *Tel*/*Etv6* has been shown to be an essential and selective regulator of adult HSC survival (137). Together, these findings suggest the existence of an adult-specific transcriptional program.

Conversely, several gene products have recently been demonstrated to be important for fetal but not adult HSCs. The first of these identified was *Sox17* which is expressed at a higher level in fetal compared to adult HSCs, using both direct measurements of gene expression and an analysis of HSCs isolated from a *Sox17* knock-in reporter mouse (138). Inducible deletion of the *Sox17* gene was then used to demonstrate an essential role for Sox17 in maintaining HSCs in fetal/neonatal mice. Importantly, *Sox17* deletion in adult mice had no effect on HSC numbers or functionality (138). Interestingly, forced expression of *Sox17* in adult murine hematopoietic cells was found to enhance the HSC-derived output of myeloid cells (a fetal HSC property) (139), consistent with a partial reactivation of the fetal program.

Another recently identified potential regulator of fetal versus adult HSC identity is *Lin28b*. *Lin28b* is expressed at higher levels in fetal as compared to adult lymphoid progenitor populations, and forced overexpression of *Lin28* in adult hematopoietic progenitors reactivates a fetal-like lymphoid differentiation program (140). These authors also found that *Lin28b* is

differentially expressed in fetal and adult HSC-containing populations (LSK cells), suggesting Lin28b may also regulate differences between their developmental states. The differential expression of *let-7b*, an important target of Lin28b, was also recently found to regulate differences in megakaryocyte size and ploidy, thus strengthening the case for Lin28b as a potential master regulator of hematopoietic developmental transitions (141).

With respect to the difference in proliferative activities of fetal compared to adult HSCs, C/EBPa was recently shown to be an important negative regulator of proliferation in murine adult BM HSCs. Furthermore, C/EBPa-null adult HSCs have a transcriptional program similar to that of fetal HSCs (142), which supports the notion that many of the transcriptional differences between fetal and adult HSCs are a consequence of their different proliferative activities. It remains unclear what factor(s) developmentally regulate the levels of C/EBPa.

1.5.2.6 Evidence suggesting a cell-intrinsic "switch" may reprogram HSC properties

Since genetic tracing (143, 144) and serial transplant experiments (70) strongly indicate that adult HSCs are derived from fetal HSCs, it follows that developing HSCs must acquire new properties and/or suppress fetal properties in order to become adult-like. This transition could theoretically take place by a gradual transformation through a number of intermediate states, or alternatively by an abrupt and coordinated switch from the fetal to the adult state. Data from our group supports the latter (3, 69, 70).

Since the cells that stimulate HSCs within the BM are thought to regulate HSC behaviour through cell-to-cell interactions and paracrine signaling (145), we first considered that the switch from a fetal to an adult set of HSC properties may be triggered by the migration of HSCs into the BM at E17. Interestingly, when E18.5 BM cells were, it was found that these HSCs were still in cycle (a fetal HSC property). This finding suggested that colonization of the BM is likely not the

immediate trigger for the transition from the fetal to adult cell-cycle state (69). Analysis of other developmental time points revealed that HSCs continue to cycle until 3-weeks of age and then rapidly acquire an adult-like quiescent state by 4-weeks of age (69).

To investigate whether other developmentally regulated HSCs properties (i.e. self-renewal capacity and granuloctye/monocyte (GM) output) are changed along with cell-cycle status 3-4 weeks after birth, a series of transplantation experiments were performed on populations of HSCs derived from E14.5 FL, E18.5 BM, 3-week BM, 4-week BM and 10-12-week BM. The results of these studies revealed that E14.5 FL, E18.5 BM, and 3-week BM-derived HSCs have nearly identical expansion rates and GM-output patterns, which are significantly different from the patterns shared by 4-week and 10-12-week-derived HSCs (70). Furthermore, since E14.5 FL HSCs transplanted into irradiated adult recipients become adult-like with roughly the same timing as if they were left *in situ* (70), it was postulated that this highly coordinated developmental switch may be under the control of a pre-programmed developmental timer that operates intrinsically within all developing HSCs. This switch parallels another developmental hematopoietic switch which determines the requirement of IL-7 and thymic stromal-derived lymphopoietin for the terminal differentiation of B-cell progenitors. Since this occurs at roughly the same time (1-2 weeks after birth) (125), a common set of mechanisms may coordinately regulate many or all hematopoietic developmental changes.

1.6 Mechanisms of developmental timing of changes in cell behaviour

Although very little is known about the mechanisms underlying the regulation of developmental timing in the hematopoietic system, a few examples of such "cell-intrinsic developmental timers" in other animals and tissues exist. In the study of *C. elegans*, worms that

have a defect in the timing of cellular fate are termed heterochronic mutants. The *let-7* miRNA was identified in a screen for such heterochronic mutants and its role has been particularly well characterized in a subset of skin stem cells called seam cells. These seam cells divide asymmetrically at each of four larval stages during development and then cease dividing at the larval-to-adult transition (146). Interestingly, *let-7* mutant worms reiterate a fourth larval fate suggesting that *let-7* expression is required for the correct timing of this L/A transition (146). Furthermore, forced early expression of *let-7* can induce a partial premature seam cell differentiation (146). Since *let-7*, along with 6 related miRNAs termed the '*let-7* family', are also known to regulate key timing events in the ventral nerve cord and the intestine (147-149), these miRNAs are considered master regulators of developmental timing in *C. elegans*.

Another example of a cell-intrinsic timer is that of the rat oligodendrocyte precursor cell. In studies performed more than three decades ago it was found that oligodendrocytes appear *in vitro* from E10 brain cell suspensions at the same time as they would if left *in situ* (150). Amazingly, the timing of this process is likely not mediated but cell division counting, since OPCs cultured at a lower temperature undergo fewer divisions but still differentiate within the same time period (151). The timer involves the progressive accumulation of the cyclin-dependent kinase inhibitors p27 and p18 (151, 152).

1.7 Thesis objectives

The overall goal of my work was to test the hypothesis that one or several factors change their levels between fetal and adult HSCs, which in turn endows these cells with distinct properties{Bowie, 2007 #24;Bowie, 2007 #25;Bowie, 2006 #26}. Since the fetal HSC state is associated with a heightened self-renewal activity (70, 123), the identification of factors that

specifically maintain the fetal program, and/or repress this program in adult HSCs, may help inform methods by which adult HSCs could be manipulated to enhance their transplantation potency. Additionally, by discerning the molecular mechanisms that distinguish the fetal and adult HSC self-renewal and differentiation programs, we may gain greater insight into the possible roles that developmentally-distinct HSC backgrounds may play in the pathogenesis of pediatric relative to adult human hematopoietic malignancies.

Although *Sox17* has been previously shown to regulate the fetal HSC transcriptional program (138), it remains unclear whether its loss in fetal HSCs alters the self-renewal process or other properties like proliferation or apoptosis. Furthermore, since *Sox17* is unlikely to be the sole regulator and specific determinant of the superior self-renewal behaviour of the fetal versus adult HSC state, the identification of other factors involved in this process warrants further investigation.

In the work described in Chapter 2, I endeavoured to perform comparisons of E14.5 FL and adult BM HSCs in order to identify candidate regulators of developmental changes in HSC self-renewal. To facilitate the most relevant comparisons, I also worked with my colleagues Claudia Benz and David Kent to design and test a novel strategy for isolation of mouse HSCs that could be used on cell populations from multiple tissues and developmental time points. Since differences in the proliferative activities of fetal and adult HSCs were predicted to be a confounding variable in my comparisons, I also developed and utilized a strategy for identifying transcripts that are directly regulated by this difference in cellular state.

Since the results generated in Chapter 2 suggested that differential expression of components of the Lin28b-let-7-Hmga2 axis might regulate developmental differences in mouse HSC self-renewal, I next undertook a series of experiments to test this model. This was

accomplished by: (i) determining whether or not high expression of Lin28 or Hmga2 are sufficient to confer a fetal-like self-renewal activity upon adult HSCs, (ii) testing the necessity of high *Hmga2* expression for the high self-renewal activity of fetal HSCs, and (iii) investigating whether Lin28 can regulate let-7 and Hmga2 levels in mouse HSCs. Since Lin28 was recently shown to regulate developmental differences in mouse HSC lymphopoietic potential (140), this property was also explored. Experiments were also undertaken to interrogate the mechanisms by which Lin28 and Hmga2 may mediate their effects.

Table 1.1 Activation state-dependent HSC cell-surface marker expression

Marker	Adult BM	Fetal liver	Activated adult BM
AA4.1	- (121)	+ (121)	n.d.
CD34	- (39)	+ (153)	+ (154)
CD38	+ (155)	- (156)	- (156)
CD45RB	- (121)	+ (121)	n.d.
Endoglin	+ (157)	n.d.	+/- (158)
Mac1	- (121)	+ (120)	+/- (121)
Mpl	+ (158)	n.d.	+/- (158)
Prp	+ (158)	n.d.	- (158)
Rho	lo (63)	+ (159)	+/- (159)
SP	+ (160)	- (159)	- (159)
Tie-2	+ (158)	n.d.	- (158)

+: positive, -: negative, n.d.: no data available. Numbers in brackets are references.

Table 1.2 Activation state-independent HSC cell-surface marker expression

Marker	Adult BM	Fetal liver	Activated adult BM
CD150	+ (38)	+ (72)	n.d.
CD244	- (38)	- (72)	n.d.
CD41	- (38)	- (72)	n.d.
CD43	+ (161)	+ (69)	n.d.
CD48	- (38)	- (72)	- (73)
c-Kit	+ (54)	+ (69)	+ (73)
EPCR	+ (67)	+ (162)	+ (162)
Lin	- (54)	- (120)	n.d.
Sca-1	+ (54)	+ (120)	+ (73)

+: positive, -: negative, n.d.: no data available. Numbers in brackets are references.

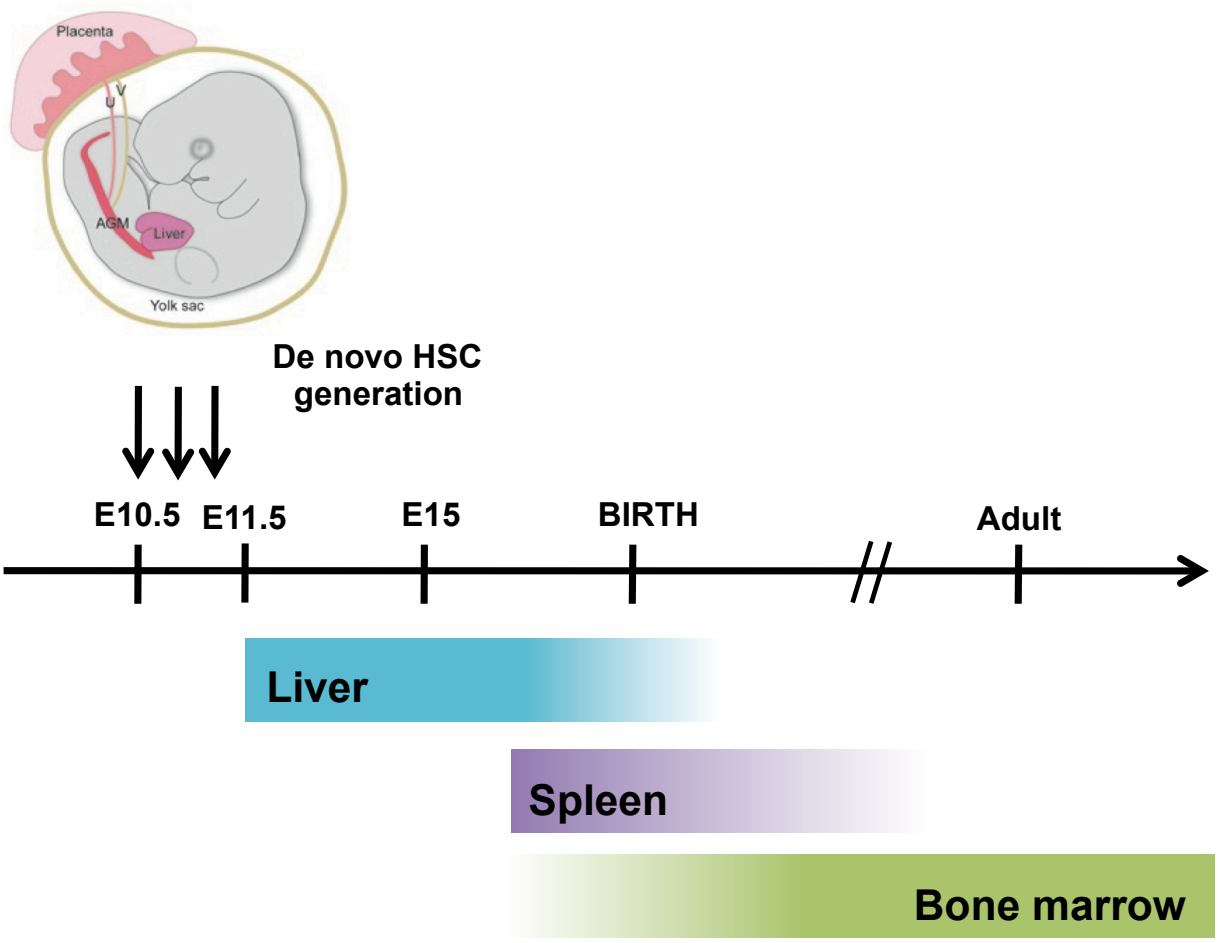

Figure 1.1 The journey of developing hematopoietic stem cell (HSCs)
Mouse hematopoietic stem cells (HSCs) generated in the aorta-gonad-mesonephros (AGM) or placenta migrate to the fetal liver and undergo an expansion in their numbers prior to their migration to the spleen and bone marrow. Figure adapted from Dzierzak et al. 2008 (163).

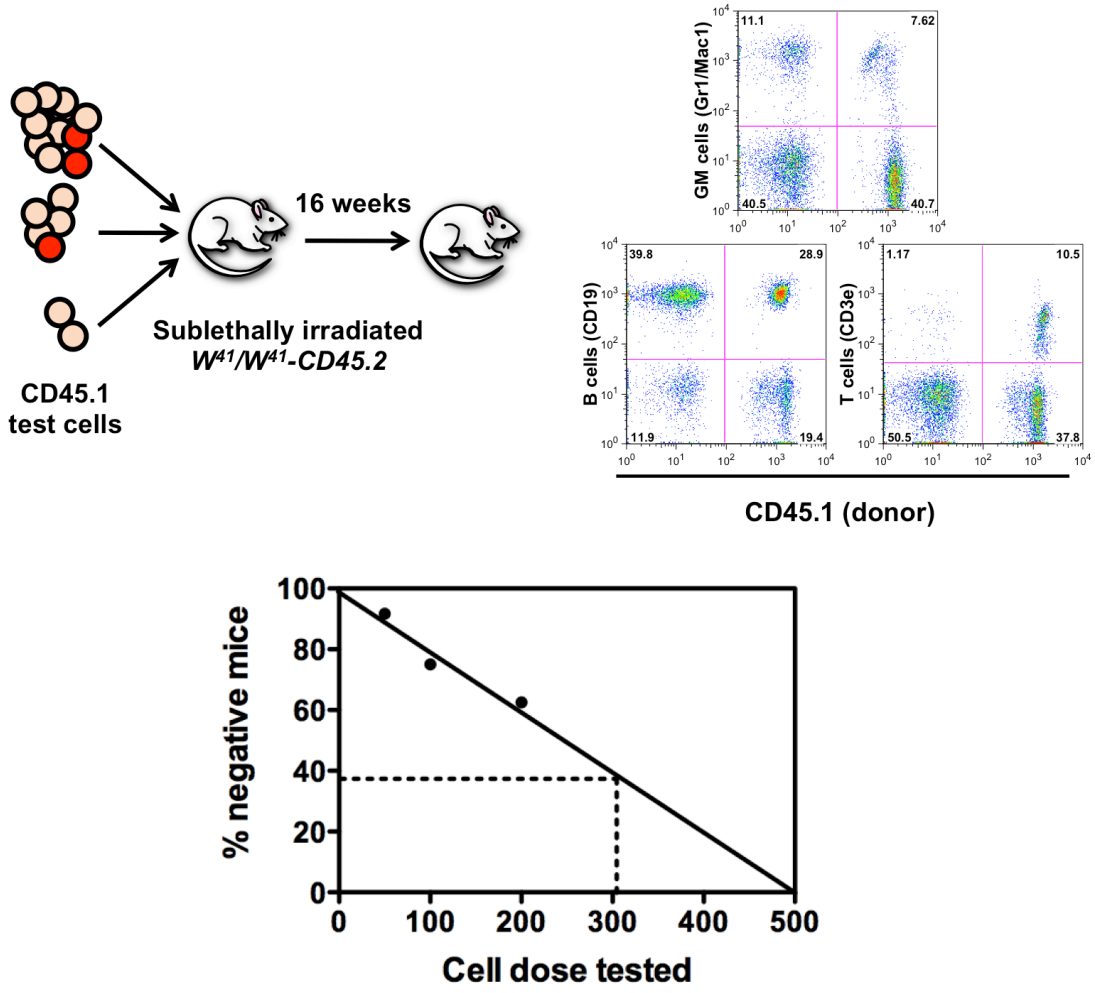

Figure 1.2 Limiting dilution competitive repopulating unit (CRU) assay
This assay utilizes the principles of limiting dilution analysis to quantify the number of test cells that have long-term repopulating capacity (represented by red cells). The recipient mouse is irradiated in order to give the test stem cells a competitive advantage; however, the mouse must also survive even if the test population contains no HSCs. Therefore, BM cells containing sufficient short-term repopulating cells are co-transplanted, or sublethally irradiated W^{41}/W^{41} hosts are used. This latter genotype is one in which c-KIT is mutated which reduces the number of HSCs in the host (129). The presence of donor origin blood cells after 16 weeks is used to infer the presence of HSCs in the injected cells. Mice are considered to be positive if their blood contains >1% donor-type blood cells overall with a >1% donor-type contribution the myeloid lineage. Poisson statistics are then used to determine the frequency of HSC in the test population.

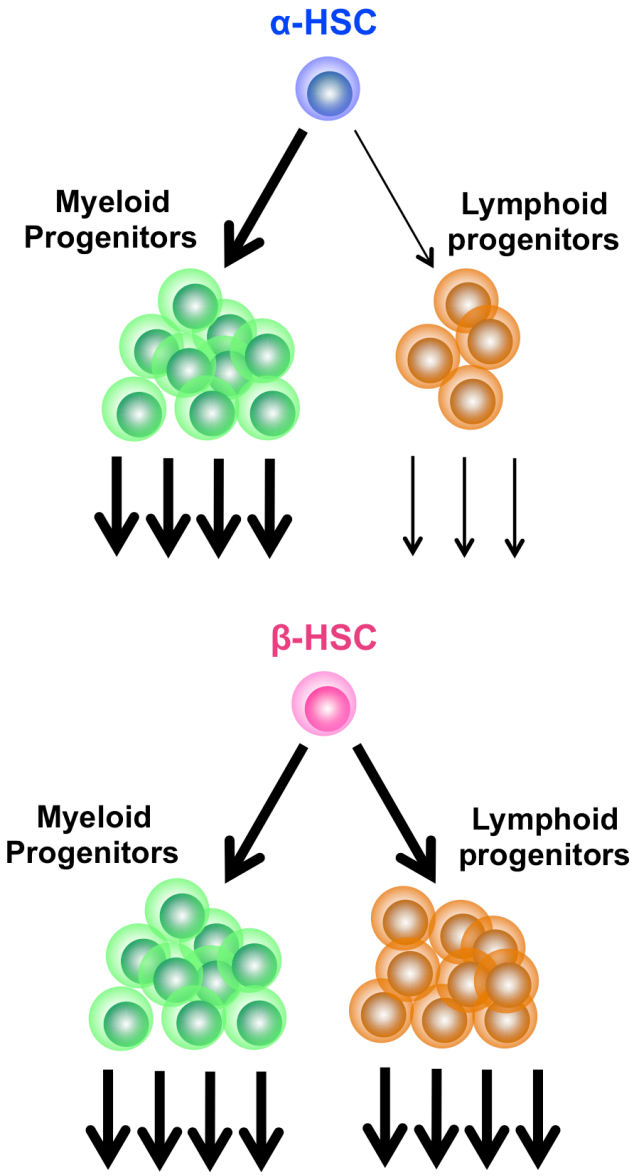

Figure 1.3 Lymphopoietic differences between HSC subtypes are manifested at multiple levels of lymphoid differentiation

HSCs with durable self-renewal consist of 2 subtypes (α-HSCs and β-HSCs). These have equivalent robust myeloid differentiation ability but they differ in their ability to produce mature lymphoid cells as shown. The lymphoid deficiency of α-HSCs results from a multi-step reduction in lymphoid cell output (2).

Chapter 2 Identification of candidate molecular and cellular determinants of the fetal HSC high self-renewal state

2.1 Introduction

HSC numbers in the developing mouse increase 10-30 fold between E12.5 and E16.5 (11, 164) within the FL. Since this rapid growth of fetal-stage HSCs is both spatially and temporally separate from *de novo* HSC generation (165), this population expansion is presumed to involve a transient developmental elevation of HSC symmetric self-renewal divisions. This possibility is supported by the finding that fetal HSCs (70, 123), like the CFU-S they produce (18), are regenerated at a faster rate, when compared to adult BM, in transplanted irradiated mice (i.e. within the same microenvironment). Nonetheless, the extent to which this enhanced expansion might represent a heightened self-renewal potential possessed uniquely by fetal HSCs was not known.

An important clue came from the discovery, in our lab, that the more rapid *in vivo* expansion behaviour of FL HSCs, persists long after these cells begin to migrate to the BM (~E17.5), and does not change until 3 weeks after birth when, within a period of 1 week, most of the HSCs enter the quiescent state that normally characterizes adult HSCs (70). These findings, along with evidence of other properties of hematopoietic cells that change in a similar time frame (70, 125), led our group to propose the existence of a cell-intrinsic fetal-stage program that maintains multiple HSC properties that appear coordinately regulated during development. One indication of the mechanism(s) involved can be inferred from the observation that fetal and adult HSCs are differentially responsive to SF stimulation *in vitro* (3). Specifically, highly purified E14.5 FL HSCs are maximally maintained *in vitro* in serum-free medium containing 50 ng/ml

SF, whereas adult BM HSCs require 300 ng/ml SF + 20 ng/ml IL-11 to achieve the same outcome.

Analyses of the transcripts present within populations of prospectively isolated HSCs, relative to their more differentiated progeny, have provided a wealth of information about the genes that regulate key HSC properties such as self-renewal. Since many of such studies have compared populations from multiple developmental sources (71, 166-169), a comparison of the HSC-enriched populations from these studies should reveal candidate developmental regulators of HSC self-renewal. Unfortunately, this interpretation is confounded by the fact that these studies relied on the use of different phenotypes to obtain the HSC-enriched populations analyzed. This was necessitated by the fact that the markers used to isolate adult HSCs lose their specificity when HSC are cycling (Table 1.1), as is the case in the fetal mouse (69). But since these populations were not "pure" HSCs, and indeed were typically enriched to different degrees, differences in the gene expression profiles obtained might well be due to cells other than the HSCs present.

The discovery that some members of the family of signaling lymphocyte-activating molecule markers (SLAM), i.e. CD48, CD150 and CD244, have similar expression patterns on steady-state as well as activated adult BM and FL HSCs appeared to offer an opportunity to overcome this barrier. Unfortunately, these SLAM markers only yield high HSC purities when combined with "unstable" markers (38, 58, 72). In contrast, EPCR is expressed on both cycling fetal and quiescent adult HSCs (4, 67). We therefore investigated the possibility of combining EPCR with the SLAM markers to isolate HSCs at high purity, independent of their cycling status. Since single-cell transplants were used to test this strategy, the HSC differentiation subtypes identified at different developmental time points were also analyzed.

To identify candidate genes involved in regulating the developmental changes in HSC self-renewal behavior, several approaches were employed. These included an analysis of candidate SF signaling genes, differentially expressed genes identified from a comparison of Serial Analysis of Gene Expression (SAGE) libraries prepared from highly enriched FL and adult BM HSC populations constructed previously in our lab (4), and by an Affymetrix array analysis of a subset containing HSC and derivative progenitors followed by confirmation of candidates in highly purified HSCs.

2.2 Materials and methods

2.2.1 Mice

C57Bl/6J:Pep3b-Ly5.1 (Pep3b) or C57Bl/6J-Ly5.2 (B6) mice were used as donors and C57Bl/6J W^{41}/W^{41} (W41) mice were used as recipients. All mice were bred and maintained in microisolators in the animal research centre at the BC Cancer Research Centre according to protocols approved by the University of British Columbia Animal Care Committee (ACC #A10-0173 and #A11-0080). W41 mice were irradiated with 360 cGy of X-rays or 400 cGy ^{137}Cs γ-rays prior to being intravenously injected with test cells. To obtain E14.5 FLs, 1-4 female Pep3b mice were placed overnight with a single male Pep3b stud and inspected for vaginal plugs on the following day. The day of plug detection was considered E0.5. For 3-week (19-20-day-old) and 4-week (29-31-day-old) mice, the day of birth was considered day 0. Unless otherwise stated, adult BM was harvested from 8-12 week-old mice.

2.2.2 Cell preparation and flow cytometry

BM cells were harvested from femurs, tibiae and pelvic bones of CO_2-euthanized mice by flushing with 3 ml of Hank's balanced salt solution (HBSS, STEMCELL Technologies, Vancouver, BC, Canada) containing 2% fetal bovine serum (HF, STEMCELL Technologies) using a 3 ml syringe and 21-gauge needle. To lyse red blood cells, 7 ml of ammonium chloride lysis solution (0.8% NH_4Cl with 0.1 mM EDTA, STEMCELL Technologies) was added to the 3 ml BM suspension and incubated on ice in the dark for 10 minutes. E14.5 FL cells were prepared by separating FLs from surrounding tissue under a dissecting microscope and forcing the cells through a 352340 Falcon 40 μm nylon cell strainer (Becton Dickinson, Franklin Lakes, NJ, USA) using the plunger of a 3 ml syringe and rinsing with 10 ml of HF. In many cases, the majority of lineage marker-positive (Lin^+) cells were depleted immunomagnetically using the EasySep negative selection kit (STEMCELL Technologies). FL cells were depleted of Ter119 only and 3-week BM were depleted of all Lin markers (anti-CD4, anti-CD8, anti-CD3ε, anti-CD5, anti-Ter119, anti-Gr1 and anti-B220). When cells were stained for SP and Rho phenotypes, they were suspended at 10^6 cells/ml in pre-warmed serum-free medium (SFM) which consisted of Iscove's modified Dulbecco's medium (IMDM) supplemented with 10 mg/ml bovine serum albumin, 10 μg/ml insulin, and 200 μg/ml transferrin (BIT, STEMCELL Technologies), 100 units/ml penicillin, 100 μg/ml streptomycin (both from STEMCELL Technologies), 10^{-4} M 2-β-mercaptoethanol (2-ME, Sigma-Aldrich, St. Louis, MO, USA) to which Rho (Molecular Probes Inc., Eugene, OR, USA) was added at a final concentration of 0.1 μg/ml. After 30 minutes of incubation at 37°C in the dark, the cells were washed with HF and resuspended at 10^6 cells/ml in the same medium without Rho. Cells were then incubated with 0.1 μg/ml Hoechst 33342 (Hst, Molecular Probes) for 90 minutes at 37°C in the dark. Cells destined for monoclonal antibody

staining were pelleted and resuspended in 25 µl of 1 mg/ml D4513 DNase (Sigma-Aldrich) followed by a further dilution in ice-cold HF plus 10% rat serum (Sigma-Aldrich) and 1.25 µg/ml mouse CD16/32 Fc receptor blocking 2.4G2 antibody (STEMCELL Technologies). Cells were stained on ice in the dark for 30 minutes for primary antibodies and 15 minutes for secondary antibodies unless otherwise stated. Phenotypes and antibodies used are listed in appendices B.1 and B.2, respectively. Cells stained with biotinylated antibodies were washed and stained for 15 minutes on ice with either streptavidin-phyco-erythrin (PE), streptavidin-PETexasRed or streptavidin-Peridinin Chlorophyl Protein Complex Cyanin 5.5 (PerCpCy5.5) (BD) and then filtered using a BD 352235 strainer cap tube and resuspended in HF containing 2 µg/ml prodidium iodide (PI, Sigma-Aldrich) or 0.1 µg/ml 4',6-diamidino-2-phenylindole (DAPI, Sigma-Aldrich). Cells were analyzed using a FACSCalibur (BD) with CellQuest software (BD) and sorted in the Terry Fox Lab Flow Cytometry Core using a FACSAria (BD) or Influx Cell Sorter (Cytopeia, Seattle, WA, USA).

2.2.3 Hmga2 protein level measurements

Western blots were performed using an anti-mouse Hmga2 antibody #5269 (Cell Signaling, Danvers, MA, USA) at 1:1000 as per the manufacturer's protocol. For intracellular flow cytometry, cells were stained for extracellular antigens, washed and fixed overnight with the Foxp3/Transcription Factor Staining Buffer Set (eBioscience, San Diego, CA, USA) according to the manufacturer's instructions. The following day, cells were washed and stained with 1:100 rabbit anti-mouse Hmga2 antibody (Cell Signaling, Danvers, MA, USA) at room temperature for 30 minutes. After washing, cells were stained with 1:2000 Alexa Fluor 594 labeled goat anti-rabbit IgG #A-1102 (Invitrogen) and re-stained with 1:100 Streptavidin-

PerCpCy5.5 (for lineage markers) for 15 minutes at room temperature. Cells were analyzed on an LSR Fortessa (BD).

2.2.4 Single-cell HSC transplantation and analysis

To assess single cells for *in vivo* repopulating activity, cells were sorted directly into separate wells of a round-bottom 96-well plate containing 100 μl of SFM in each well. Plates were centrifuged briefly at 120 g to pellet cells. Each well was then visually inspected for the presence or absence of a single cell and the plate put on ice until the cells were harvested. This was performed by removing the entire volume of each well containing a single cell into a 1 ml U-100 insulin syringe (BD) pre-loaded with 200 μl of phosphate-buffered saline (PBS) and then taking the volume up and down several times. Cells were then injected into the tail vein of sub-lethally irradiated *W41* recipients as described in section 2.2.1. Unless otherwise stated, donor cells were from female mice and injected into either female or male recipients. Male mice were only injected into male recipients to avoid inactivation of HSC by natural antibodies against male-specific antigen(s). To assess donor-derived repopulation, ~100 μl of PB was obtained from the tail vein of recipients 16 weeks post-transplant and lysed with 2 ml of ammonium chloride lysis solution for 10 minutes on ice in the dark. Remaining white blood cells (WBCs) were then stained with anti-CD45.1-FITC and anit-CD45.2-APC in combination with either anti-Ly6g-PE and anti-Mac1-PE to detect GM, anti-B220- or CD19-PE to detect B-cells (B) or anti-CD5- or CD3ε-PE to detect T-cells (T). Stained cells were resuspended in 100 μl of HF containing 2 μg/ml PI. Recipients were considered to have received an HSC if the WBCs at 16-weeks post-transplant contained greater than 1% donor-type cells. Subtypes were defined at 16-weeks post-transplant by donor-derived GM:(B+T) ratios of ≥2, 2-0.5 and <0.5 for α, β and γ/δ, respectively. γ and δ subtypes were distinguished by >1% and <1% donor contribution to the

GM compartment, respectively (24). Frequencies of HSCs were calculated directly in single-cell experiments by the proportion of positive mice (α, β, γ or δ).

2.2.5 *In vitro* liquid cultures

Cells destined for liquid cultures were sorted directly into 100 μl of SFM in the wells of round-bottom 96-well plates, centrifuged, and the presence of cells in each well verified as for *in vivo* assays. Just prior to transfer to a 37°C 5% CO_2 incubator, 100 μl of 2x 300 ng/ml murine SF (STEMCELL Technologies) + 20 ng/mL human interleukin (IL)-11 (Genetics Institute, Cambridge, MA) or 50 ng/mL SF alone was added to each well. Cultured cells were visualized at the end of the culture period to confirm division and survival. Wells were harvested with 3 washes of 200 μl of ice-cold SFM.

2.2.6 RNA isolation, cDNA synthesis and quantitative reverse-transcription (qRT)-PCR

Cells destined for RNA isolation and cDNA synthesis were either directly sorted into a 1.5 mL microcentrifuge tube containing HF, or transferred to the tube from a 96-well plate post-culture. Cell suspensions were centrifuged at 5000 g for 5 minutes and supernatants removed. RNA was extracted using the Picopure RNA isolation kit (Arcturus, Mountain View, CA, USA), TRIzol Reagent (Invitrogen, Burlington, ON, Canada) or RNeasy Mini Spin Columns (QIAGEN), and cDNA was generated with the SuperScript III First-Strand Synthesis System for RT-PCR (Invitrogen). qRT-PCR analyses were performed with Power SYBR Green PCR Master Mix (Applied Biosystems, Foster City, CA). For a list of qRT-PCR primers used see Appendix B.3. Let-7 miRNA reverse transcription was performed using the TaqMan miRNA Reverse Transcription Kit (ABI) and miRNA-specific stem-loop RT primers. Let-7 transcript levels were determined relative to sno-RNA202 using Taqman probes specific for human let-7a-f and the TaqMan Fast Universal PCR Master Mix (ABI). Mean and SEM calculations were made using

log-transformed relative expression data ($1/^{2Ctx-CtGapdh}$) from 2 to 4 separate qRT-PCR analysis experiments.

2.2.7 Affymetrix gene array analysis

RNA was isolated from 2 biological replicates each of LSK cells from E14.5 FLs and adult (8-12 week-old) BM using RNeasy Mini Spin Columns (QIAGEN, Toronto, ON) and subjected to amplification with the Agilent RNA 6000 Nano Kit (Agilent, Mississauga, ON). Affymetrix (Santa Clara, CA, USA) Mouse Gene 1.0 ST Arrays were RMA normalized using the Bioconductor (170) package 'xps' in R (http://www.R-project.org/) including the metacore probesets grouped by exon. Gene annotation data was added using a combination of the NetAffx (Release 32) annotation files as well as the Bioconductor packages 'mogene10sttranscriptcluster.db' and 'Org.Mm.eg.db'. Probesets which did not map to an Entrez Gene identifier were discarded. Data Above Background (DAB) scores were calculated for each probe set and those probe sets with a DAB *P*-value of 0.05 or less in at least one chip were retained. In the case of multiple probe sets mapping to the same Entrez Gene identifier, the mean intensity value was used and differential expression between FL and adult BM LSK cells tested using the R package 'limma' with a false discovery rate correction for multiple testing.

2.2.8 Statistical analyses

Unless otherwise stated, all values represent the mean ± the s.e.m. and *P* values were derived using Student's *t*-tests in MS Excel.

2.3 Results

2.3.1 The ESLAM phenotype of both FL and adult BM contains HSCs at very high frequencies

To examine the potential of high EPCR expression in combination with the $CD150^{+}CD48^{-}$ (SLAM) subset (38), adult BM cells were co-stained with these markers in addition to CD45, a pan-HSC marker that simplifies gating of $EPCR^{+}$ cells (Figure 2.1). We found the $EPCR^{+}CD45^{mid}$ population of FL SLAM cells to be a rarer subset (~10% of the $CD150^{+}CD48^{-}$ subset; Figure 2.1) than the previously described $CD41^{-}$ fraction (~50% of the $CD150^{+}CD48^{-}$ subset) (72). This suggested that isolation of the $CD45^{+}EPCR^{+}CD48^{-}CD150^{+}$ (ESLAM) subset might provide a markedly greater enrichment of FL HSCs than is achieved with the SLAM markers alone. Furthermore, since EPCR (67, 162) and SLAM (38, 72) are stable markers of FL and adult BM HSCs, we hypothesized that this phenotype may enable isolation of HSCs at similarly high purities from different developmental sources.

To test this, hematopoietic tissues from different aged mice (E14.5, 3-week, 4-week and 10-12 week) were analyzed for their content of ESLAM cells (Figure 2.2A-D) and this population was then assayed for HSCs using a single-cell transplantation assay (Figure 2.2E). We found the ESLAM population to be a very rare population ($2.9x10^{-3}$ to $7.6x10^{-3}$ % of total cells) in all of the samples tested from different developmental time points. Moreover, the frequency of directly detectable HSCs was consistently high (24% - 44%). Furthermore, since the E14.5 FL and 3-week BM HSCs are known to be entirely cycling (69), the frequencies of HSCs within ESLAM cells isolated from these tissues likely represent underestimates by a factor of ~2-fold due to the homing deficit of HSCs in the S, G2 and M stages of the cell cycle (69).

2.3.2 HSC subtype prevalence is not altered as part of the HSC developmental switch

Since a developmental reprogramming of multiple HSC properties (discussed previously) is known to occur between 3 and 4 weeks of age, we analyzed mice transplanted with single ESLAM cells from different developmental sources to determine if the HSC subtype composition is also altered by this 3-4 week HSC developmental switch. From an analysis of ~400 transplant recipients, it was determined that all HSC subtypes (α, β, γ and δ) (24) are detectable in hematopoietic tissues of E14.5 FL, 3-week BM, 4-week BM and adult BM (Figure 2.3A). Interestingly, however, there was a dramatic (~5-fold) increase in the proportion of α-HSCs between E14.5 and 3 weeks of age, but with no significant changes between 3 and 4 weeks (Figure 2.3B). The relative proportions of the other HSC subtypes (β, γ and δ) were also unchanged between 3 and 4 weeks and continued to remain relatively constant into adulthood (Figure 2.3B). In conclusion, although significant differences in the subtype composition of the HSC compartment were found between fetal and adult life (i.e. an increase in the α-HSC content), these subtype changes do not appear to be controlled by the 3-4 week development switch since changes in subtype proportions greatly precede this time point.

2.3.3 Comparison of transcripts related to SF signaling

As a first strategy towards identifying genes that are differentially expressed between fetal and adult HSCs, we made use of the observation that fetal compared to adult HSCs are ~6-fold more sensitive to SF stimulation (3). We therefore hypothesized that one or several mediators of SF-induced mitogenesis (*Ccnd1*, *Ccnd2*, *Ccnd3*, *Cdkn2c*, *Cdkn1a* and *Cdkn1b*) or SF-stimulated self-renewal (*Jak2*, *Stat3*, *Stat5a*, *Sh2b3*, *Cdh2* and *Inpp5d*), may be differentially expressed between prospectively isolated populations of E14.5 FL and adult BM HSCs (171). Since this study was performed prior to validation of the ESLAM phenotype, FL and adult BM

HSCs were necessarily isolated using $Lin^{-}Sca1^{+}CD43^{+}Mac1^{+}$ (~1/5 HSCs) (70) and $Lin^{-}Rho^{-}CD45^{mid}SP$ (~1/3 HSCs) (24), respectively. Levels of transcripts for 3 of the 12 genes investigated (*Jak2*, *Stat3* and *Stat5a*) were found to be significantly ($P<0.05$) higher in adult BM compared to FL HSCs by quantitative reverse transcription-polymerase chain reaction (qRT-PCR) analysis (Figure 2.4A). Additionally, expression of *Cdkn2c* and *Inpp5d* were found to be ~10-fold higher in adult as compared to fetal HSCs; however, these latter differences did not reach statistical significance.

To test whether similar differences in expression of the same candidate genes were preserved when both types of HSCs were proliferating (hence not specific to their different cell-cycle states), an aliquot of purified E14.5 FL and adult BM HSCs were cultured for 48 hours under serum-free conditions previously shown to stimulate all of these cells to divide while optimizing their generation of daughter HSCs (70). Comparison of the expression of the same genes in extracts of these 48 hour cultures showed that transcripts for only one of the 3 genes (*Stat3)* that were present at a higher level in freshly isolated adult BM HSCs, remained significantly ($P<0.05$) higher in proliferating adult as compared to fetal HSCs (Figure 2.4B). However, transcripts for 2 others (*Cdkn1a* and *Cdkn2c*) became significantly higher after culturing. In addition, *Jak2, Stat5a* and *Inpp5d* transcripts, previously found to be present at higher levels in freshly isolated adult as compared to fetal HSCs, lost their differential expression pattern after culturing. One possible explanation for this finding was that the differential expression of these genes was a consequence of the different cell-cycle states of the freshly isolated cells fetal and adult HSCs. Of the 12 genes studied, only 2 (*Stat3* and *Cdkn2c*) met the criteria of being differentially expressed between fetal and adult HSCs before and after *in vitro* stimulation.

2.3.4 Comparison of transcripts identified by Long-SAGE and Affymetrix profiling

To search more broadly for differentially expressed genes in FL and adult BM HSCs, we compared Long-SAGE libraries prepared from $Lin^-Sca1^+CD43^+Mac1^+$ E14.5 FL and $Lin^-Rho^-CD45^{mid}SP$ adult BM cells (4) using Discovery Space SAGE software with a 99.9% cut-off (172). This analysis identified 52 genes expressed at higher levels in FL cells and 442 expressed at higher levels in adult BM cells. A parallel comparison of the gene expression profiles obtained from Affymetrix microarray analysis of similarly enriched populations of E14.5 FL and adult BM HSC (71) using the GEO analysis tool (http://www.ncbi.nlm.nih.gov/geo) and a one-tailed *t*-test at 0.1 significance stringency, identified 2061 genes that were more highly expressed in FL HSCs and 2342 more highly expressed in adult BM HSCs. Further comparison of these results with a similarly acquired dataset for HSCs isolated from adult BM 5 days after being injected with 150 mg/kg of 5-fluorouracil (5-FU), which stimulates ~50% of phenotypically defined HSCs to be in S/G2/M (173), identified 1824 genes that were more highly expressed in FL HSCs and 1960 that were more highly expressed in the post-5-FU BM HSCs. Finally, when all lists were compared (SAGE, GEO FL vs BM and GEO FL vs post-5-FU BM), 5 genes (*Hmga2, Lyl1, G3bp1, Eif1a* and *Tubb5*) were found to be consistently more highly expressed in the FL HSCs. A similar comparison of those consistently higher in adult BM HSCs revealed another 8 (*Psap, Pld3, Vwf, Prnp, Rhob, Mlx, Car3 and Plp1*).

Based on these comparisons, transcript levels for these latter 13 genes, plus another 6 of the genes whose expression was most upregulated in adult BM HSCs compared to progenitors (Lin^- cells) cells in the Long-SAGE library analysis (*Chd4*, *Smarcc2*, *Hdac3*, *Smarcc1*, *Trim27* and *Cul4a*), were then re-examined by qRT-PCR analyses of E14.5 FL and adult BM ESLAM cells. Expression of 4 of the 5 genes predicted to be expressed at a higher level in fetal as

compared to adult HSCs were confirmed, but for only one of these (*Hmga2*) was the increase significant ($P<0.05$, Figure 2.5A). Transcript levels for another 5 of the 8 predicted upregulated genes in fetal HSCs were also higher than in adult BM HSCs, but none of these 5 reached significance. For candidates predicted to be upregulated in adult BM HSCs as compared to progenitors, only *Smarcc1* showed a significant differential expression pattern by qRT-PCR ($P<0.05$). Interestingly, many of these predicted candidate genes were significantly differentially expressed by qRT-PCR when Lin^- subsets were compared (Figure 2.5B). Overall, only 2 of 19 predicted candidates (*Smarcc1* and *Hmga2*) were found to be differentially expressed in FL and adult BM HSCs isolated using the same (ESLAM) protocol.

As a final survey, we performed an Affymetrix comparison of LSK cells from FL and adult BM sources (Figure 2.6A-B) as a means to identify further candidate regulators of developmental differences in HSC self-renewal. From this comparison, we identified *Lin28b* as the protein-coding gene with the greatest differential (higher) expression in FL as compared to adult BM cells (Figure 2.6A and Appendix A.1). This difference was confirmed by qRT-PCR analysis of FL and adult BM LSK cells (Figure 2.6C) and was found to apply also to more highly purified ESLAM populations.

2.3.5 Let-7 miRNA and let-7 target profiling of fetal and adult hematopoietic stem and progenitor cells

Since Lin28b is a known inhibitor of let-7 miRNA biogenesis (174-176), it was of interest to determine whether let-7 miRNAs are also differentially expressed in highly purified FL and adult BM HSCs. We found that 2 of the 6 let-7 miRNAs profiled are present at lower levels in FL LSKs and 3 are decreased in FL HSCs as compared to their adult BM counterparts (Figure 2.6D). We also identified let-7 binding sites in 6 of the other most highly upregulated

transcripts in FL LSK cells (*Lin28b*, *Igf2bp2*, *Igf2bp3*, *Igf2bp1, Slc31a1* and *Hmga2*; purple bars, Figure 2.6A). Except for *Slc31a1,* these differentially expressed let-7 target genes were confirmed by qRT-PCR analysis of FL and adult BM LSK cells (Figure 2.6C). However, only *Lin28b*, *Hmga2* and *Igf2bp3* were differently expressed in purified FL and adult BM HSCs (Figure 2.6C). Consistent with a higher activity of let-7 miRNAs in adult as compared to fetal HSCs, we also found that only one of the 25 most highly upregulated genes in adult BM LSKs (*Gdpd1*) was a predicted let-7 target (Figure 2.6B).

2.3.6 Hmga2 is downregulated between fetal and adult HSCs independent of their cell-cycle status

Since *Hmga2* was identified as being expressed higher in fetal than adult HSCs by both our Long-SAGE and Affymetrix profiling approaches, we were interested in interrogating this difference further. Firstly, we investigated the influence of the cycling status of HSCs on the expression of this gene. This was done by performing qRT-PCR analyses on 48-hour cultures of E14.5 FL and adult ESLAM cells (70). Although this resulted in a decrease in the *Hmga2* transcript levels in the cultured FL cells resulting in a reduced difference when compared to the cultured adult BM cells, this difference remained significant ($P<0.01$, Figure 2.7A). In contrast, the original difference in *Smarcc1* expression between freshly isolated fetal and adult ESLAM cells was lost in the cycling cells (Figure 2.7A). Thus, *Hmga2*, but not *Smarcc1*, expression appears to be a stable (i.e. cell-cycle independent) distinguishing feature of fetal and adult HSCs. In addition, Hmga2 protein levels were dramatically different between fetal and adult lin^- cells (Figure 2.7B and $lin^-Sca1^+c\text{-}Kit^+$ (LSK) cells (Figure 2.7C); with no difference between fetal and adult Lin^+ cells (Figure 2.7C).

We also asked whether the timing of change in *Hmga2* expression between FL and adult BM HSCs would occur coincident with the other developmental changes that take place in HSCs between 3 and 4 weeks after birth. However, a qRT-PCR comparison of *Hmga2* transcript levels in Lin^- cells isolated from E14.5 FL, 3-week BM, 4-week BM and adult BM indicated that *Hmga2* levels decrease gradually between fetal and adult life, with little change between 3 and 4 weeks (Figure 2.7D).

2.4 Discussion

In this study we describe a series of experiments designed to identify transcript differences that might be relevant to the different self-renewal activities that fetal and adult HSCs display in transplanted mice. Until very recently (44), developmental comparisons of HSCs (70, 71, 166, 169) have necessarily utilized distinct strategies to isolate HSC-enriched populations from fetal and adult hematopoietic tissues. This fact, coupled with the relatively low HSC content of such populations (10-50%), has made it difficult to distinguish biologically relevant differences from those related to technical factors. Accordingly, as a first step, we developed and functionally validated a protocol that enables fetal and adult HSCs to be isolated at similar, very high purities (~40%-50%) using the same phenotypic markers.

From the surveys and analyses performed, we found that some candidate differentially expressed genes (e.g. *Jak2, Stat5a,* and *Smarcc1*) do indeed lose this differential when quiescent adult BM HSCs are cycling under similar conditions as the FL HSCs to which they are being compared. Importantly, however, this is not a common feature of all differentially expressed candidates, as shown here for *Stat3* and *Hmga2*.

We also show that the specific phenotype of the HSC-enriched populations being compared may indeed influence the HSC specificity of the differences detected. This was

exemplified by the finding that only 2 of the 19 candidate genes (*Hmga2* and *Smarcc1*) identified from a comparison of Long-SAGE libraries of $Lin^-Sca1^+CD43^+Mac1^+$ FL cells and $Lin^-SPRho^-CD45^{mid}$ adult BM cells, were confirmed by qRT-PCR analysis of FL and adult BM ESLAM cells. Notably, since a qRT-PCR confirmation was not performed using the original phenotypes (i.e. $Lin^-Sca1^+CD43^+Mac1^+$ for FL cells and $Lin^-SPRho^-CD45^{mid}$ for ABM cells), another explanation for the low proportion of confirmed candidates could be inaccuracies in the SAGE analysis. It is interesting to note that the differential expression of genes eventually found to be most relevant to the developmentally-determined biological changes in HSCs (see Chapter 3), proved not to be HSC-specific and persisted in LSK cells (~10-fold lower HSC content). Thus, while it was important to have confirmed expression of candidates in highly purified HSC populations, a search for differences exclusive to these cells was not warranted.

Of the several genes found likely to be differentially expressed in fetal and adult HSCs, *Hmga2* was the only one identified using multiple strategies. The differential expression of *Hmga2* was also found to not be sensitive to the cycling status of the cells being compared. High mobility group AT-hook 2 (*Hmga2*), also known as *Hmgic,* is one of a family of 4 (*Hmga1a*, *Hmga1b*, *Hmga1c* and *Hmga2*) non-histone chromatin proteins in mice that bind the minor groove of AT-rich DNA sequences via AT-hooks and influence gene expression directly or by recruitment of transcriptional regulators (177). *Hmga2* is widely expressed during embryogenesis but is absent from nearly all adult tissues, except for a low level of expression in human $CD34^+$ HSCs (178), proliferating preadipocytic mouse cells (179), and secondary spermatocytes and spermatids (180, 181). Furthermore, $Hmga2^{-/-}$ mice have a pygmy phenotype with adult heterozygous and homozygous mutant mice manifesting a 20% and 60% reduced size, respectively (182). More recently, it was reported that neural stem cells from $Hmga2^{-/-}$ fetal mice

show decreased self-renewal and/or proliferation *in vitro* (183). Thus, evidence is accruing to suggest that *Hmga2* could play a role in regulating stem cells more generally.

Several studies have also provided mechanistic clues supporting this thesis. This includes the finding that chromosomal rearrangements resulting in overexpression of *Hmga2* can be found in a wide variety of benign and metastatic tumours of multiple tissues (184). For example, in 6 patients with various myeloid malignancies, the *HMGA2* gene was found to be involved in translocations that ultimately lead to its overexpression (185). Although relevant disruption or activation of other genes may have occurred, the most likely explanation for the dysregulation of *HMGA2* expression is the loss of the 3'-UTR in these translocations. The *Hmga2* 3'-UTR contains multiple let-7 miRNA target sites that when mutated block this let-7-*Hmga2* pairing and thus permit higher transcript and protein levels of HMGA2 (186, 187). Additionally, let-7 overexpression and knockdown have been shown to reduce and enhance tumorigenicity, respectively (186, 187).

In *C. elegans*, let-7 is a heterochronic gene that is upregulated during the later stages of larval development and is required at the larval to adult transition to trigger hypodermal blast cells (seam cells) to cease dividing and exit the cell cycle (146). Misexpression of let-7 is also sufficient to specify early adult fates (188). Our finding that let-7 miRNAs are expressed in an inverse pattern to *Hmga2* during development in HSCs suggested that an analogous, highly-conserved developmental timer might also be active in mouse HSCs to regulate their self-renewal activity. Since we found *Lin28b*, a negative regulator of let-7 biogenesis, to also be differentially expressed in FL and adult BM HSCs (ESLAM cells), we speculated that this gene might serve as the upstream master determinant of fetal versus adult HSC identity.

The availability of a new method to obtain HSCs at high purities, independent of their cycling status, enabled several additional important studies of HSCs during fetal and neonatal development, a time during which a "switch" in their cycling behavior and self-renewal properties occurs. These included the demonstration that *Hmga2* expression changes within HSCs between E14.5 and adulthood. In addition, we found from analyses of mice transplanted with single ESLAM cells isolated from 3- or 4-week-old BM, that these contained a similar (adult-like) distribution of HSCs according to their differentiation programs. ESLAM cells from all sources contained detectable α, β, γ and δ HSCs; however, a shift occurs from very few α-HSCs and prominent β-HSCs in E14.5 FL, to prominent α-HSCs and fewer β-HSCs in adult BM (2). Surprisingly, an adult-like subtype distribution was already attained in 3-week BM, suggesting that the factors regulating the selective expansion of α-HSCs during development does not appear to be linked closely with the 3-4 week switch in other HSC properties. Additional data showing that the E18.5 fetal BM already contains a higher proportion of α-HSCs than age-matched FL (2), suggests that this phenomenon is likely regulated by extrinsic factors (i.e. the BM niche).(177)

In summary, these studies provide a powerful new method to validate gene expression differences in phenotypically identical (ESLAM) subsets of cells from different in *vivo* sources that are ~40%-50% pure HSCs. By coupling this approach to multiple gene expression comparisons, we identified the Lin28-let7-Hmga2 pathway as a potential upstream regulator of the unique self-renewal properties of FL HSCs.

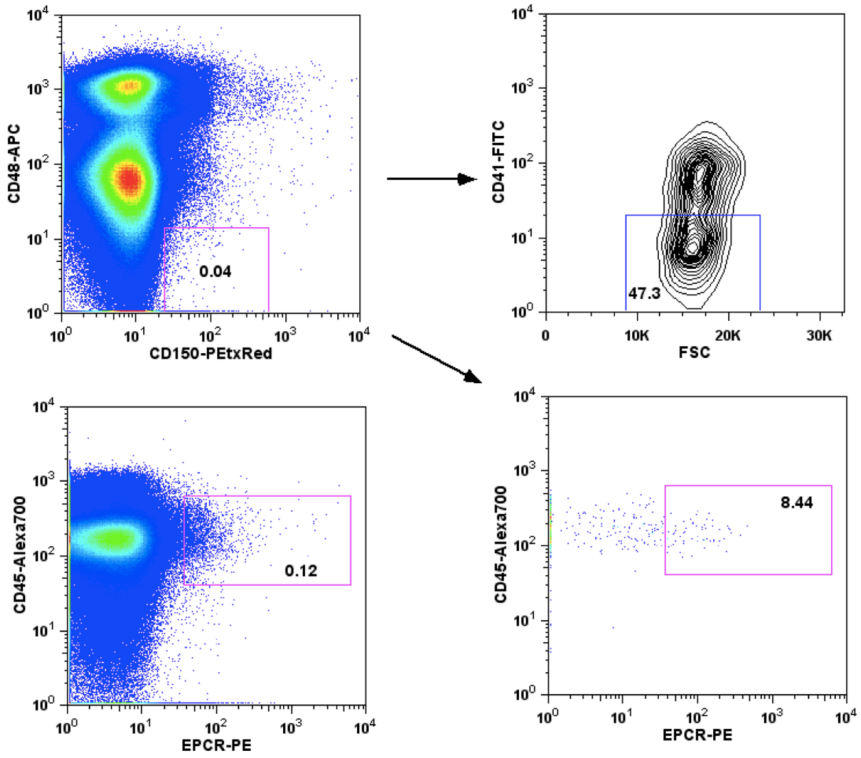

Figure 2.1 Subfractionation of the adult BM SLAM subset using EPCR and CD41
The proportion of viable $CD150^{+}CD48^{-}$ (SLAM) cells that are $EPCR^{+}CD45^{mid}$ and $CD41^{-}$ is shown. The $EPCR^{+}CD45^{mid}$ gate was drawn on the upper ~0.1% of $EPCR^{+}$ viable cells.

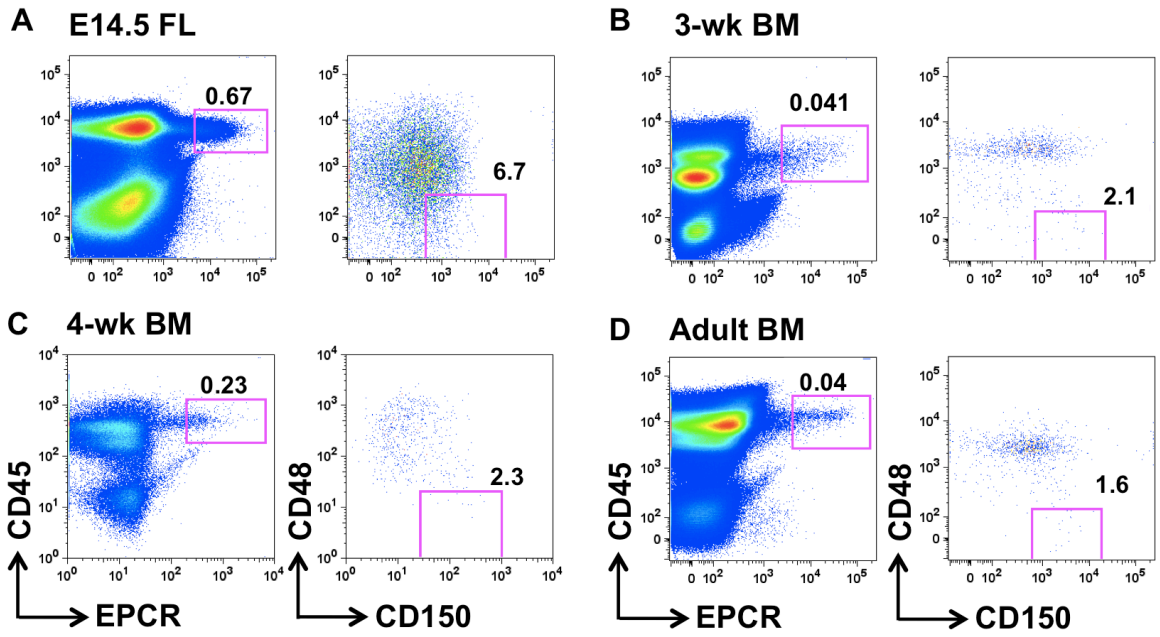

E

	E14.5 FL	3-wk BM	4-wk BM	Adult BM
% ESLAM ($x10^{-3}$)	7.6	3	2.9	3.5
% HSCs in ESLAM	24	31	36	44
Total transplants	141	72	53	133

Figure 2.2 HSC isolation by the ESLAM strategy yields high purities
(A-D) FACS profiles of $EPCR^+CD45^+CD150^+CD48^-$ (ESLAM) cells. FL=fetal liver, adult BM = 8-12 week-old. **(E)** Frequency of cells with the ESLAM phenotype in each tissue examined and the HSC purity of each ESLAM population determined from the frequency of single transplanted ESLAM cells that produced >1% of the circulating WBCs present at 16 weeks post-transplant.

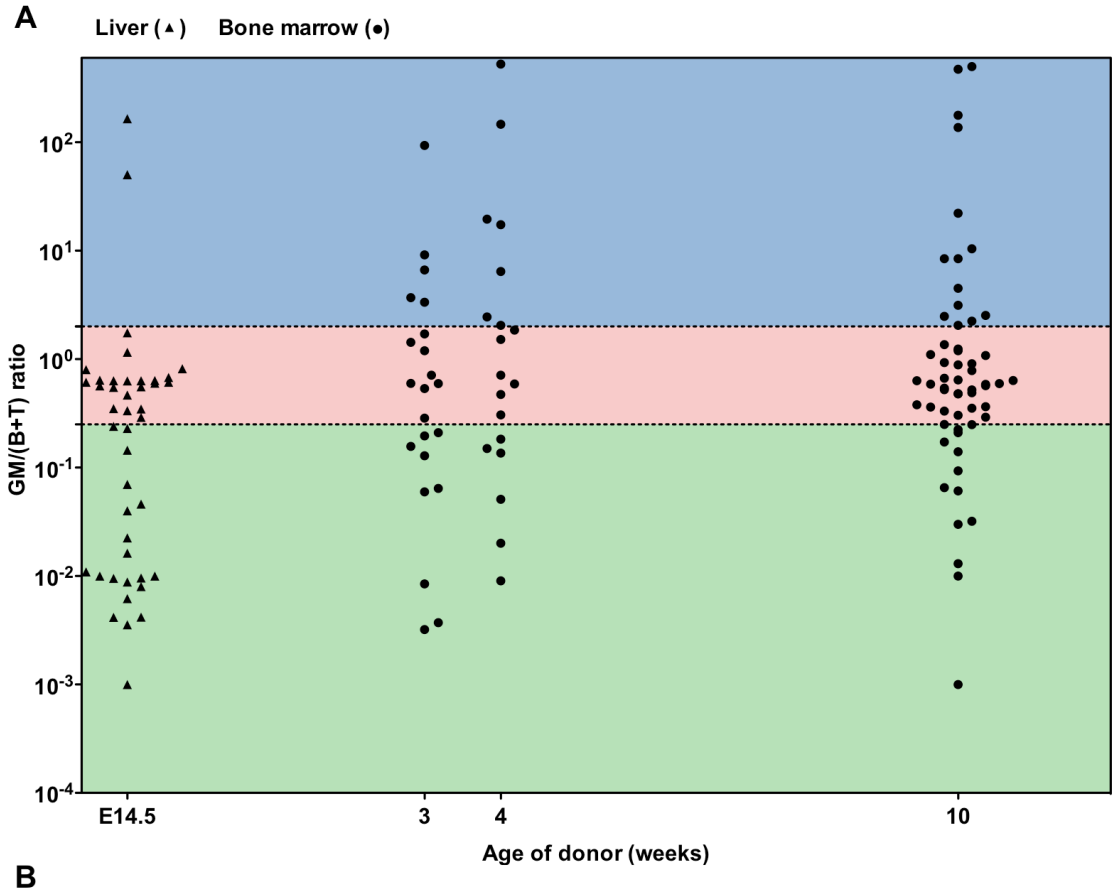

B

	E14.5 FL	3-wk BM	4-wk BM	Adult BM
% α-HSCs of α+β+γ/δ	5	23	36	27
% β-HSCs of α+β+γ/δ	49	36	32	51
% γ/δ-HSCs of α+β+γ/δ	46	41	32	22
% α-HSCs of α+β	9	39	54	35
% β-HSCs of α+β	91	61	46	65

Figure 2.3 ESLAM-isolated HSCs show subtype-specific differences in their prevalence across development

(A) Distributions of GM/(B+T) values for all HSCs detected in hematopoietic tissues of mice analyzed at different times throughout their development. GM/(B+T) values were calculated as described in the methods and are plotted as a function of the age of the donor from which the original ESLAM HSC transplanted was obtained. The solid and dotted horizontal lines indicate GM/(B+T) values of 2 and 0.25 that distinguish clones derived from α- (>2; blue), β- (0.25-2; pink) or γ/δ- (<0.25; green) HSCs as defined by Dykstra et al. (24). **(B)** Prevalence and purities of HSC subtypes in the ESLAM population present in hematopoietic tissues at different times in development of the mouse as determined from analyses of recipients of single ESLAM cell transplants.

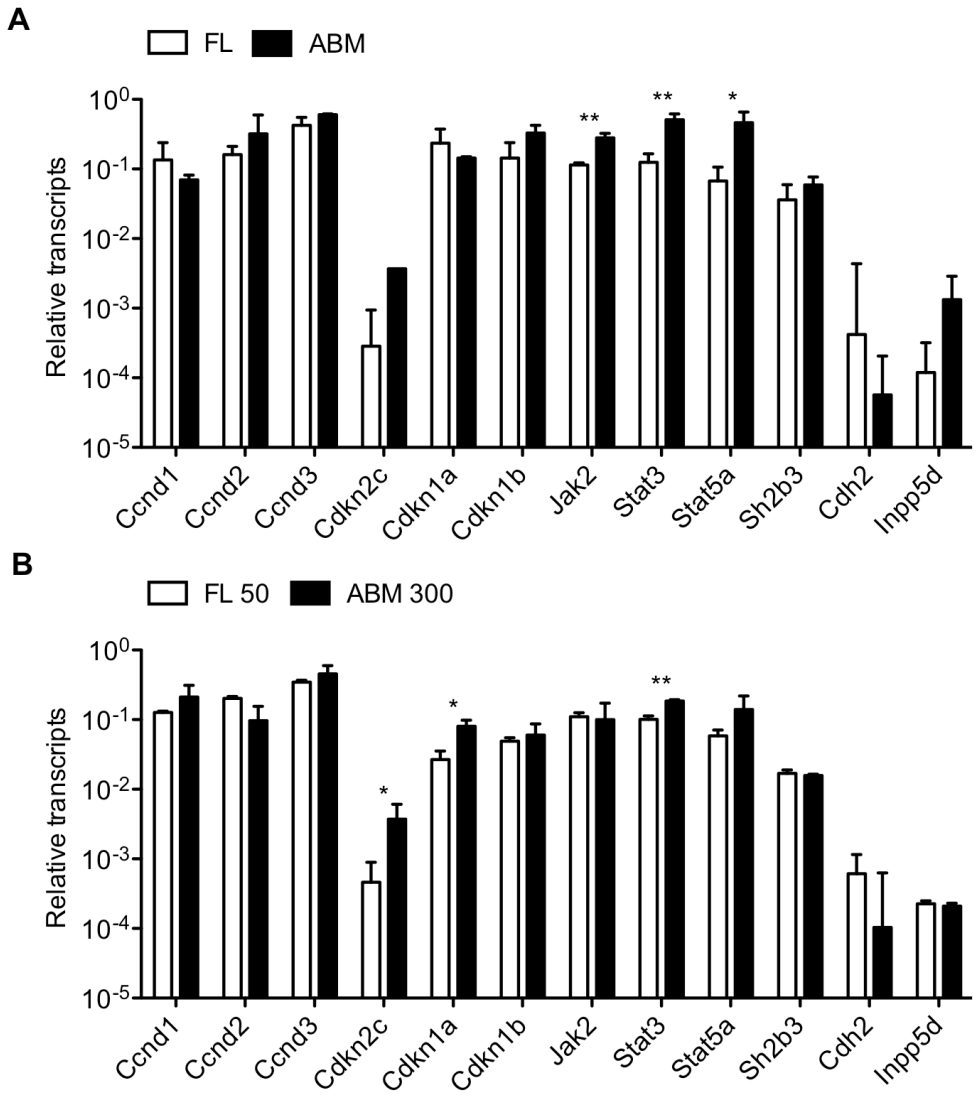

Figure 2.4 Gene expression comparison of SF signaling intermediates in FL and adult BM HSCs before and after *in vitro* stimulation

(A) Transcript levels for each gene were determined by qRT-PCR relative to *Gapdh*. Highly purified suspensions of HSCs from E14.5 FL (white bars) and adult (8-12-week-old) BM (ABM; black bars) were isolated by FACS sorting the $Lin^-Sca1^+CD43^+Mac1^+$ and $Lin^-Rho^-SPCD45^{mid}$ subsets, respectively. **(B)** Transcript levels in FL (white bars) and ABM (black bars) cultured for 48 hours under serum-free conditions with growth factors that optimize HSC maintenance (50 ng/ml SF for FL cells or 300 ng/mL SF plus 20 ng/ml IL-11 for ABM cells). Results are the mean ± s.e.m. of data from 2 to 3 experiments, in each of which qRT-PCR measurements were performed in triplicate. Significant differences between FL and ABM values ($P<0.05$) were determined by a Student's *t*-test and are indicated by an asterisk.

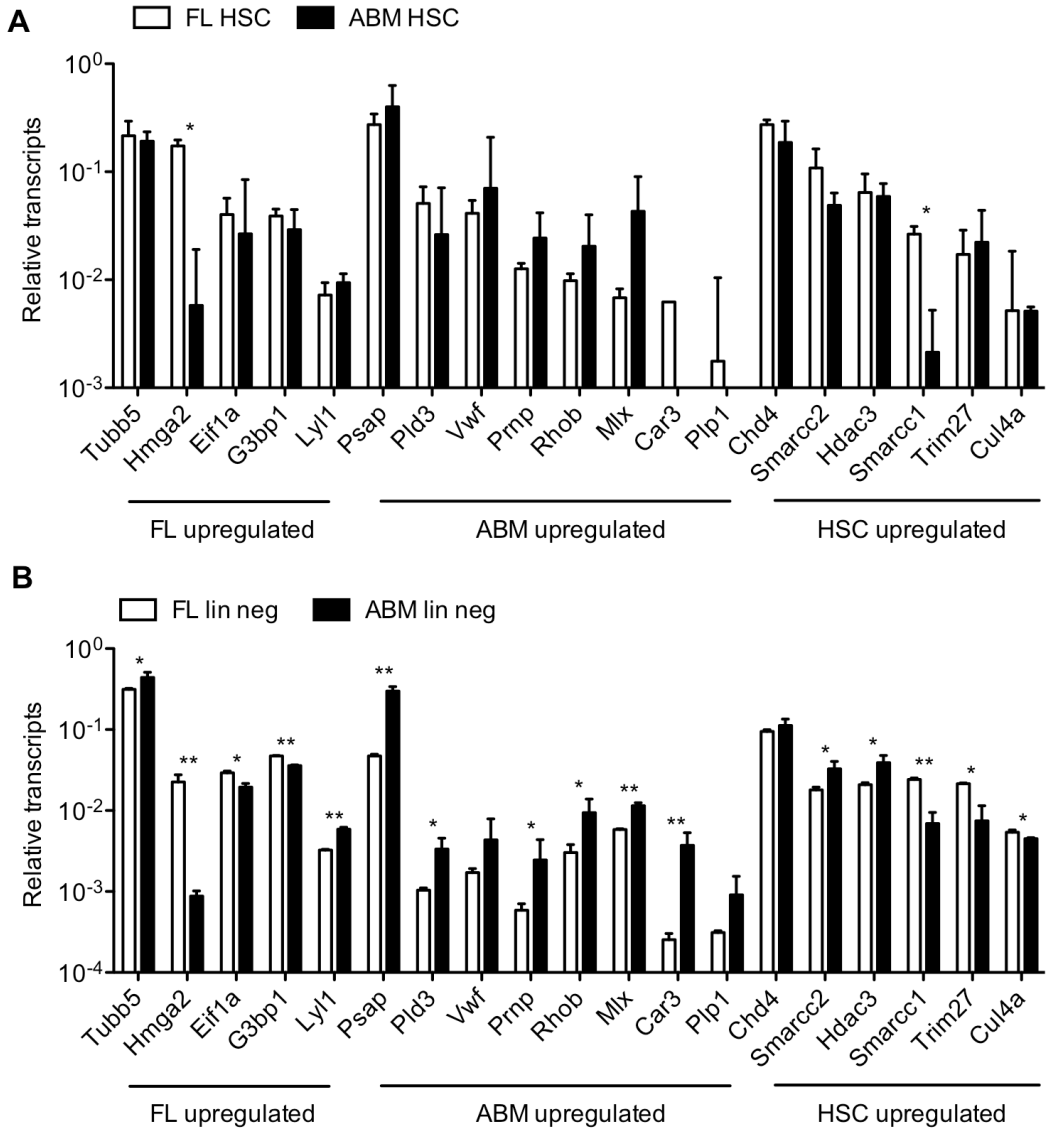

Figure 2.5 Gene expression comparison of SAGE-identified candidate genes between fetal and adult hematopoietic stem and progenitor cells

(A) Transcript levels for each gene were determined by qRT-PCR relative to *Gapdh* for highly purified suspensions of HSCs from E14.5 FL (white bars) and adult BM (black bars) by FACS isolation of the $EPCR^{+}CD150^{+}CD48^{-}CD45^{mid}$ (ESLAM) subset. **(B)** Transcript levels relative to *Gapdh* for hematopoietic progenitor-enriched populations isolated by FACS isolation of the lineage negative (lin neg) subset of E14.5 FL (white) and ABM (black). Results are the mean ± s.e.m. of data from 2 to 3 experiments, in each of which qRT-PCR measurements were performed in duplicate. Significant differences between FL HSC and ABM HSC values ($P<0.05$) were determined by a Student's *t*-test and are indicated by an asterisk.

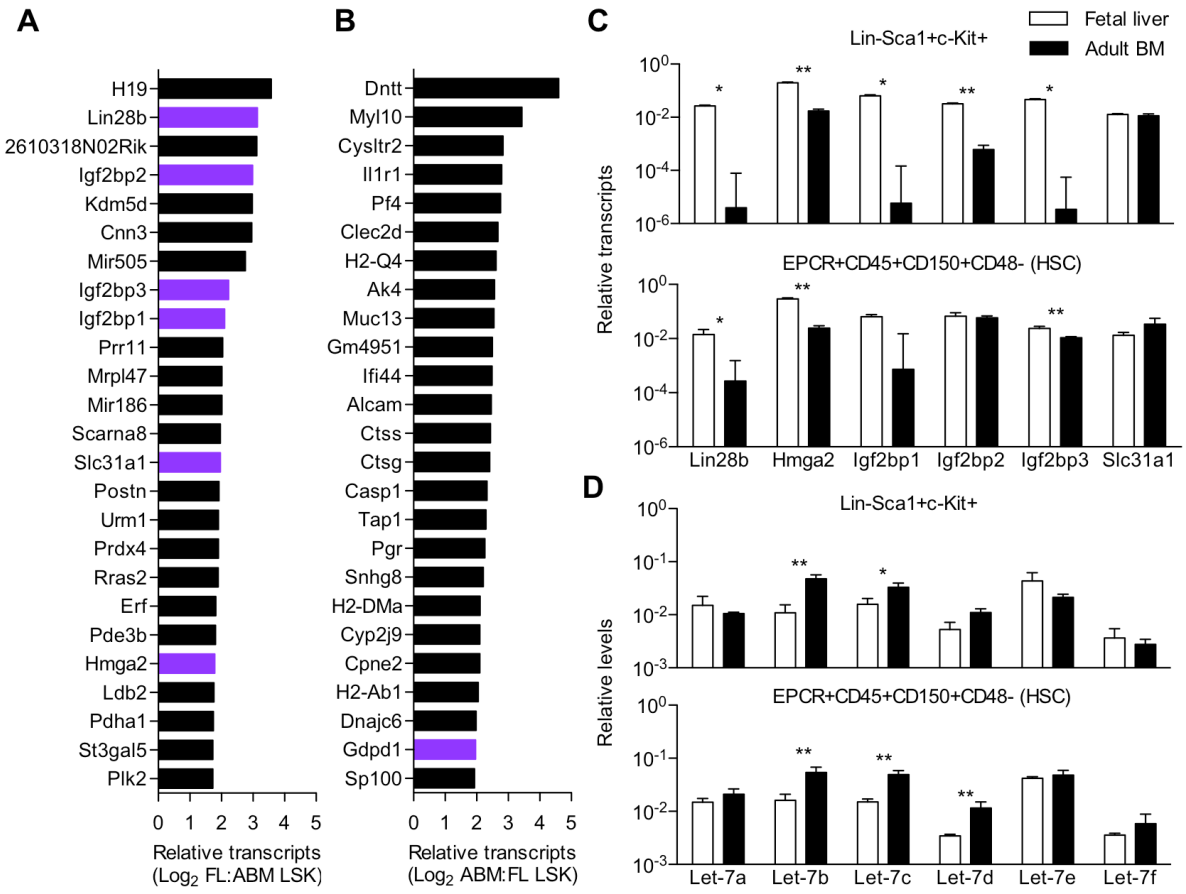

Figure 2.6 Lin28b, let-7 targets and let-7 microRNAs are differentially expressed between fetal and adult HSCs

(A) Transcript levels of genes expressed highest in E14.5 FL relative to ABM, and vice versa for **(B)**, in Lin$^-$Sca1$^+$c-Kit$^+$ (LSK) cells as determined by Affymetrix analysis (Appendix A.1). Purple bars indicate predicted let-7 target genes by TargetScan (www.targetscan.org/mmu_50). **(C)** qRT-PCR analysis of transcripts in LSK cells and HSCs (n=3). **(D)** qRT-PCR analysis of let-7 levels in LSK cells and HSCs (n=3-4). All data represent the mean ± s.e.m. relative to *Gapdh* and sno-RNA202 for mRNA and let-7 quantification, respectively. One-tailed Student's *t*-tests were used to assess statistical significance. **P*<0.05, ***P*<0.01.

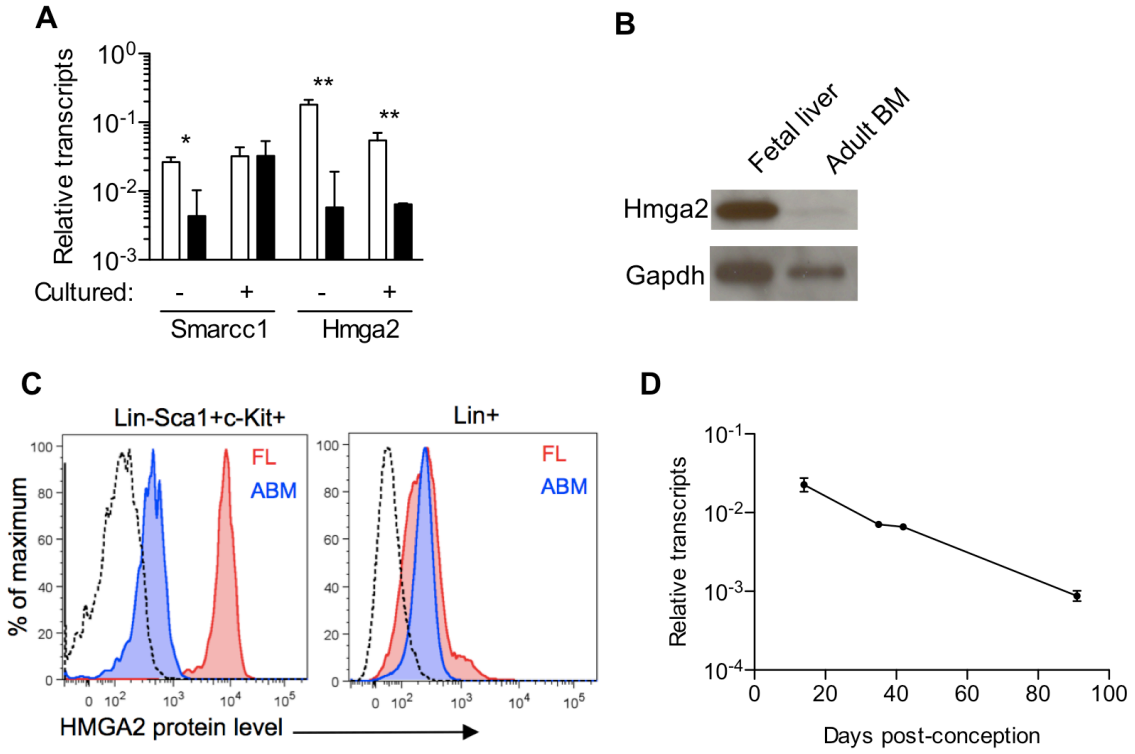

Figure 2.7 Hmga2 is stably expressed at higher levels in fetal compared to adult hematopoietic stem and progenitor cells

(A) Transcript levels relative to *Gapdh* of FL (white bars) and ABM (black bars) ESLAM cells before (-) and after (+) 48 hours of culture under serum-free conditions with growth factors that optimize HSC maintenance (50 ng/ml SF for FL cells or 300 ng/mL SF plus 20 ng/ml IL-11 for ABM cells). **(B)** Western blot of ~20,000 Lin$^-$ cells per lane. **(C)** Representative fluorescence activated cell sorting (FACS) plot for Hmga2 intracellular staining in FL and adult BM subsets. Dotted line represents the unstained control. **(D)** *Hmga2* transcript levels relative to *Gapdh* in Lin$^-$ cells isolated from different developmental time points. All data represent the mean ± s.e.m. One-tailed Student's t-tests were used to assess statistical significance. $*P < 0.05$, $**P < 0.01$.

Chapter 3 The Lin28b-let-7-Hmga2 axis determines the higher self-renewal potential of fetal hematopoietic stem cells

3.1 Introduction

The physiologic demands of fetal-stage somatic stem cells are distinct from those of their adult counterparts. For many tissues, the stem cells present in the fetus must not only generate high numbers of differentiated cell types, but also rapidly expand their numbers in order to establish a pool sufficient to meet the needs of lifelong tissue maintenance. In the blood-forming system of the mouse, the HSC pool expands from a few cells to thousands in less than 2 weeks (2, 11, 164). Previous studies have identified factors expressed on fetal liver stromal cells (i.e. insulin-like growth factor 2 (189) and angiopoietin-like factors (190)) that may provide different extrinsic signals to facilitate the execution of such fetal stage-specific demands. In addition, studies comparing transplanted fetal versus adult HSCs have provided evidence for intrinsically endowed differences in their expansion activities in irradiated hosts (120, 122, 191, 192). These differences seem to be regulated at the level of HSC self-renewal since transplanted fetal HSCs produce daughter HSCs more rapidly than their adult counterparts, and the in vitro survival and cell-cycle transit time of these populations are similar (70). Fetal HSCs also generate higher numbers overall following their transplantation (123). Interestingly, this high self-renewal fetal HSC behaviour is associated with a selectively elevated output of myeloid cells at 16-weeks post-transplant and an increased proliferative activity. All 3 of these distinctive properties (i.e. increased self-renewal, elevated output of myeloid cells and increased cycling) change coordinately between 3 and 4 weeks after birth in mice (69, 70). These observations, led us to propose that one or several intrinsic master regulators of the HSC developmental state are altered

between fetal and adult life to facilitate the determination of, and transition between, these fetal and adult HSC states.

In Chapter 2, we identified developmental differences in the components of the Lin28b-let-7-Hmga2 axis as being highly differentially expressed between fetal and adult HSCs. We therefore hypothesized that Lin28b might acts as a master determinant of fetal HSC identity through its ability to inhibit the biogenesis of let-7 miRNAs (174, 193) and thus permit the expression of let-7 targets (194).

3.2 Materials and methods

3.2.1 Mice

All experiments used B6 or B6.Cg-*Hmga2*$^{pg\text{-}Tg40BCha}$ (*Hmga2*$^{-/-}$; KO) mice obtained from the Jackson Laboratory (Bar Harbor, ME, USA) (195) as donors, and Ly5-congenic sublethally irradiated W41 mice as recipients. Transplantations were performed as described in Chapter 2 in accordance with approved institutional protocols (ACC #A10-0173 and #A11-0080). *Hmga2*$^{-/-}$ mice were genotyped by PCR using a protocol adapted from the Jackson Laboratory for strain 002644. Briefly, DNA was extracted from E14.5 tail or adult ear tissue using the prepGEM^{TM} DNA extraction kit (Zygem, Hamilton, NZ). Oligonucelotides used were 5'-ATTCTGGAGACGCAGGAAGA-3'(sense primer for detection of gene-targeted allele), 5'-TGCTCCTGGGAGTAGATTGG-3'(antisense primer for detection of gene-targeted allele), 5'-CCCACTGCTCTGTTCCTTGC-3'(sense primer for detection of wild-type allele), 5'-GTGTCCCTTGAAATGTTAGGCG-3'(antisense primer for detection of wild-type allele), 5'-CAAATGTTGCTTGTCTGGTG-3'(sense internal positive control primer), 5'-GTCAGTCGAGTGCACAGTTT-3'(antisense internal positive control primer). The PCR cycle

was 94°C for 3 minutes, followed by 35 cycles of 94°C for 30 seconds, 60°C for 1 minute and 72°C for 1 minute, followed by a final cycle of 72°C for 2 minutes. E14.5 FL and adult BM cells were prepared, isolated and stained as described in Chapter 2. All antibody incubation steps were performed on ice for 30 minutes for primary antibodies and 15 minutes for secondary antibodies. Analyses and sorting of cell populations were performed with the phenotypes listed in Appendix B.1 and antibodies listed in Appendix B.2. The lineage cocktail used contained anti-CD4, anti-CD8, anti-CD3ε, anti-CD5, anti-Ter119, anti-Gr1 and anti-B220. Sorting was performed in the Terry Fox Lab Flow Cytometry Core using a FACSAria (BD, Franklin Lakes, NJ, USA) or Influx Cell Sorter (Cytopeia, Seattle, WA, USA).

3.2.2 Affymetrix gene array analyses

For the comparison of gene expression between LSK cells isolated from control, Hmga2-transuced or Lin28-transduced mice, donor-derived transduced (YFP^+) LSK cells were isolated by FACS from secondary recipient mice 8-10 months post-transplant. Since control mice did not contain sufficiently high numbers of YFP^+ donor-derived LSK cells, the YFP^- donor-derived LSK cells were isolated from these mice. RNA was isolated from 2 biological replicates from each group using RNeasy Mini Spin Columns (QIAGEN, Toronto, ON, Canada) and subjected to amplification with the Agilent RNA 6000 Nano Kit (Agilent, Mississauga, ON, Canada). Affymetrix (Santa Clara, CA, USA) Mouse Gene 1.0 ST Arrays were RMA normalized using the Bioconductor50 package 'xps' in R (http://www.R-project.org/) including the metacore probesets grouped by exon. Gene annotation data was added using a combination of the NetAffx (Release 32) annotation files as well as the Bioconductor packages 'mogene10sttranscriptcluster.db' and 'Org.Mm.eg.db'. Probesets which did not map to an Entrez Gene identifier were discarded. DAB scores were calculated for each probe set and those probe

sets with a DAB *P*-value of 0.05 or less in at least one chip were retained. In the case of multiple probe sets mapping to the same Entrez Gene identifier, the mean intensity value was used and differential expression between FL and adult BM LSK cells tested using the R package 'limma' with a false discovery rate correction for multiple testing.

For the comparison of gene expression between *Hmga2* KO and *Hmga2*$^{+/+}$ (WT) E14.5 FL LSK cells, RNA was isolated from 3 biological replicates each of LSK cells from *Hmga2*$^{+/+}$ or *Hmga2*$^{-/-}$ FLs using RNeasy Mini Spin Columns (QIAGEN, Toronto, ON, Canada) and subjected to amplification with the Agilent RNA 6000 Nano Kit (Agilent, Mississauga, ON, Canada). Data processing was then performed as above. However, in cases where multiple probe sets mapped to the same Entrez Gene identifier, only the probe set with the highest maximum absolute deviation was retained. This allows minimization of multiple testing while still retaining probes with the greatest signal and thus maximizing the power to detect differences. Differential expression was then tested between *Hmga2* WT or KO cells as described above.

3.2.3 qRT-PCR

See Chapter 2 for details. Unless otherwise stated, unamplified targets were assigned a value corresponding to the background (as determined by no template control) or limit of detection (calculated by the number of pcr cycles performed). qRT-PCR primers are listed in Appendix B.3.

3.2.4 Apoptosis and proliferation of HSCs

BM cells were enriched for Sca1^{+} cells using the EasySep Mouse Sca1 positive selection kit (STEMCELL Technologies) and stained for extracellular antigens. After washing, cells were stained for 30 minutes on ice with eFluor780 fixable viability dye (eBioscience) at 1:10000, followed by Annexin V-PerCp-eFluor710 (eBioscience) according to the manufacturer's

instructions. Pelleted cells were then fixed (for 1 hour at 4°C) and permeabilized using the Foxp3/Transcription Factor Staining Buffer Set (eBioscience). Finally, permeabilized cells were stained with 1:50 BD Ki-67 -V450 (clone B56) for 30 minutes at room temperature. Stained cells were then analyzed on a BD LSR Fortessa (BD).

3.2.5 Lentivirus production and transfection

The pCCL.PPT.MND.PGK.YFP lentiviral vector was adapted from a vector (196, 197) obtained from D. Kohn (UCLA, Los Angeles, CA, USA). All cloning was performed using a single site immediately downstream of the MNDU3 promoter and an insert derived from PCR amplification with restriction site-containing primers. To clone murine *Hmga2* (GenBank BC052158.1), an amplicon was generated by PCR with the following primers: 5'-TCAGATGAATTCACCGGTAGAGGCAGTGGTAG-3' (sense primer containing an *EcoR*I site), 5'-TCAGATGAATTCTGCAGTG TCTTCTCCCTTCA-3' (antisense primer containing an *EcoR*I site). To clone murine *Lin28* (GenBank BC068304.1), an amplicon was generated by PCR with the following primers: 5'-ATACGAGAATTCACGGGC TCAGCAGACGAC-3' (sense primer containing an *EcoR*I site), 5'-TCAGATGAATCCA CCCCCACTTTCTCCACTCT-3' (antisense primer containing an *EcoR*I site). To clone murine *Lin28b* (NM_001031772.2), an amplicon was generated by PCR with the following primers: 5'-TCAGATGAATTCATGGCCGAAGGCGG-3' (sense primer containing an *EcoRI* site), 5'-TCAGATGAATTCCTAAGTCTTTTTCCGTTTCTGAATCA-3' (antisense primer containing an *EcoRI* site). Virus was then produced using a standard calcium phosphate transfection of HEK293T cells in 10 cm tissue culture dishes, collected, filtered, concentrated and titred on Hela cells, as previously described (198). Cell populations to be transduced were sorted by FACS into separate wells of a 96-well round bottom plate containing 50 μl of Iscove's modified Dulbecco's

medium (IMDM) supplemented with 10 mg/ml bovine serum albumin, 10 μg/ml insulin, 200 μg/ml transferrin (BIT, STEMCELL Technologies), 100 units/ml penicillin, 100 μg/ml streptomycin (both from STEMCELL Technologies) and 10^{-4} M 2-β-mercaptoethanol (2-ME, Sigma-Aldrich). Prior to addition of virus, 50 μl of the above medium containing 600 ng/ml Steel factor (SF, STEMCELL Technologies) and 40 ng/ml human interleukin (IL)-11 (Genetics Institute, Cambridge, MA, USA) were added to each well followed by 2 μl of concentrated virus. Cells were incubated with virus at 37°C in a 5% CO_2 incubator for 3-4 hours and washed 3 times with 100 μl of medium prior to further experimentation. Gene transfer efficiencies were determined from the frequency of YFP^+ colonies assessed after 7-10 days in methylcellulose assays (MethoCult M3234, STEMCELL Technologies, Vancouver, BC, Canada) containing 50 ng/ml SF, 10 ng/ml IL-3, 10 ng/ml IL-6 and 3 U/ml erythropoietin. Colonies were then removed individually, analyzed by FACS, and considered to have derived from a transduced ESLAM cell if >25% of the cells in the colony were YFP^+.

3.2.6 CFC assays

YFP^+ BM cells were isolated by FACS and seeded at $2.0x10^4$ cells per dish in Methocult M3434 (STEMCELL Technologies) containing 50 ng/ml SF, 10 ng/ml IL-3, 10 ng/ml IL-6 and 3 U/ml erythropoietin. Dishes were incubated at 37°C and 5% CO_2 for 12 days after which colonies were enumerated. Colony counts are derived from the sum of 2 dishes per sample. Each dish was scored for colonies derived from a large erythroid (burst)-forming unit-erythroid (BFU-E), a colony forming unit-granulocyte macrophage (CFU-GM) or a colony forming unit-granulocyte erythrocyte macrophage megakaryocyte (CFU-GEMM) using standard criteria to recognize the presence of maturing erythroblasts, granulocytes and macrophages, and all of these, respectively.

3.2.7 LDA of the extent of HSC expansion in primary recipient mice

To quantify the 6-week output of transplanted HSCs *in vivo*, 3-4 mice were each transplanted with 40 transduced adult BM ESLAM cells, $1.7x10^5$ E14.5 *Hmga2*$^{+/+}$ or *Hmga2*$^{-/-}$ FL cells, or $2.0\text{-}7.0x10^5$ *Hmga2*$^{+/+}$ or *Hmga2*$^{-/-}$ adult BM cells. Mice were then sacrificed 6 weeks later and the BM cells combined from both tibiae and both femurs of all mice in the same group. Decreasing equivalent aliquots of these BM cell suspensions were then injected into secondary irradiated W^{41}/W^{41} recipients and the HSC content per primary mouse calculated assuming the BM content of 2 tibiae and 2 femurs contains 25% of the entire BM of a mouse (199). All LDA calculations and statistical testing were performed using ELDA (http://bioinf.wehi.edu.au/software/elda/index.html) (200).

3.2.8 Weight gain and glucose handling measurements

For measurements of weight gain, mice were initiated on a high fat diet (9% fat, 2019 Teklad global 19% protein extruded rodent diet, Harlan Laboratories, Madison WI, USA) and weighed at 2 weeks intervals starting at 8 weeks post-transplant. Fasting glucose measurements were performed by transferring mice to a new cage without food or corn-cob bedding 12 hours prior to isolation of ~5 μl of blood obtained from the tail vein. Mice were not heated or placed in a restrainer to reduce stress. Blood glucose was measured using a handheld glucose monitor (OneTouch Ultra2). Glucose tolerance testing was subsequently performed on fasting mice by introduction of 1g/kg glucose by intraperitoneal injection. Blood glucose was then measured at 15, 30, 60 and 120 minutes following the glucose challenge.

3.2.9 Statistical analyses

Unless otherwise stated, all values represent the mean ± the s.e.m. and p values were derived using Student's *t*-tests in MS Excel. Statistical analyses of LDA were performed using ELDA (200) and are given as the mean ± 95% c.i.

3.3 Results

3.3.1 Lin28, Lin28b or Hmga2 overexpression can activate fetal-like properties in adult HSCs

To test our hypothesis that the Lin28b-let-7-Hmga2 axis regulates developmental differences in HSC properties, we first asked whether let-7 inhibition in adult BM HSCs would confer upon them the high self-renewal potential characteristic of fetal HSCs. A permanent suppression of let-7 levels was achieved by lentivirus (LV)-mediated transfer of a construct containing the cDNA of mouse *Lin28*, a homologue of *Lin28b* with a similar capacity to inhibit let-7 biogenesis (140, 176). Use of a short (3-4 hour) transduction protocol resulted in high gene transfer efficiencies (72% and 40% for the control-LV and Lin28-LV exposed cells, respectively), with no differences in toxicity, as determined by measuring the subsequent clonogenic efficiencies of the transduced cells in methylcellulose cultures (Figure 3.1). Identical numbers of transduced HSCs from each group, chosen to mimic previously published experiments (70), were transplanted immediately post-transduction into irradiated W^{41}/W^{41} congenic mice (40 total ESLAM cells assumed to contain ~20 transplantable HSCs (2, 4) per mouse of which ~14 would have been transduced with the control-LV and ~8 would have been transduced with the Lin28-LV; Figure 3.2A).

Analysis of the progeny of the transduced cells present in the BM of the primary recipients 6 weeks later, showed that *Lin28* mRNA levels were ~45-fold higher in the LSK cells derived from the *Lin28*-transduced HSCs as compared to control-transduced HSCs (Figure 3.2B). We also found that let-7a, b, d and f levels were, as predicted, significantly reduced in the LSK progeny of the *Lin28*-transduced HSCs (Figure 3.2C). *Hmga2* transcripts were also elevated (Figure 3.2B) and, by flow cytometry, increased Hmga2 protein could be seen in all of the LSK progeny of *Lin28*-transduced HSCs at levels equivalent to those produced by direct Hmga2 overexpression (Figure 3.2D-F), and in unmanipulated FL LSK cells (Figure 2.6D). Interestingly, however, the differential expression of Hmga2 in cells derived from the *Lin28*-transduced adult HSCs was limited to the LSK population and not apparent in their mature (Lin^+) progeny (data not shown), as is also the case for unmanipulated FL cells (Figure 2.6D). These findings support the concept that increasing Lin28 expression in adult HSCs results in an inhibition of let-7 levels and a consequent increase in Hmga2, thus mimicking the pattern seen in fetal HSCs.

We then assessed the effects of enforced elevation of Lin28 in adult BM HSCs on their self-renewal activity. This involved quantifying the number of daughter HSCs produced 6 weeks after transplantation of the LV-exposed HSCs into primary recipients. This was accomplished using a limiting dilution analysis (LDA) approach (36) to quantify the proportion of BM cells from primary recipients that regenerated multi-lineage hematopoiesis in secondary recipients for at least 16 weeks (Figure 3.2A). An initial indication of a marked positive effect of increasing Lin28 expression was clearly evident from the levels of chimerism obtained in the secondary recipients of the highest dose of BM cells from the primary recipients (Figure 3.3A, orange line vs black line for controls). It can be seen that the progeny of the *Lin28*-transduced (YFP^+) cells

subsequently produced greater numbers of all 3 lineages of mature white blood cells. This advantage progressively increased over the entire 16-week follow-up period, and was primarily due to an enhanced output of myeloid and B-cells, although a greater output of T-cells was also observed at early time points. To confirm that this effect was not specific to the Lin28 homologue being overexpressed in these experiments, we performed the same experiment using Lin28b and found a similar phenotype (i.e. progressively increasing transduced cell-derived contributions in secondary recipients, Figure 3.3B).

Assessment of the secondary recipients of all doses of primary recipient BM cells after 16 weeks showed that the initial *Lin28*-transduced adult BM HSCs had expanded their numbers significantly more than control-transduced HSCs (Figure 3.3C-D and Appendix A.2), with an estimated expansion of 95-fold (750 HSCs produced from ~8 transduced HSCs, see above). In contrast, control HSCs expanded only ~9-fold. These HSC expansions are remarkably similar to our previous results for unmanipulated fetal and adult BM HSCs, respectively (70). These data provide strong evidence that inhibition of let-7 biogenesis, by overexpression of either Lin28 or Lin28b, can activate fetal-like self-renewal properties in adult HSCs.

We next examined the effects of direct Hmga2 overexpression to investigate whether Lin28-mediated activation of Hmga2 levels are wholly or partially responsible for the induction of fetal-like self-renewal properties in adult HSCs. Using the same experimental design (Figure 3.2A), we found that Hmga2 overexpression, similarly to Lin28 and Lin28b overexpression, resulted in a progressively increasing YFP^+ chimerism in secondary recipients of a high dose of BM cells from the initial recipients of the *Hmga2*-transduced cells (Figure 3.3A, blue line). LDA results provided a more quantitative confirmation that Hmga2 overexpression enables the initially transduced adult BM HSCs to execute a fetal-like expansion of their numbers (~150-

fold) during their first 6 weeks in the primary recipients (Figure 3.3D). We also found that after a more extended period in secondary recipients (8 to 10 months), the number of *Hmga2*-transduced adult BM HSCs had expanded to the level seen in the BM of unmanipulated mice (Figure 3.3E and Appendices A.3-A.4), an outcome that is also eventually attainable by transplants of normal fetal but not adult HSCs (123).

Our finding that Hmga2 overexpression can phenocopy the ability of Lin28 overexpression to induce a fetal-like self-renewal potential, provides strong evidence that Lin28 exerts this effect by derepression of Hmga2 expression. However, these data do not formally exclude the alternative explanation that Lin28 and Hmga2 overexpression are able to activate distinct pathways with overlapping outcomes. To further investigate this we designed an experiment to test whether or not Hmga2 is *required* for Lin28-induced activation of a fetal-like self-renewal in adult HSCs. By using the same experimental design to that shown in Figure 3.2A, however, adult HSCs were instead isolated from *Hmga2* KO mice (195). Since we had previously established that the high self-renewal phenotype of Lin28- and Hmga2-overexpressing adult HSCs is associated with a progressively increasing pattern of transduced-HSC-derived chimerism in secondary recipient animals (see Figure 3.3A), we used this endpoint. As expected, overexpression of Hmga2 generated a progressively increasing fetal-like reconstitution pattern, whereas control-transduced HSCs displayed a stable pattern (Figure 3.4A). Astonishingly, Lin28-overexpression in *Hmga2*-null adult HSCs lead to a complete loss (<1% in all lineages) of transduced-HSC-derived (YFP^+) hematopoiesis, in spite of appreciable donor-derived chimerism (25-70% at the 12-week timepoint). Also, this was not a consequence of a failure of the initial HSCs to receive virus since the primary mice contained a substantial number of transduced-HSC-derived LSK cells at the time of secondary transplants (Figure 3.4B).

This data supports a model whereby Hmga2 is a key downstream mediator of Lin28-induced fetal-like reprogramming of adult HSC self-renewal, and further suggests that Hmga2 may be necessary for the maintenance of self-renewal in the context of the increased proliferation caused by derepression of other let-7 targets such as k-Ras and c-Myc (201).

Igf2bp2 is a well-established transcriptional target of Hmga2 (202-204) that we also identified as showing higher levels of expression in fetal as compared to adult LSK cells (Figure 2.6A). It was therefore of interest to measure the transcript levels of this gene following Hmga2 and Lin28 overexpression. The results showed a significant increase in *Igf2bp2* expression in the LSK progeny of both *Hmga2*- and *Lin28*-transduced adult HSCs (Figure 3.5A). To determine if other genes are altered as a consequence of Hmga2 overexpression in adult HSCs, the LSK progeny of Hmga2-transduced HSCs (isolated from the BM of secondary recipient animals 8-10 months post-transplant) were compared with equivalent cells from control-transduced-HSC transplanted animals, FL and adult BM, using Affymetrix profiling. To accomplish this, we purified YFP^+ LSK cells from mice transplanted 8-10 months earlier with a high dose of primary BM from *Hmga2*-overexpressing HSC-transplanted mice (see Figure 3.1A) and compared the transcriptome of these cells with E14.5 FL LSK cells, adult BM LSK cells and control LSK cells. Since control-transduced HSC transplanted mice contained very few YFP^+ LSK cells, donor-derived YFP^- LSK cells were used as a control in this experiment. Using a gene signature defined by genes differentially expressed between FL and adult BM LSK cells, the biological replicates for all 4 conditions clustered closest to one another, as would be expected. Interestingly, the transcriptional signature of Hmga2-overexpressing LSK cells was not more similar to fetal LSK cells than the control cells (Figure 3.5B). Surprisingly, only 3 of these genes

(*Hmga2, Igf2bp2 and Plk2*) were re-activated to fetal levels upon Hmga2 overexpression (Figure 3.5B), suggesting that *Igf2bp2* is a rare target of this manipulation.

We also looked for evidence of changes in apoptosis or proliferation in the transduced HSCs, since these parameters are regulated by HMGA proteins (184), and changes in either of these could affect the rate of HSC regeneration in our transplantation model. Comparison of the proportion of proliferating (Ki-67$^+$) or apoptotic (Annexin V$^+$) cells in the *Lin28*- or *Hmga2*-transduced (YFP$^+$) ESLAM compartment and the matching non-transduced (YFP$^-$) ESLAM cells in secondary recipients, showed no significant differences in either of these parameters (Figure 3.6), although a trend towards fewer apoptotic ESLAM cells overexpressing either of these genes was noted.

To investigate the differentiation behaviour of Hmga2- and Lin28-overexpresing HSCs, we first compared the composition of the donor-derived PB compartment arising from transduced (YFP$^+$) and untransduced (YFP$^-$) HSCs in secondary recipients of a high-dose of primary marrow. At the 16-week time point, we found that control-transplanted mice, as expected, contained similar proportions of myeloid, B-cells and T cells in the YFP$^+$ and YFP$^-$ fractions (Figure 3.7A). Interestingly, we also found the YFP$^+$ cells in the PB of recipients of Hmga2-overexpressing HSCs to contain an increased myeloid and decreased lymphoid (B-cell and T-cell), with an opposite pattern in the YFP$^-$ fraction (Figure 3.7A). This pattern was similar to that which we observed previously within recipients of unmanipulated FL cells (70), thus providing evidence that Hmga2 regulation may extend to other fetal-specific HSC properties. Curiously, we did not observe evidence of a fetal-like myeloid-biased differentiation pattern in recipients of *Lin28*-transduced HSCs, suggesting that the concurrent activation of *Hmga2* and other let-7 targets in these cells can suppress this phenotype.

Colony forming cell (CFC) assays performed on transduced HSC-derived (YFP^+) BM cells showed an increase (as compared to controls) in the frequency of BFU-Es following overexpression of Hmga2, but not Lin28 (Figure 3.7B), consistent with a reported role for Hmga2 as a positive regulator of erythropoiesis (205). Both Lin28 and Hmga2 overexpression also increased the output of CFU-GEMMs with no effect on CFU-GMs (Figure 3.7B).

Together, these data provide strong evidence that Hmga2 overexpression in adult HSCs replicates the ability of Lin28-mediated let-7 repression to elicit a fetal-like self-renewal activity and enhance expression of *Igf2bp2*. Furthermore, these observations make it likely that the increased expansion of HSCs enabled by overexpression of Lin28 or Hmga2 in adult HSCs is a consequence of an increased frequency of their executing symmetric self-renewal divisions.

3.3.2 Hmga2 is not a downstream target of Lin28-induced activation of fetal-like lymphopoietic potential in adult HSCs

Overexpression of Lin28 in adult BM cells can also activate a fetal-like lymphoid program including an enhanced frequency of B1a B cells and a reduced frequency of B2 B cells present in the peritoneal cavity of recipient mice (140). Therefore, we asked whether this outcome might be similarly mediated by Hmga2. Examination of the B cells produced from transplanted Lin28 overexpressing HSCs confirmed the reported alteration of donor-derived B1a and B2 cell numbers in the recipients (Figure 3.8A-D). However, we found that the same changes were not replicated in recipients of Hmga2-transduced HSCs (Figure 3.8A-D). We also observed that the large change in the proportions of follicular zone B (FoB) and marginal zone B (MzB) cells in the spleen, that is conferred by Lin28 overexpression (140), is not fully activated by Hmga2 overexpression (Figure 3.8E-G). Interestingly, a small increase in MzB cells was noted, suggesting that Hmga2 may partially activate the same pathway required for this Lin28-

mediated effect. This inability of Hmga2 to activate the production of fetal-like B cell subsets may also explain the differences in transduced HSC-derived B-cell chimerism that we observed in comparing recipients of Lin28- and Hmga2-overexpressing HSCs (Figures 3.3A and 3.7A). These findings suggest that unlike Lin28, which can activate both fetal HSC self-renewal potential and multiple features of fetal B cell lymphopoiesis, Hmga2 plays a more limited role in regulating the likelihood that these cells can execute a symmetric self-renewal division.

3.3.3 Hmga2 is necessary for fetal HSCs to execute a high self-renewal activity

To determine whether Hmga2 is *required* for the enhanced self-renewal activity displayed by fetal HSCs, we compared the regenerative properties of HSCs from *Hmga2* KO and WT mice (195). *Hmga2* KO fetal mice are normal in size, but show reduced growth after birth and hence become smaller than their WT littermates (182) (Figure 3.9A). Similarly, their FLs have a normal cellularity and composition (Figure 3.9B-D). However, by adulthood, the BM of the KO mice contains ~2.5-fold fewer cells of all subsets of primitive hematopoietic cells (Figure 3.9B-C), but with no significant changes in the frequencies of any of these (Figure 3.9D). This was evident from measurements of all hematopoietic cell types in the BM of the adult *Hmga2* KO mouse, which included functionally-defined HSCs as measured by LDA analysis (Figures 3.9C-D and F, and Appendices A.4 and A.5). We also found that the ESLAM cells from *Hmga2* KO animals are highly enriched in HSCs (as shown by single ESLAM cell transplants) and contain a full complement of HSC differentiation subtypes (2, 24) (α, β, γ and δ; Figure 3.9E). Thus, Hmga2 is not required for the creation of an HSC state, for the generation of different HSC lineage subtypes, or for efficient homing of HSCs into the BM.

To compare the self-renewal activity of HSCs from the FL of *Hmga2* KO and WT mice, where we anticipated an effect due to the lack of Hmga2, we used the same general protocol as

for the Lin28 and Hmga2 overexpression studies. However, in this case, the cells transplanted were bulk, untransduced FL cells containing an estimated 4-5 HSCs (based on the frequencies shown in Figure 3.9F). Quantification of the frequency of donor-derived LSK cells present 6 weeks later in the BM of the primary recipients of the KO cells, revealed these to be already significantly reduced as compared to the recipients of WT E14.5 FL cells (~2-fold, Figure 3.10B-C). Unexpectedly, when adult BM cells were transplanted, a smaller number of LSK cells were generated from the recipients of KO compared to the WT cells (Figure 3.10D). This suggests that the lower level of expression of *Hmga2* in adult HSCs may also function to regulate self-renewal activity.

Not surprisingly, analysis of the secondary recipients of the 6-week cells obtained from the primary recipients of the *Hmga2* KO FL cells showed these also produced fewer mature cells in the secondary mice when compared to recipients of the WT cells (Figure 3.10E), with an equivalent reduction in all lineages (myeloid, B-cell and T-cell). A comparison by LDA of the extent of HSC expansion that had occurred in the 2 groups of primary mice also showed a significantly reduced expansion (~10-fold) of daughter HSCs from the *Hmga2* KO E14.5 FL cells relative to the WT controls (Figure 3.10F). Interestingly, the magnitude of expansion observed for fetal *Hmga2* KO HSCs (~12-fold, 60 HSCs produced from an estimated input of 5 HSCs) is remarkably similar to that observed for control-transduced adult BM HSCs (Fig. 3.3E) and for unmanipulated adult BM HSCs (70), suggesting that the self-renewal potential of *Hmga2* KO fetal HSCs reverts to an adult-like self-renewal capability. These findings point to a role for Hmga2 as a regulator of the *elevated* self-renewal potential of fetal HSCs, but not as a necessary requirement for the establishment or maintenance of a baseline self-renewal capability.

3.3.4 *Hmga2*-null fetal HSCs express lower levels of *Igf2bp2*

To identify transcriptional targets responsible for the decreased self-renewal activity of *Hmga2* KO fetal HSCs, we performed a comparative Affymetrix array analysis of RNA obtained from E14.5 *Hmga*2 KO and WT FL LSK cells. This comparison revealed 7 differentially expressed genes (FDR<0.1; Appendix A.7), of which only 2, *Hmga2* and *Igf2bp2,* were also found in our original fetal-defined signature (Figure 2.7A). qRT-PCR assessment of the level of expression of these 7 genes in both LSK and ESLAM cells isolated from KO and WT FL showed *Hmga2* and *Igf2bp2* to be significantly downregulated in both KO cell compartments (Figure 3.11). Remarkably, our finding that *Igf2bp2* represents a strong, if not exclusive, target of *Hmga2* in FL HSCs and progenitors may extend beyond the haematopoietic system since a similar comparison using E12.5 whole embryos yielded the same result (202). Since Igf2bp2 or related homologues have been shown to regulate the self-renewal of mouse myoblasts (204) and developmental changes in *Drosophila* germline stem cells (206), we speculate that it may play a similar role downstream of Hmga2 in mouse HSCs.

3.3.5 Evidence of IGF-2 secretion following Lin28 and Hmga2 overexpression

Insulin-like growth factor 2 mRNA binding protein 2 (Igf2bp2) binds its mRNA targets and either positively or negatively regulates its translation rates (207). Through this mechanism, Igf2bp2 has been found to increase the levels of Insulin-like growth factor 2 (IGF-2) (208, 209). IGF-1 and IGF-2 bear structural similarities to insulin and act to regulate organismal growth through their mitogenic and anti-apoptotic actions (210). At high concentrations, IGFs can also recapitulate the activities of insulin including increased uptake of glucose, decreased lipolysis in adipocytes, and increased synthesis of glycogen, lipids and proteins (210). We were therefore

interested in testing whether the Lin28- or Hmga2-induced increased expression of *Igf2bp2* resulted in increased IGF-2 secretion as evidenced by alterations in recipient mouse metabolism.

This was first tested by measuring blood glucose levels in the secondary recipients from the experiment shown in Figure 3.2A. Astonishingly, when the fasting glucose was measured at 8 weeks post-transplant, recipients of Hmga2- and Lin28-overexpressing BM cells were found to have significantly lower levels than control mice (Figure 3.12A). Glucose handling was then measured using a glucose tolerance test. Following the intraperitoneal injection of 1 g/kg glucose, blood glucose levels increased in all groups (Figure 3.12B); however, recipients of Lin28-overexpressing BM cells displayed a more rapid glucose clearance that was most apparent at 30 minutes following the glucose challenge (Figure 3.12B). Interestingly, the glucose handling of recipients of Hmga2-overexpressing BM cells was not different from control mice (Figure 3.12B).

We also tracked the weight gain of transplant recipients since insulin signaling-mediated alterations in glucose uptake and/or lipid metabolism would be expected to increase the rates of weight gain. To enhance this effect, mice were fed a high-fat diet starting at 8 weeks post-transplant. Recipients of Lin28- and Hmga2-overexpressing cells indeed displayed a more rapid weight gain phenotype, which was most dramatic within the first 2 weeks after being initiated on a high-fat diet (Figure 3.12C). This trend was continued for Lin28-overexpressing BM recipients; however, Hmga2-overexpressing BM recipients were not significantly different from control mice after 14 weeks post-transplant (Figure 3.12C).

Since *Igf2bp2* overexpression in hepatocytes can increase IGF-2 expression and stimulate lipid accumulation within these cells (209), we stained liver sections of samples isolated from recipients of control, Hmga2-overexpressing, or Lin28-overexpressing BM cells with the

lipophilic dye Oil Red O. As shown in the representative examples, lipid accumulation was evident in the hepatocytes within recipients of the highest dose of Hmga2-overexpressing and Lin28-overexpressing BM cells, but was never found in control-transplanted mice (Figure 3.12D). Although striking, the size and density of lipid droplets was highly variable and could not be detected at all in one recipient of Lin28-overexpressing BM cells.

Together, these findings provide evidence that Lin28 and Hmga2 overexpression can induce a heightened expression of *Igf2bp2* in blood cells, which in turn can lead to the production of one or several paracrine or endocrine regulators of glucose and lipid metabolism. This factor appears most likely to be IGF-2, since it is a known target of Igf2bp2 (209), although further studies will be required to exclude a role of IGF-1 or insulin. Since IGF-2 has been shown to support HSC self-renewal divisions in vitro (189), this molecule may also be a key mediator of the increased self-renewal phenotype that results from Lin28 and Hmga2 overexpression in adult HSCs.

3.4 Discussion

Our finding that *Lin28b* is present at higher levels in fetal compared to adult HSCs, coupled with the demonstration that Lin28 or Hmga2 overexpression can activate a fetal-like self-renewal activity in adult HSCs, strongly implicate the Lin28b-let-7-Hmga2 axis as a primary determinant of the alterations in HSC self-renewal activity that occur between fetal and adult life. Notably, since most of the overexpression studies were performed with Lin28 instead of Lin28b, we cannot exclude the possibility that Lin28 may be an important and/or sole contributor to the high self-renewal phenotype of fetal HSCs. However, we feel that Lin28b is likely the

most important since it is the isoform that is differentially expressed between E14.5 FL and adult BM HSCs.

Together with evidence that Lin28b regulates fetal lymphopoiesis (140), these results support a role for Lin28b as a master regulator of fetal HSC identity. Acquired translocations or viral insertions that prevent the ability of let-7 miRNAs to regulate *Hmga2* transcript activity in HSCs would thus be anticipated to induce a fetal-like high self-renewal state in these cells and lead to the genesis of dominant clones. Interestingly, several examples of such a consequence of this type of *Hmga2* mutation in both mice and humans have recently been documented (50, 51, 205, 211, 212).

Previous studies have identified *Bmi1* (135), *Gfi1* (136), *Tel/Etv6* (137) and c-Kit activation (55) as being selectively dispensable for fetal, but not adult, HSCs. Conversely, *Sox17* (138) and *Ezh2* (213) are specifically required for the maintenance of fetal-stage HSCs. Here we provide the first evidence of a gene, *Hmga2*, that controls the higher self-renewal potential of fetal HSCs, but is not required for the baseline maintenance of fetal or adult HSCs. Hmga2 is a non-histone chromatin protein with a specific affinity for the minor groove of AT-rich DNA sequence (184). It also regulates the expression of *Igf2bp2* (202), as shown here for HSCs. Since overexpression of an isoform of this gene can increase levels of IGF-2 (209), a cytokine that can support the growth of murine HSCs *in vitro* (189), Igf2bp2 may ultimately mediate its downstream effects of Hmga2 through this mechanism.

Since neural stem cells from *Hmga2* KO mice have also been found to display a fetal-specific defect in self-renewal, our discovery of a similar phenotype in HSCs from these mice suggests that this gene may play a similar role in other tissues. This possibility is further supported by the elevated *Hmga2* expression characteristic of multiple fetal mouse tissues (182),

the pygmy phenotype of *Hmga2* KO mice (182, 195, 214), and evidence in humans of growth disorders involving deletion (215, 216) or variants (217) of *HMGA2*. Thus the LIN28B-let-7-HMGA2 axis may play a more generic role in the growth regulation of human, as well as mouse, tissues and organs through effects operating at the stem cell level. This idea is additionally supported by the fact that alterations in the growth hormone-insulin-like growth factor endocrine pathway, which are the underlying abnormality in most spontaneous mutant mice with deficient growth, do not account for the pygmy phenotype of *Hmga2*-null mice (218-221). Instead, the phenotype of these mice, and in human growth disorders involving *HMGA2*, may represent a consequence of cell-intrinsic stem cell self-renewal deficits acting in parallel across multiple tissue and organ systems.

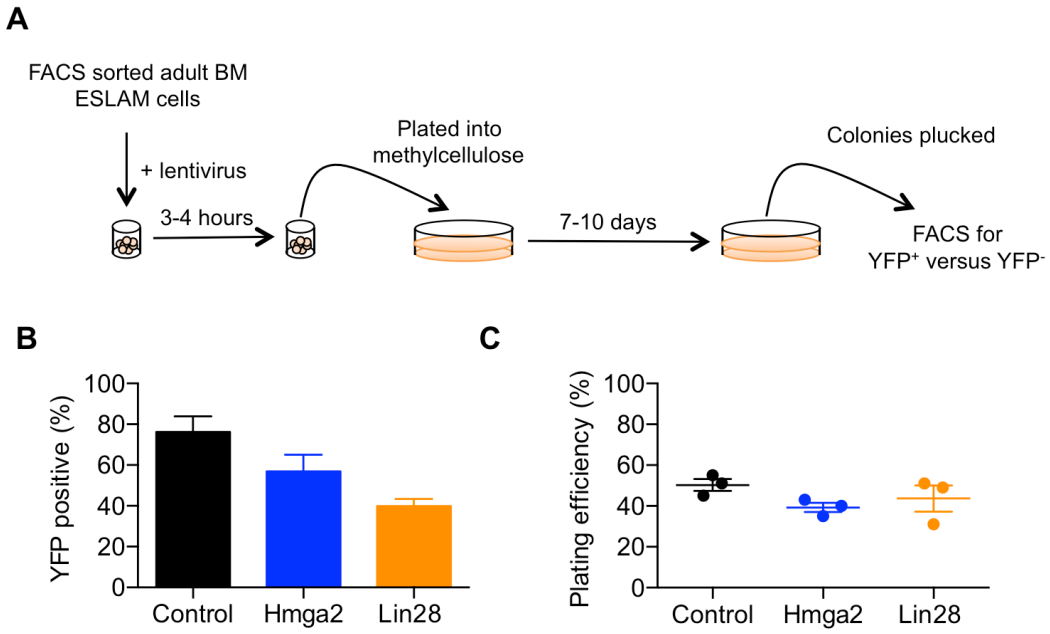

Figure 3.1 Gene transfer and plating efficiencies for adult BM ESLAM cells following lentivirus transduction

(A) Viral transduction efficiencies for control, *Hmga2* and *Lin28* lentiviruses were determined by exposing adult BM $CD45^+EPCR^+CD48^-CD150^+$ (ESLAM) to virus and plating into methylcellulose. Colonies produced were analyzed by FACS for YFP content (see Materials and methods for details). **(B)** Proportion of YFP^+ colonies derived from transduced adult BM ESLAM cells. Mean ± s.e.m. of data from 5 separate experiments where 4-18 colonies were analyzed per group per experiment. **(C)** Colony formation efficiencies for freshly transduced ESLAM cells. 47-213 cells plated per treatment per experiment. Mean ± s.e.m. from 3 experiments.

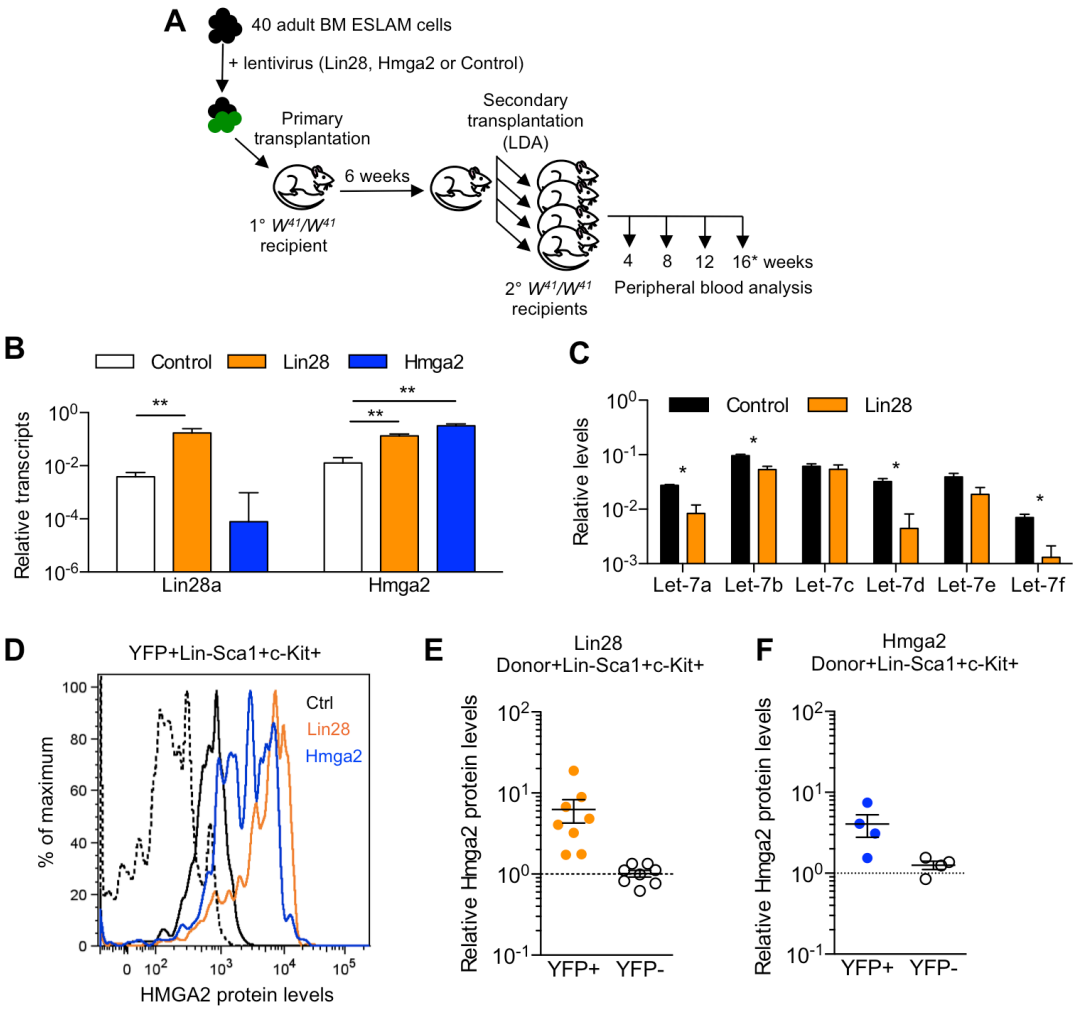

Figure 3.2 Lin28 overexpression in adult HSCs leads to a decrease in let-7 miRNA levels and a subsequent derepression of Hmga2 expression

(A) Schematic representation of the experimental design involving the transplantation of 40 adult BM ESLAM cells following their exposure to a *Lin28*, *Hmga2* or control (YFP) lentivirus. Daughter HSCs produced after 6 weeks *in vivo* were measured by limiting dilution analysis (LDA). Asterisks indicate the HSC-defining PB analysis time point. **(B)** qRT-PCR analysis of transcripts relative to *Gapdh* in Lin$^-$Sca1$^+$c-Kit$^+$(LSK) YFP$^+$ cells from mice transplanted 6 weeks earlier with control (white bars), *Lin28* (orange bars) or *Hmga2* (blue bars) lentivirus-transduced adult BM ESLAM cells (n=3-7). **(C)** Let-7 miRNA levels relative to sno-RNA202 in the YFP$^+$ LSK progeny of control- or *Lin28*-lentivirus-transduced adult BM ESLAM cells 6 weeks following transplantation (n=3-7). **(D)** Representative fluorescence activated cell sorting (FACS) plot for Hmga2 measurement by intracellular flow cytometry (see Materials and methods) within the 6-week LSK progeny of transduced HSCs. The dotted line represents the unstained control. Hmga2 protein levels in the YFP$^+$ and YFP$^-$ LSK progeny of **(E)** *Lin28* and **(E)** *Hmga2* lentivirus-exposed HSCs. All levels were normalized to the same subset within recipients of HSCs exposed to a control lentivirus (8 mice from 3 experiments). All data represent the mean ± s.e.m. One-tailed Student's *t*-tests were used to assess statistical significance. **P*<0.05, ***P*<0.01.

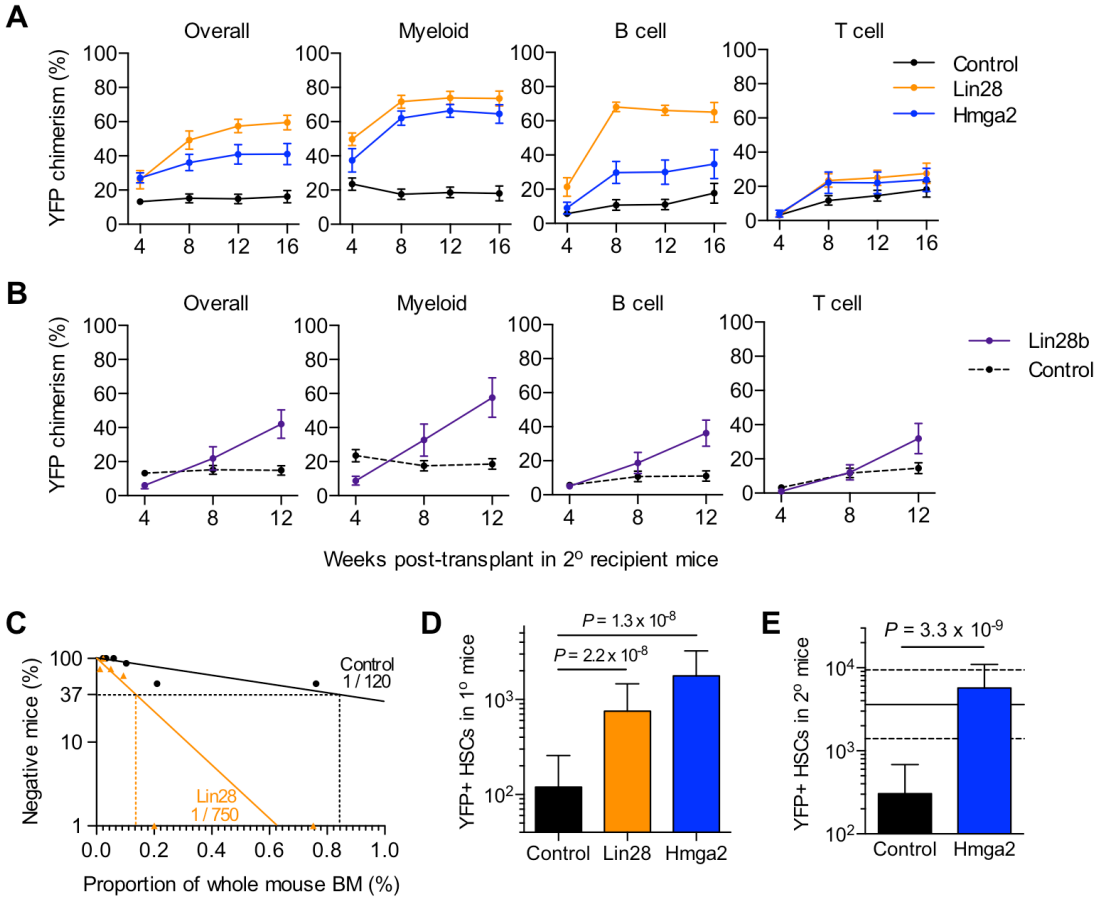

Figure 3.3 Lin28, Lin28b or Hmga2 overexpression can activate a fetal-like heightened self-renewal activity in adult HSCs

(A) PB chimerism in secondary recipients of the highest dose of BM cells obtained from primary recipients (estimated as 8% of the total mouse BM assuming 2 femurs plus 2 tibiae represent 25% of the total BM) of control, *Lin28*-transduced or *Hmga2*-transduced adult BM HSCs (199). Values shown are the mean ± s.e.m of 12 mice per group from 3 experiments. **(B)** PB chimerism in secondary recipients of a high dose of BM cells obtained from the primary recipients (estimated as 8% of the total mouse BM) of Lin28b-transduced adult BM HSCs. Control values (dotted black line) are redrawn from (A). **(C)** Graphical representation of HSC frequency determination by limiting dilution analysis (LDA) that were used to derive the values in (D). **(D)** Numbers of transduced (YFP^+) HSCs (mean ± 95% c.i.) within primary recipients of control, *Lin28* or *Hmga2* lentivirus-transduced HSCs, 6-weeks following transplantation. LDA calculations and statistical comparisons were performed using the ELDA software (200) on groups of transplanted mice (see Appendix A.2) from 3 separate experiments in which 4-12 mice were tested at each of 7 different doses. **(E)** Transduced (YFP^+) HSC numbers (mean ± 95% c.i.) regenerated in secondary recipients of the highest dose of primary mouse BM (8% of the total) and determined by LDA assays in tertiary recipients 8-12 months post-transplant. LDA calculations and statistical comparisons were performed using the ELDA software (200) on groups of transplanted mice (see Appendix A.3) from 3 separate experiments in which pools of BM from 2 secondary recipients were assayed per experiment, see Appendix A.3). Solid and dashed horizontal lines correspond to the mean and 95% c.i, respectively, of HSC numbers in WT adult mice (see Appendix A.4).

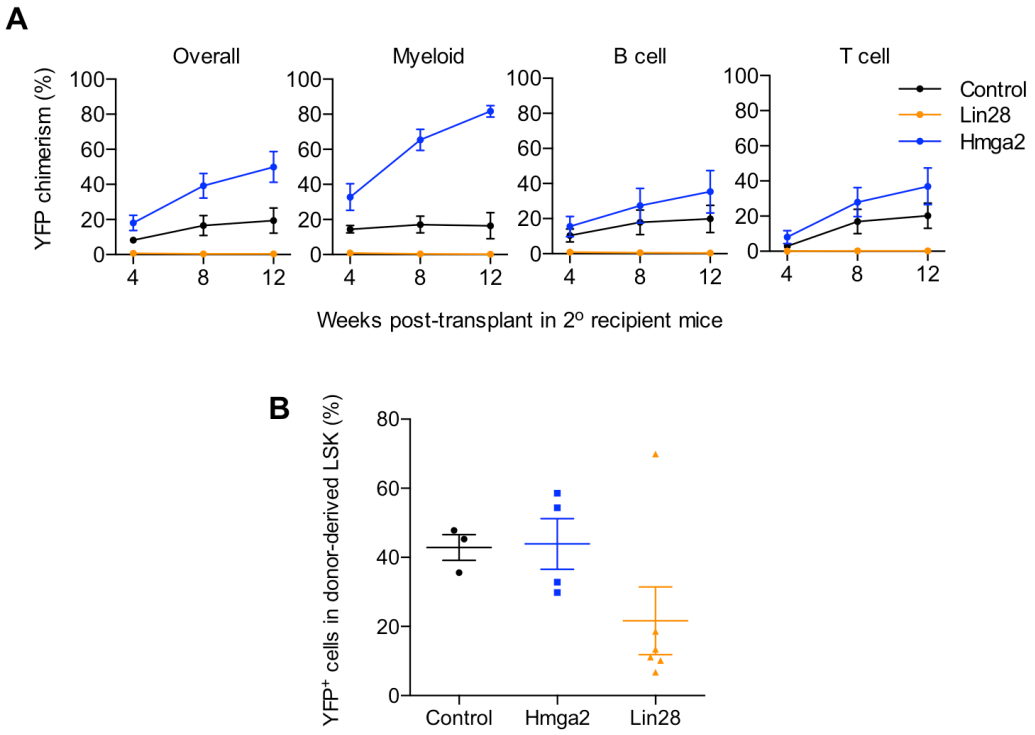

Figure 3.4 Hmga2 expression is required for Lin28-mediated activation of a fetal-like high self-renewal in adult HSCs

(A) PB chimerism in secondary recipients of a high dose of BM cells obtained from primary recipients (estimated as 8% of the total mouse BM assuming 2 femurs plus 2 tibiae represent 25% of the total BM) of adult BM HSCs from an experiment designed similarly to that depicted in Figure 3.2A, but instead using *Hmga2*$^{-/-}$ mice as donors. Values shown are the mean ± s.e.m of 6-8 mice per group from 2 experiments. **(B)** Percentage YFP^{+} cells within the donor-derived LSK compartment of the primary recipient marrow used to transplant the secondary recipient mice shown in (A). Mean ± s.e.m of 3-6 mice per group from 2 experiments.

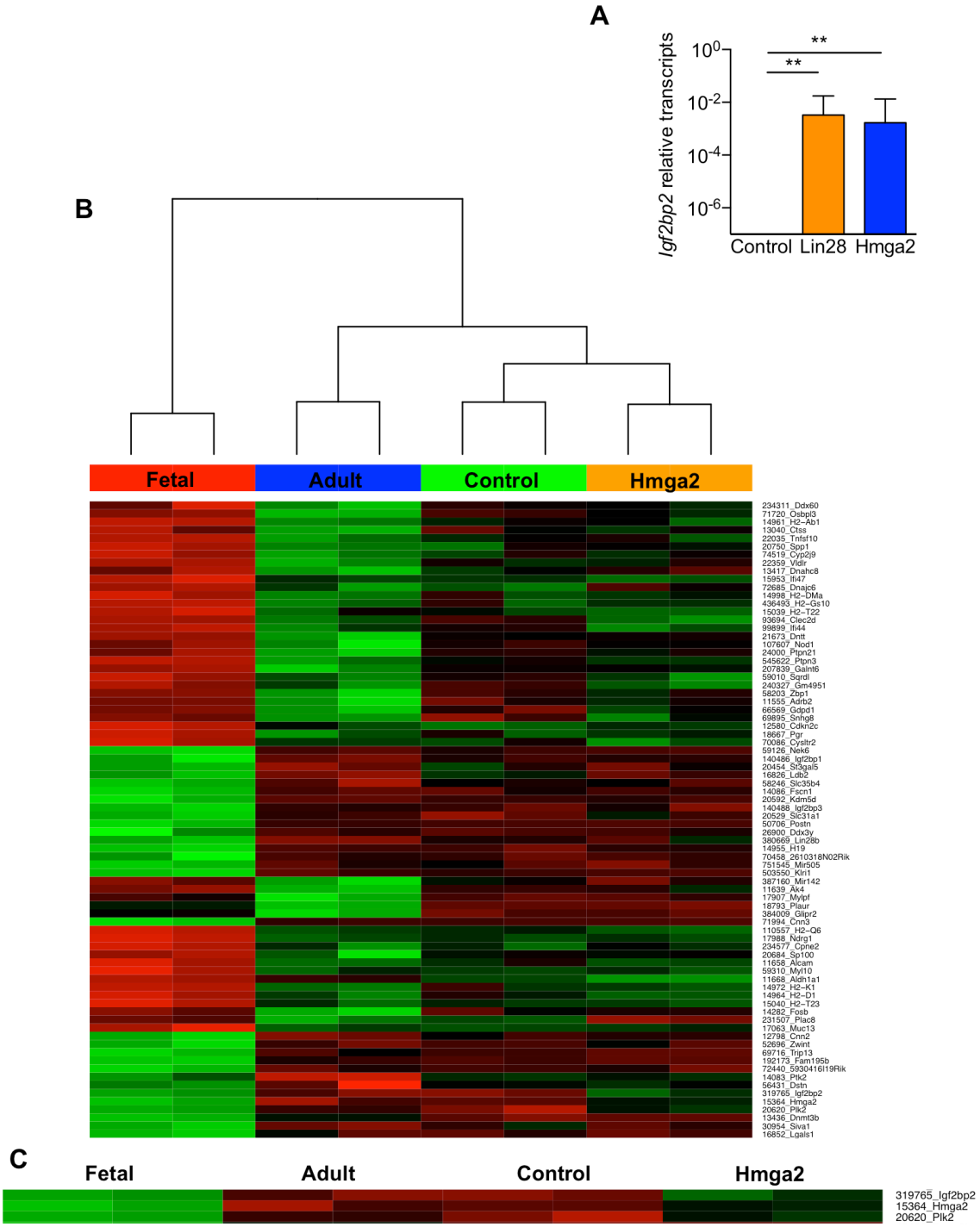

Figure 3.5 Hmga2 and Lin28 ovexpression in adult HSCs activate a fetal-like pattern of Igf2bp2 expression.

(A) qRT-PCR analysis of *Igf2bp2* transcripts in LSK cells from mice transplanted 6 weeks earlier with control, *Lin28*-transduced or *Hmga2*-transduced adult BM HSCs in the experiment detailed in Figure 3.2A (3 to 7 mice per group). **(B)** Affymetrix array analysis of LSK cells from E14.5 fetal liver (fetal) or adult BM (adult) as compared to the donor-derived BM cells from secondary recipients of the highest dose of BM from the experiment described in Figure 3.2A 8-

10 months post-transplant. Note that the YFP^+ and YFP^- fractions were necessarily used for the Hmga2 and Control arms, respectively, since a limiting number of YFP^+ cells could be recovered from control animals. Each column represents one biological replicate and displays a set of genes selected by their differential expression between fetal and adult control subsets. **(C)** Subset of genes from (B) that show a fetal-like gene expression pattern in Hmga2 compared to Control cells.

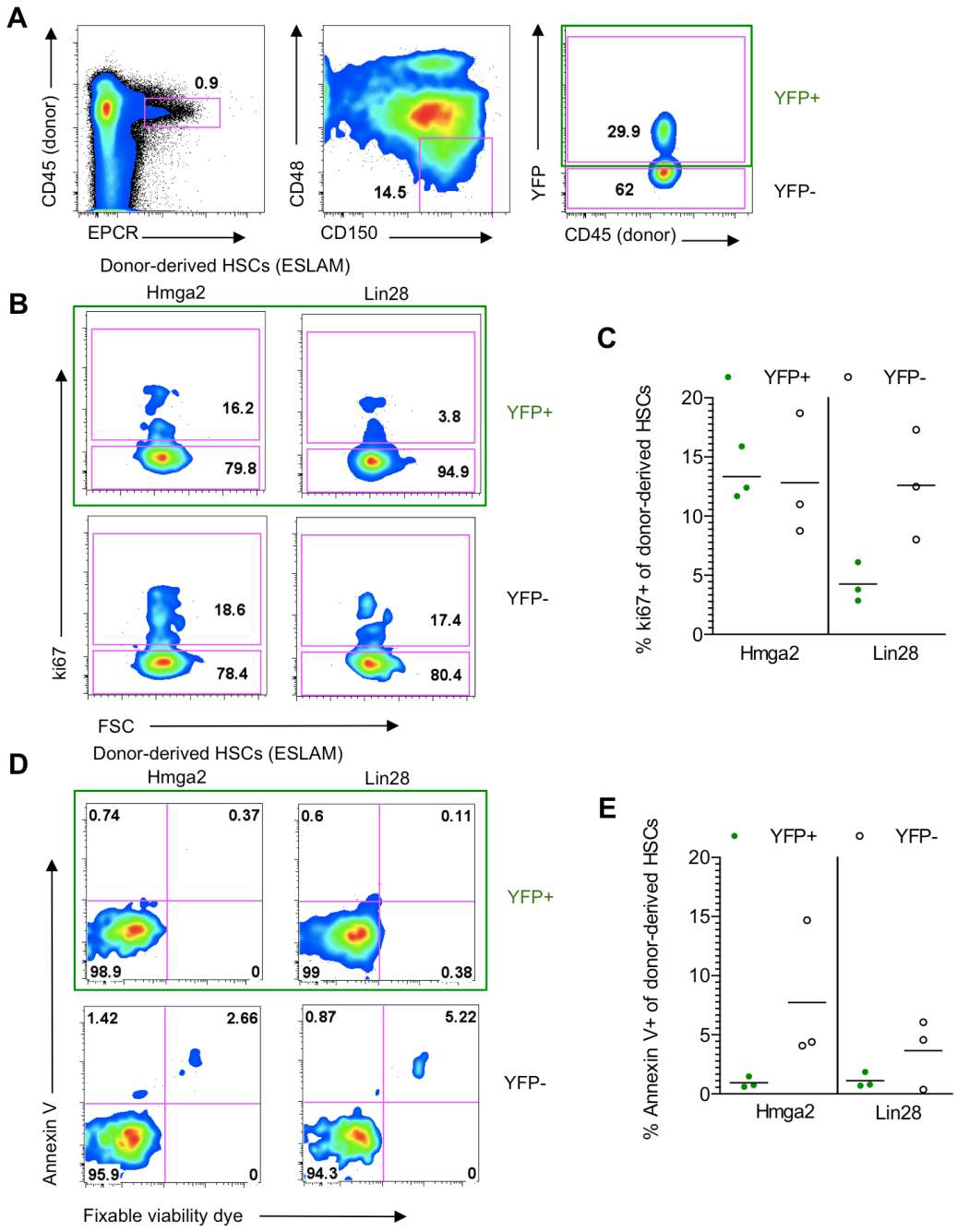

Figure 3.6 Proliferation and apoptosis following Hmga2 and Lin28 overexpression in adult BM HSCs

(A) FACS gating strategy for donor-derived ESLAM cells, followed by separation of transduced (YFP^+) and untransduced (YFP^-) cell fractions. Recipients were analyzed 24 weeks following secondary transplantation with the highest cell dose from the experiment detailed in Figure 3.2A. Representative FACS plots of donor-derived HSCs stained for **(B)** Ki-67, and **(D)** Annexin V/fixable viability dye as described in the Methods. Percentages of **(C)** Ki-67^+ cells and **(E)** Annexin V^+ cells among the YFP^+ and YFP^- subsets of donor-derived ESLAM cells. The means and individual data points for 3 mice per group are plotted. Paired two-tailed Student's *t*-tests were used to assess statistical significance.

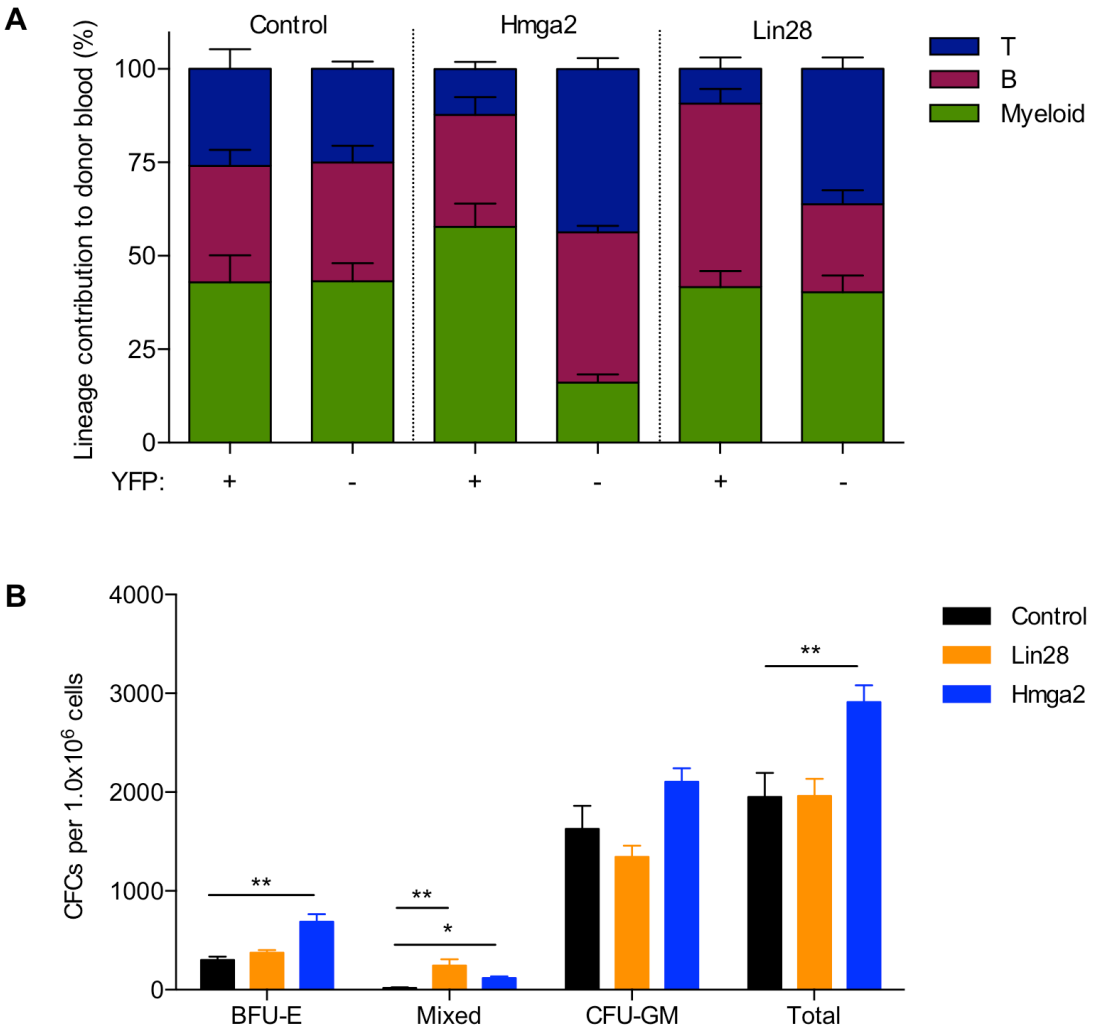

Figure 3.7 Hematopoietic differentiation patterns following Lin28 and Hmga2 overexpression in adult BM HSCs and progenitors

(A) Pairwise comparison of the myeloid, B-cell and T-cell proportions within the YFP$^+$ and YFP$^-$ donor-derived PB fractions of secondary recipients 16 weeks following transplantation of the highest dose of BM from the primary recipients (see Figure 3.2A). Mean ± s.e.m. of 12 mice per group from 3 separate experiments. **(B)** Numbers of day 12 CFCs observed upon seeding 2x10^4 FACS-sorted YFP$^+$ BM cells from 24-week reconstituted secondary recipients (see Figure 3.2A) into methylcellulose supplemented with cytokines (see Materials and methods). Samples were plated in duplicate. Colonies were typed based on morphology as burst forming unit-erythroid (BFU-E), colony forming unit-granulocyte erythrocyte macrophage megakaryoctye (CFU-GEMM), colony forming unit-granulocyte macrophage (CFU-GM). All data represent the mean ± s.e.m of 4 samples per group. One-tailed Student's *t*-tests were used to assess statistical significance. **P*<0.05, ***P*<0.01.

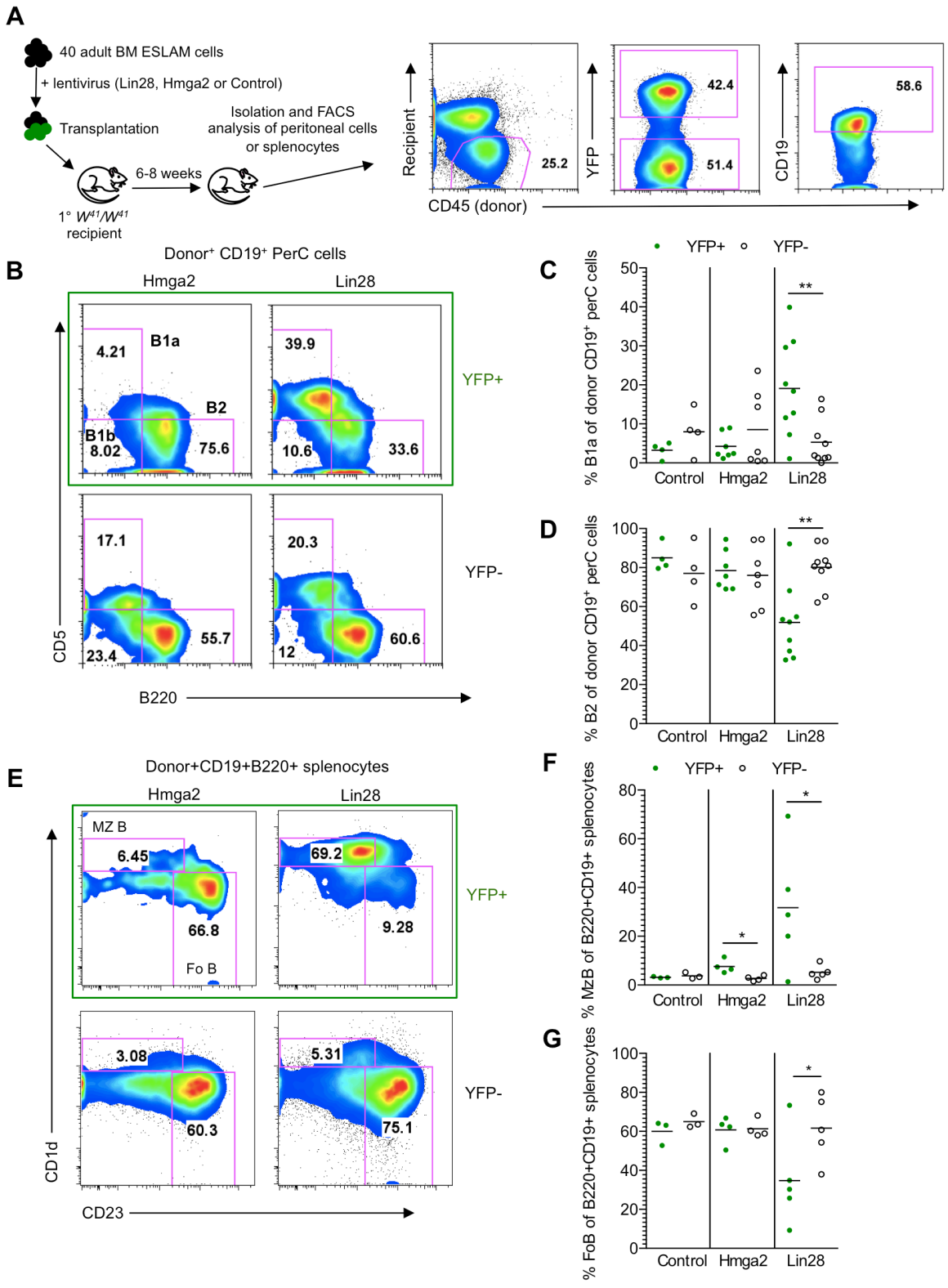
A
40 adult BM ESLAM cells
+ lentivirus (Lin28, Hmga2 or Control)
Transplantation
Isolation and FACS analysis of peritoneal cells or splenocytes
6-8 weeks
1° W41/W41 recipient
Recipient
CD45 (donor)
25.2
YFP
42.4
51.4
CD19
58.6
B
Donor+ CD19+ PerC cells
Hmga2
Lin28
YFP+
YFP-
4.21
B1a
B2
B1b
8.02
75.6
39.9
10.6
33.6
17.1
55.7
23.4
20.3
12
60.6
CD5
B220
C
YFP+ YFP-
% B1a of donor CD19+ perC cells
Control
Hmga2
Lin28
D
% B2 of donor CD19+ perC cells
E
Donor+CD19+B220+ splenocytes
MZ B
6.45
66.8
Fo B
69.2
9.28
3.08
60.3
5.31
75.1
CD1d
CD23
F
% MzB of B220+CD19+ splenocytes
G
% FoB of B220+CD19+ splenocytes

Figure 3.8 Hmga2 overexpression does not recapitulate the Lin28-mediated activation of fetal-like B cell differentiation programs within adult HSCs

(A) Schematic representation of the experimental design involving the transplantation of 40 adult BM ESLAM cells following their exposure to a Lin28, Hmga2 or control lentivirus. Six to 8 weeks following transplantation, peritoneal cavity (perC) cells were harvested and the donor-derived YFP^+CD19^+ and YFP^-CD19^+ cells were compared by FACS. **(B)** Representative FACS plots of PerC $CD19^+$ donor-derived cells. Proportion of **(C)** B1a and **(D)** B2 cells in the YFP^+ and YFP^- fractions of $CD19^+$ donor-derived perC cells (4 to 9 mice per group from 3 experiments). **(E)** Representative FACS plots of YFP^+ and YFP^- fractions of $CD19^+$ donor-derived splenocytes. Proportions of **(F)** marginal zone B (MzB) and **(G)** follicular zone B (FoB) cells in the YFP^+ and YFP^- fractions of $CD19^+B220^+$ donor-derived perC cells (3 to 5 mice per group from 3 experiments). Black lines represent the mean. Paired one-tailed Student's *t*-tests were used to assess statistical significance. $*P<0.05$, $**P<0.01$.

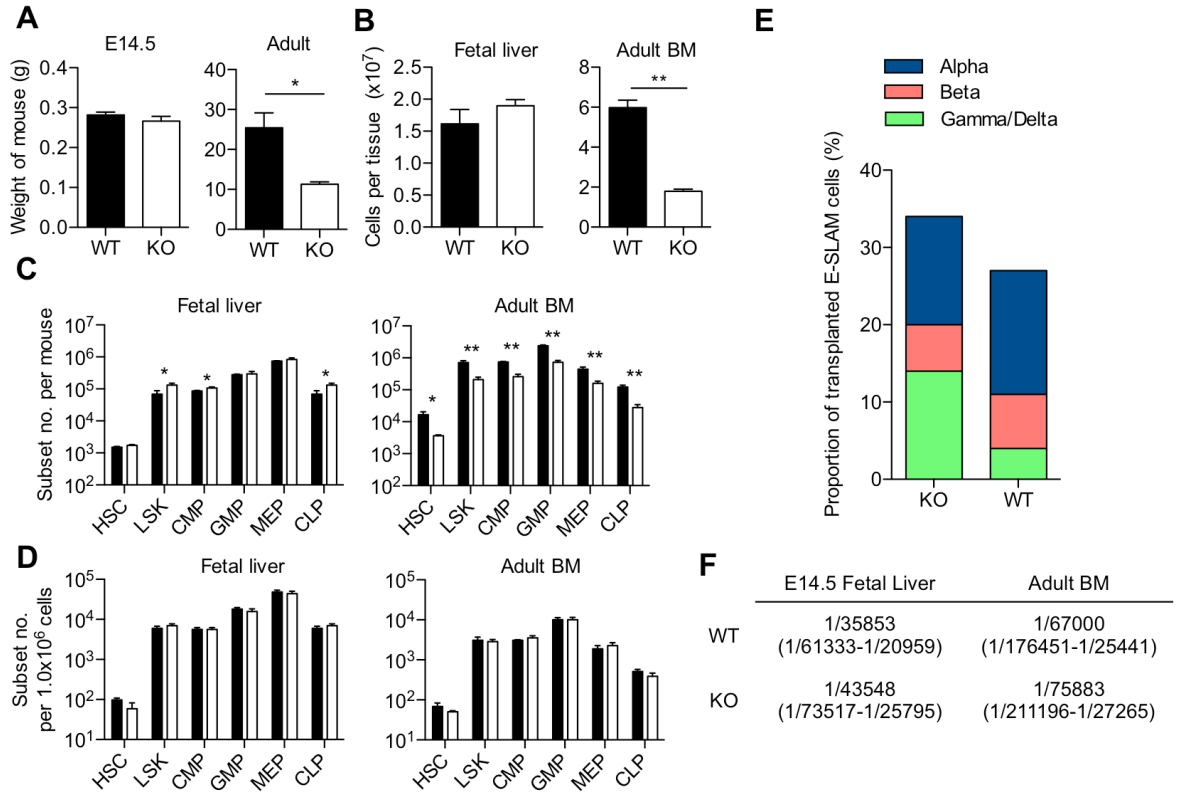

Figure 3.9 Hmga2 KO adult mice manifest an absolute deficiency in HSC and progenitor numbers

(A) Weight of *Hmga2*$^{+/+}$ (WT) or *Hmga2*$^{-/-}$ (KO) mice (n=3 to 4). **(B)** Nucleated cell counts for E14.5 FL or the BM from 8-12 week old (adult) mice (2 femurs and 2 tibiae). **(C)** Absolute numbers of phenotypically defined subsets of E14.5 FL and adult BM of WT and KO mice (n=3 to 4). **(D)** Frequencies of phenotypically defined subsets of E14.5 FL and adult BM of WT (black bars) and KO (white bars) mice (n=3 to 4). **(E)** Single ESLAM cells from 36-58 week-old *Hmga2* KO mice were transplanted into sublethally irradiated recipient mice and the HSC subtype was determined by the relative donor-type chimerism at 16 weeks post-transplant (50 recipients) as described previously (24). Data for wild-type (WT) mice are from the 36-48 week old group from our previously published study (2) (71 recipients). **(F)** LDA-determined HSC frequencies and 95% c.i. (in brackets) (see Appendices A.4 and A.5). Values shown are the mean ± s.e.m. One-tailed Student's t-tests were used to assess statistical significance. **P* < 0.05, ***P* < 0.01.

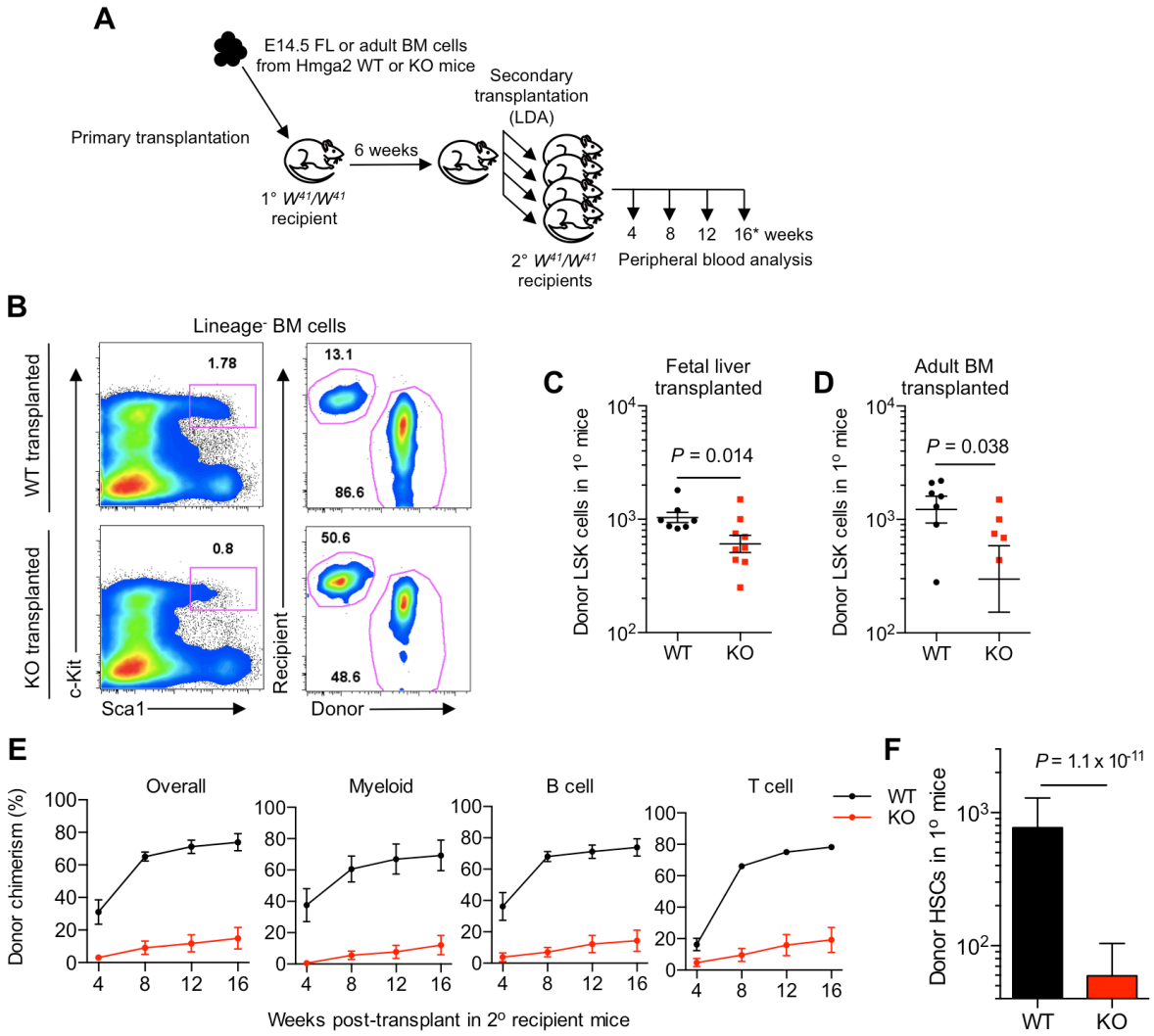

Figure 3.10 Hmga2 is required for the high self-renewal activity of fetal HSCs

(A) Schematic representation of the experimental design involving the transplantation of $1.7x10^5$ E14.5 fetal liver (FL) or $2.0x10^5$ adult BM cells from *Hmga2* KO or WT mice. 6 weeks later, daughter HSCs produced *in vivo* were measured by LDA. Asterisks indicate the HSC-defining PB analysis time point. **(B)** Representative FACS plots showing donor and recipient chimerism within the LSK fraction of the recipients' BM 6-weeks following transplantation with $1.7x10^5$ E14.5 FL cells from WT or KO mice. Frequency of donor-type LSK cells per $1.0x10^6$ total cells in the BM of recipients of WT or KO **(C)** E14.5 FL or **(D)** adult BM cells 6-weeks after transplantation. Mean ± s.e.m for 7-9 mice per group from 2 experiments. **(E)** PB chimerism in secondary recipients of the highest dose of BM cells obtained from the primary recipients of $1.7x10^5$ WT or KO E14.5 FL cells (2.5% of the total primary recipient BM). Values shown are the mean ± s.e.m, 10 mice per group from 2 experiments. **(F)** Donor HSCs (mean ± 95% c.i.) in primary recipients of $1.7x10^5$ WT or KO FL cells as determined by ELDA software on groups of transplanted mice (see Appendix A.6). Data are from 3 separate experiments in which 4-12 mice were tested at each of 7 different transplant doses. One-tailed Student's *t*-tests were used to assess statistical significance unless otherwise indicated.

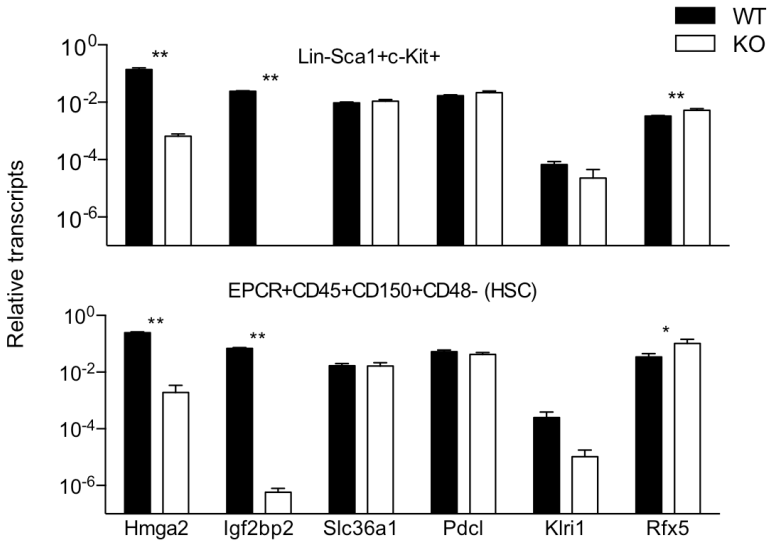

Figure 3.11 Fetal *Hmga2* KO HSCs and progenitors express lower levels of *Igf2bp2*
(A) qRT-PCR analysis of transcripts relative to *Gapdh* in LSK cells and HSCs isolated from *Hmga2*$^{+/+}$ (WT; black bars) and *Hmga2*$^{-/-}$ (KO; white bars) E14.5 fetal livers. *Aktip* was tested but could not be detected above background in any samples. Candidate genes were identified by an Affymetrix comparison of E14.5 FL LSK cells from Hmga2 KO and WT littermates (see Appendix A.7). All data represent the mean ± s.e.m. of 3-5 samples per group. One-tailed Student's *t*-tests were used to assess statistical significance. **P*<0.05, ***P*<0.01.

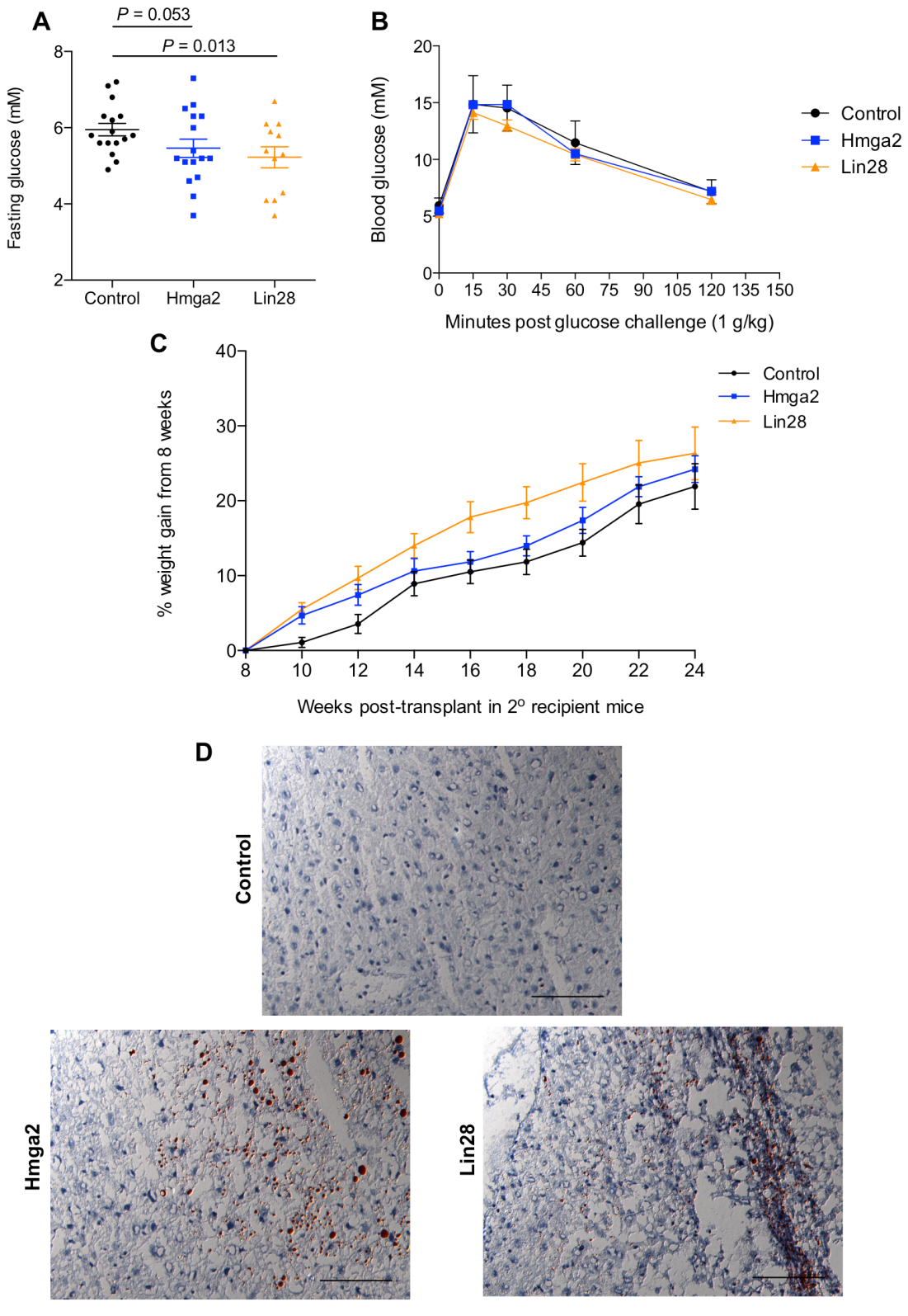
A
P = 0.053
P = 0.013
Fasting glucose (mM)
8
6
4
2
Control
Hmga2
Lin28
B
Blood glucose (mM)
20
15
10
5
0
0 15 30 45 60 75 90 105 120 135 150
Minutes post glucose challenge (1 g/kg)
Control
Hmga2
Lin28
C
% weight gain from 8 weeks
40
30
20
10
0
8 10 12 14 16 18 20 22 24
Weeks post-transplant in 2º recipient mice
Control
Hmga2
Lin28
D
Control
Hmga2
Lin28

Figure 3.12 Recipients of Hmga2 and Lin28 overexpressing BM cells display evidence of altered glucose and lipid handling

(A) Blood glucose levels in secondary recipients of a high dose of BM cells obtained from primary recipients (estimated as 8% of the total mouse BM assuming 2 femurs plus 2 tibiae represent 25% of the total BM) of adult BM HSCs from an experiment designed similarly to that depicted in Figure 3.2A. Recipients groups were age and sex matched and analyzed at 8 weeks post-transplant following an overnight fast. Values shown are the mean ± s.e.m. for 16 mice per group from 4 separate experiments. **(B)** Blood glucose levels at 8 weeks post-transplant following a 1g/kg glucose challenge. Values shown are the mean ± s.e.m. for 16 mice per group from 4 separate experiments. **(C)** Weights (normalized to 8-week starting point) of mice analyzed in (A) after being initiated on a high-fat diet. Values shown are the mean ± s.e.m. for 16 mice per group from 4 separate experiments. **(D)** Cryosections of liver tissue isolated from secondary recipients of the mice analyzed in (A) 24 weeks post-transplant. Mice were fed a high-fat diet for the preceding 16 weeks. Oil Red O stained. Bar in the bottom right is a scale bar representing 100 μm.

Chapter 4 Discussion

4.1 Major contributions

The overall goal of the work described in this thesis was to elucidate the molecular and cellular mechanisms responsible for the higher self-renewal activity of fetal compared to adult HSCs. Herein, I describe a series of experiments that together point to Lin28b as the master regulator of the high self-renewal potential of fetal HSCs. This action is ultimately mediated through inhibition of let-7 miRNAs, which in turn leads to the upregulation of Hmga2.

In Chapter 2, I describe experiments in which prospectively isolated populations of HSCs from different developmental sources were compared. Since the interpretation of previous studies of a similar nature are confounded by the relatively low HSC content of the populations being compared (169) and/or the different phenotypes that were required to isolate highly-enriched HSCs from fetal compared to adult sources (4, 70, 71), I worked with David Kent and Claudia Benz to establish a new HSC-isolation strategy that would partially circumvent these issues. This involved combining the EPCR (67) and SLAM ($CD150^{+}CD48^{-}$) (38, 72) HSC markers with CD45, to simplify gating of the required populations, in order to ultimately yield the ESLAM strategy (2, 4). Isolation of ESLAM cells from E14.5 FL, 3-week BM, 4-week BM and adult BM enables recovery of HSCs at extremely high frequencies (~1 in 2), and also permits a common phenotype to be applied. Since single cell transplants were performed as a means to determine HSC frequencies, we were also able to characterize the differentiation patterns of the transplanted HSCs in a similar manner to that previously determined for adult BM HSCs (i.e. α, β, γ or δ) (24). Interestingly, the relative proportions of these HSC subtypes were found to change most dramatically between E14.5 and 3-weeks of age, with little change between 3 and 4 weeks. This therefore suggests that the mechanisms responsible for the

generation and expansion of specific HSC subtypes are not directly linked to the fetal-to-adult developmental transition that occurs between 3 and 4 weeks of life (70), but rather parallel the expansion in numbers that occurs throughout fetal and neonatal life (2). Using multiple strategies for the identification of candidate developmentally-regulated HSC genes (i.e. Long-SAGE and Affymetrix), *Hmga2* was identified as being expressed at a higher level in fetal HSC-containing populations. Additionally, unlike many other candidate genes, the differential expression pattern of *Hmga2* was retained within fetal and adult ESLAM cells. I also found an inverse pattern of expression of several let-7 family miRNAs, and a parallel expression pattern of the let-7 inhibitor Lin28b. Although several other studies have similarly identified a differential expression of Lin28b, let-7 and Hmga2 between fetal and adult hematopoietic sources (140, 183), this is the first demonstration that these differences also apply to highly-enriched HSCs. An additional contribution of this work is the finding that *Hmga2* expression in fetal HSCs is not a direct consequence of their rapid cycling (69), but rather a stable, developmentally-regulated feature of these cells. Another candidate gene identified in this study, *Smarcc1*, was found to represent a consequence of the greater proliferative activity of fetal HSCs. This finding indicates that it will be important to consider the contribution of this difference in cellular state (i.e. cycling versus non-cycling) in future studies comparing FL and adult BM HSC populations.

In the work described in Chapter 3, I performed a series of experiments designed to investigate the functional consequence(s) of the developmentally-regulated expression patterns of components of the Lin28b-let-7-Hmga2 axis. Using a combination of lentivirus-mediated overexpression and an *Hmga2* knockout mouse model (195), I found that a high level of Hmga2 expression is both necessary and sufficient for the fetal HSC high self-renewal state. This finding suggests that the competitive advantage endowed upon both mouse and human HSCs following

mutations that truncate the let-7 miRNA binding sites within the *Hmga2* transcript (51, 205, 212), may involve an activation of a fetal-like self-renewal within these cells. In these experiments, I also found that Hmga2 protein levels in adult HSCs can be altered by inhibition of let-7 miRNAs. Since Lin28b is expressed higher in fetal compared to adult HSCs, and can also induce a fetal-like pattern of HSC regeneration following its overexpression, Lin28b is likely the ultimate upstream regulator of fetal Hmga2 levels. These findings are summarized in Figure 4.1.

An additional contribution of this work was the finding that Lin28b-controlled developmental differences in HSC lymphopoietic potential (140), unlike the Lin28b-controlled self-renewal differences, are *not* regulated through induction of Hmga2 expression. Therefore, my findings not only strengthen the previously-proposed role for Lin28b as a master regulator of fetal HSC identity (140), but also suggest that Lin28b-mediated inhibition of let-7 levels has consequences beyond the derepression of Hmga2 expression. A model summarizing this proposed molecular control of the distinct branches of fetal HSC properties is shown in Figure 4.2.

Concerning the mechanism by which Hmga2 alters the self-renewal activity of fetal HSCs, my finding that *Hmga2*-null fetal HSCs show a substantial alteration in their levels of *Igf2bp2* suggest that it may play an important role. Specifically, Igf2bp2-mediated activation of autocrine and/or paracrine production of its target, IGF-2 (208, 209), could provide a mechanism by which ectopic Hmga2 overexpression in adult HSCs, or physiologic Hmga2 expression in fetal HSCs, exerts its effect. This notion is strengthened by the observation that murine HSC self-renewal divisions can be supported in vitro by recombinant IGF-2 (189).

Together, these findings provide evidence that the cell-intrinsic down-modulation of murine HSC self-renewal potential is a consequence of a reduced level of expression of Lin28b,

which in turn inhibits let-7 miRNA biogenesis, and permits a higher level of Hmga2 expression. These molecules are altered within HSCs themselves, strengthening the concept that the 3-to-4 week post-natal developmental switch in HSC properties (70) is regulated by cell-intrinsic mechanisms. Interestingly, since I have suggested that autocrine and/or paracrine production of IGF-2 may act downstream of Hmga2 in fetal HSCs, this "cell-intrinsic" process may in fact involve a non cell-autonomous mechanism whereby the progeny of seeded HSCs establish a supportive "hematopoietic island", which in turn activates a higher self-renewal of HSCs.

4.2 Implications and future directions

4.2.1 Regulation of organismal growth

Regulation of embryonic, fetal and post-natal mammalian growth is typically considered an endocrine-mediated process. The most central of such endocrine growth regulators is growth hormone (GH), also known as somatotropin, which is released from the anterior pituitary in response to growth hormone-releasing hormone. Binding of GH to the GH receptor, found on many tissues including liver and muscle, triggers the expression and release of IGF-1 (222). Intriguingly, this pathway is only a relative requirement for normal growth since GH receptor deletion and IGF-1 deletion both result in viable mice that are substantially smaller in size than their wild-type counterparts (223, 224). IGF-2-null mice also have a growth defect, however, unlike IGF-1-null mice, the decreased growth rate is limited to the time before birth (225). This pattern is consistent with the prenatal-restricted pattern of IGF-2 expression within rodents (226).

As mentioned previously, Hmga2-null mice have a remarkably similar phenotype to IGF-1- or IGF-2-null mice and only reach ~40% the size of their wild-type littermates as adults (214). Interestingly, unlike other naturally occurring dwarf mice, pituitary and serum GH levels in

Hmga2-null mice are normal (220). My finding that fetal HSCs isolated from Hmga2 KO mice and transplanted into WT recipients maintain a lower self-renewal phenotype, suggests that the HSCs themselves possess a cell-intrinsic defect. This also implies that the smaller number of HSCs present in *Hmga2* KO mice is not a consequence of an endocrine abnormality. A cell-intrinsic defect has also been observed for neural stem cells isolated from these mice (183). These findings, together with the observation that *Hmga2* is expressed in multiple fetal tissues (182), and that fetal neural (183), neural crest (227) and mammary stem cells (Makarem et al., Unpublished) also display a cell-intrinsic heightened self-renewal potential, indicate that the pygmy phenotype of Hmga2 KO mice may be the result of a pan-tissue cell-autonomous growth deficiency that is ultimately mediated by defects in the stem cells that supply these tissues.

4.2.2 Timing of developmental transitions

The developmental downregulation of HSC self-renewal that occurs between 3 and 4 weeks after birth in mice can also proceed when fetal HSCs are transplanted into adult mice (70). This observation indicates that the factor(s) responsible for regulating the execution and timing of this transition are active within HSCs themselves, and not provided as a paracrine or endocrine message. In contrast to many of the transcripts identified in our previous study, which change their levels rapidly and dramatically between 3 and 4 weeks of age (70), *Hmga2*, *Lin28b* (140) and let-7 miRNAs (140) change their levels gradually between fetal and adult life (Figure 4.1). This suggests that these genes may be components of a developmental clock, in which the timing is determined by accumulation and/or titration of these molecules. Interestingly, the Lin28-let-7 pairing has been implicated in the regulation of such a developmental transition in *C. elegans*. This larval-to-adult transition, which involves a switch from cycling to quiescence of a stem-like population known as seam cells, is regulated by the downregulation of Lin28, which in

turn triggers an up-regulation of let-7 (201). In let-7 mutant animals, the seam cells do not exit the cell-cycle but instead reiterate a larval fate (201). Thus, the timing mechanism of this transition is thought to involve the accumulation of let-7 miRNAs.

Our finding that let-7 levels increase in HSCs between fetal and adult life bears a striking resemblance to this larval-to-adult transition of *C. elegans*. Thus, the developmental downregulation of Lin28b, which regulates the differences in the self-renewal activities of fetal compared to adult HSCs, may also be responsible for the timing of this transition that occurs between 3 and 4 weeks of age. This raises the possibility that such cell-intrinsic development timing mechanisms represent highly evolutionarily conserved processes.

Developmental transitions of hematopoietic cells not only occur in HSCs, but also in megakaryocyte progenitors (113, 114), myeloid progenitors (116, 228), CFU-E (117), B-progenitors (124, 125) and T cells (127). Since I have found the differential expression pattern of Lin28b, let-7 miRNAs and Hmga2, to extend into the LSK compartment, the components of this HSC developmental timer may remain active within more differentiated hematopoietic subsets. This is supported by the recent evidence that let-7 miRNAs also regulate developmental differences in B-cells, T-cells (140) and megakaryocytes (141).

4.2.3 Pathogenesis of childhood cancers

Approximately 2% of all cancer cases in Western countries occur within childhood, a period spanning from birth to 15 years of age (229). These include, in descending order of prevalence, leukemia, lymphoma, CNS tumors, neuroblastomas, soft-tissue sarcomas, nephroblastomas (Wilms' tumour), bone tumors, retinoblastomas, hepatoblastomas and germ-cell tumors (229). In contrast to adult leukemias, which are most frequently myeloid diseases, the vast majority of childhood leukemias are acute lymphoblastic leukemias (ALL) (230).

Interestingly, the incidence of ALL does not increase gradually throughout childhood, but rather shows a peak at approximately 5 years of age (229). It may therefore be speculated that the microenvironment and/or leukemia initiating cells undergo a transition in their susceptibility to oncogenic transformation during early childhood.

This concept is strengthened by the observation of pediatric-exclusive mutations and susceptibility syndromes, and examples of spontaneous age-associated tumour regression. The *TEL-AML1* fusion oncogene is the most frequent mutation found in pediatric ALL, present in ~25% of all cases (231), but is rarely, if ever, found in adult ALL (232). While the reasons for this remain unknown, a possible explanation could be the absence or presence of different protective or cooperating factors in the hematopoietic cells of children but not adults. This explanation could also apply to the window of early childhood in which patients with Noonan syndrome are at an increased risk of developing a myelproliferative disorder, a risk which returns to baseline after this window despite the responsible genetic lesions remaining (233). Additional evidence of age-specific cooperating oncogenic factors can be derived from examples of spontaneously improving pediatric leukemias. Although rare, cases of juvenile myelomonocytic leukemia have been found to spontaneously regress, even in the absence of treatment (234). Furthermore, a megakaryoblastic leukemia that occurs exclusively in children with Down syndrome, known as the transient myeloproliferative disorder, spontaneously resolves within the first 3 months of life, and is therefore only treated based on the patient's symptoms (235).

Lin28b and Hmga2 are oncogenes (184, 236), and let-7 miRNAs are tumor suppressors (237). Thus, the expression pattern of these genes in fetal and neonatal hematopoietic cells would be anticipated to create a "primed" background for the generation of leukemia. Furthermore, these genes are cell-intrinsically programmed to switch their expression pattern during the

transition to adulthood, which might serve as a mechanism responsible for the occasionaly observed spontaneous regression of certain fetal/neonatal onset leukemic disorders. In these cases, the "developmental hits" which are cooperating with acquired or genetic lesions, would be predicted to be downregulated during early life, thus leading to a collapse of the molecular program driving the progression of these diseases. It is fascinating to note that spontaneous regression also occurs in some pediatric solid tumours (229). This raises the possibility that the embryonic/fetal expression of components of the Lin28b-let-7-Hmga2 axis may be more broadly applicable to pediatric malignancies and perhaps related to a more general role in fetal-adult changes in tissue homeostasis. The recently elucidated requirement for the HMGA2-IGF2BP2 axis in the pathogenesis of NRAS mutant embryonic rhabdomyosarcoma (238) lends further support to this idea.

LIN28A and LIN28B are frequently upregulated in adult malignancies and are associated with advanced forms of many of these diseases (236). Thus, the LIN28B-let-7-HMGA2 pathway may also be relevant to the pathogenesis and treatment of adult malignancies. Of particular interest is our discovery that Lin28 overexpression in Hmga2-null adult HSCs leads to a failure of HSC generation, as evidenced by a lack of hematopoiesis in secondary recipients of their progeny. In normal HSCs and/or progenitors, *Hmga2* expression is required downstream of Lin28 in order for Lin28 overexpression to create a fetal-like state. Although it remains unclear how this mechanism operates, perhaps the upregulation of Lin28 in the absence of Hmga2 can actually block HSC self-renewal capability. If this is indeed true, mimicking this approach might provide a novel treatment modality for malignancies where LIN28 and/or HMGA2 are deregulated. This might be accomplished through inhibition of pathways downstream of LIN28 using small molecular inhibitors such as rapamycin (239) and metformin (240), although these

would be also be anticipated to interfere with normal cell function since the targets of these drugs are components of many normal signaling pathways. In contrast, LIN28A and LIN28B are not normally expressed in adult tissues and therefore their direct blockade may enable a more specific targeting of cancer cells where they are upregulated. Such an effect might also be achieved by antagonizing the pri- or pre-let-7 binding activity of LIN28B and LIN28A, respectively (176). The preliminary evidence provided in Chapter 3 that Hmga2 may mediate at least some of its effects through activation of IGF-2 expression suggests that antagonizing IGF-2 (e.g., using blocking antibodies) might offer another approach to achieve this effect.

4.2.4 HSC transplantation

HSC transplantation is a well-established technique that has been used to treat over 30 different types of familial and acquired hematologic diseases (241). A major barrier to patient access to allogeneic HSC transplantation is the requirement to have a human leukocyte antigen (HLA)-matched donor. Currently, ~30% of patients requiring allogeneic HSC transplantation are not candidates for this life-saving procedure due to lack of a suitable donor (241).

Three general strategies have been proposed to improve the supply of HSC transplantation sources in order to permit more patients access to this treatment. The first of these, sometimes referred to as the "holy grail" of translational HSC research, is the *ex vivo* expansion of HSCs. Since this occurs readily *in vivo* (i.e. following HSC transplantation or during growth and development), it should theoretically be possible to replicate these conditions *in vitro*, and thereby enable the generation of a limitless supply of HSCs even using autologous sources when these may be limiting. In spite of substantial efforts being applied to this area, the most recent protocols offer only modest if any net increases in HSC numbers (242). Another approach has been to direct the differentiation of embryonic stem cells or induced pluripotent

stem cells to a hematopoietic fate. This has also been met with limited success to date and has netted only convincing evidence for the generation of hematopoietic progenitors (243). The third of such strategies has been the use of alternate sources of HSCs, most notably of umbilical cord blood (CB) HSCs. Since CB is an easily harvested product that is normally discarded, it represents a source that can be easily banked and used for both research and clinical use. CB is routinely used in the pediatric setting, however, transplantation in adults is performed less frequently due to the limiting numbers of repopulating cells in CB samples (244).

An additional strategy, informed by some of the results described in this thesis, could be the manipulation of HSCs *ex vivo* in a manner that would increase their expansion following transplantation. This could theoretically increase the effective cell dose, and in turn broaden the utility of CB and/or *ex vivo* expanded HSCs. Evidence of such an effect is found in the dominant clones containing *HMGA2* insertional mutations observed in several clinical gene therapy trials. Using new sequencing technologies, the clonal dynamics of HSC and progenitor cells within patients undergoing gene therapy for hematologic conditions can be studied. In a recent report of 8 patients that were being monitored following a transplantation of lentivirus-corrected autologous bone marrow cells for treatment of their X-linked severe-combined immunodeficiency, 2 patients were found to harbor clones where the viral cassette had inserted within the large third intron of the *HMGA2* gene. In both of these cases, the *HMGA2* insertional mutant clone demonstrated a dominant behaviour, with one clone representing 6% of all transduced cells (50). In both of these cases, the mutation generated a truncated transcript lacking the let-7 miRNA binding sites, thus leading to derepression (i.e. overexpression) of *HMGA2*. A similar mutation and case of clonal dominance was recently reported in a patient undergoing gene therapy treatment for β-thalassemia. Interestingly, in this case, the clonal dominance was

responsible for the therapeutic effect since it permitted the pool of corrected HSCs to reach a therapeutic threshold (51). This finding suggests that deliberate overexpression of *HMGA2* in parallel with the transgene of interest may enhance the efficacy of such therapies. This might be particularly useful in cases like β-thalassemia where a large portion of HSCs must be corrected in order to achieve a therapeutic effect. A potential consequence of permanently activating *HMGA2* expression in HSCs could be an increase the incidence of leukemia. However, this was not observed in my mice containing Hmga2-overexpressing HSCs after a follow-up period of greater than 600 days (data not shown), nor has it been reported for patients transplanted with HSCs harboring insertional *HMGA2* mutants.

As mentioned, HSCs from 3-week old mice reconstitute the HSC compartment of recipient mice with the same initially rapid kinetics of fetal HSCs, but cells isolated from donors only 1 week older display a lower, adult-like, reconstitution pattern in the same type of experiment (70). Since the reconstitution kinetics are measured by transplanting HSCs, and fetal HSCs are known to undergo the fetal-to-adult transition, even when transplanted (70), it follows that the fetal (and 3-week BM) reconstitution pattern is likely to be a consequence of differences that occur within the first week post-transplant. If this were not the case, 3-week HSCs would be expected to produce a fetal/adult hybrid pattern of reconstitution, since the 3-week HSCs become the equivalent of 4-week HSCs, within 1 week after transplantation. An important implication of this observation is that any pre-transplantation manipulation of HSCs aimed at activating a fetal-like self-renewal would only need to be transiently, not permanently, operational. This could be achieved using transient, non-genetic techniques, such as recombinant HMGA2 fused to cell-penetrating peptides (245). Another strategy, that was recently found to lead to HMGA2 derepression in HeLa cells, is let-7-seed-targeting using tiny locked nucleic acids (LNAs) (246).

These 8-mer LNAs are complementary to the seed-region of miRNA target sites within the 3' UTRs of target transcripts, and thus block the repressive action of their corresponding miRNA families and derepress the expression of target genes. These small molecules can enter cells without the aid of transfection reagents and can also be used *in vivo* (246). These properties make such reagents attractive to consider for treatment of cells destined for transplantation into patients.

4.3 Concluding comments

The results provided in this thesis directly demonstrate that mouse fetal HSCs undergo a molecular transition that is responsible for the decreased self-renewal activity of these cells in the adult mouse (70). Interestingly, components of the Lin28b-let-7-Hmga2 axis, and its downstream target Igf2bp2, are known to be both differentially expressed across development and/or responsible for developmental differences in stem cell properties of other tissue-specific stem cells across different species (183, 201, 204, 206, 227). Together, these findings suggest developmental modulation of self-renewal activity may be not only a tissue-wide, but also a developmentally conserved, regulatory mechanism for the control of tissue, organ and organismal growth. This cell-autonomous mechanism may be particularly necessary for tissues, such as the blood and nervous systems, that cannot be regulated by cell density mediated regulators of organ size, such as that of the Hippo pathway (247). In support of this concept is the finding that permanent inhibition of Hippo signaling within the hematopoietic system of transgenic mice does not alter HSC numbers or function, as it does in many other tissues (248). Thus, a downregulation of the Lin28b-let-7-Hmga2 axis may act in a partially overlapping fashion, along with a decrease in the activity of the endocrine GH-IGF-1 axis and an increase in

Hippo signaling, to control the growth of tissues in adults. These mechanisms may also serve to protect tissues from malignant transformation.

An important follow-up to this work would be an investigation of the relevance of the findings to human HSC biology. Observations of dominant *HMGA2*-activated clones in patients undergoing gene therapy treatments (50) provides convincing evidence that the let-7-HMGA2 pairing is active in human HSCs, and that HMGA2 may activate a fetal-like self-renewal in these cells. It is also established that Lin28b is expressed at significantly higher levels in human fetal liver and CB as compared to adult hematopoietic tissues (BM, thymus and lymph nodes) (140). It will also be interesting to investigate the consequences of the expression of LIN28 on the susceptibility of naïve human HSCs to transformation and the fetal-specific pathways that are aberrantly activated following LIN28, LIN28B or HMGA2 mutations in adult malignancies.

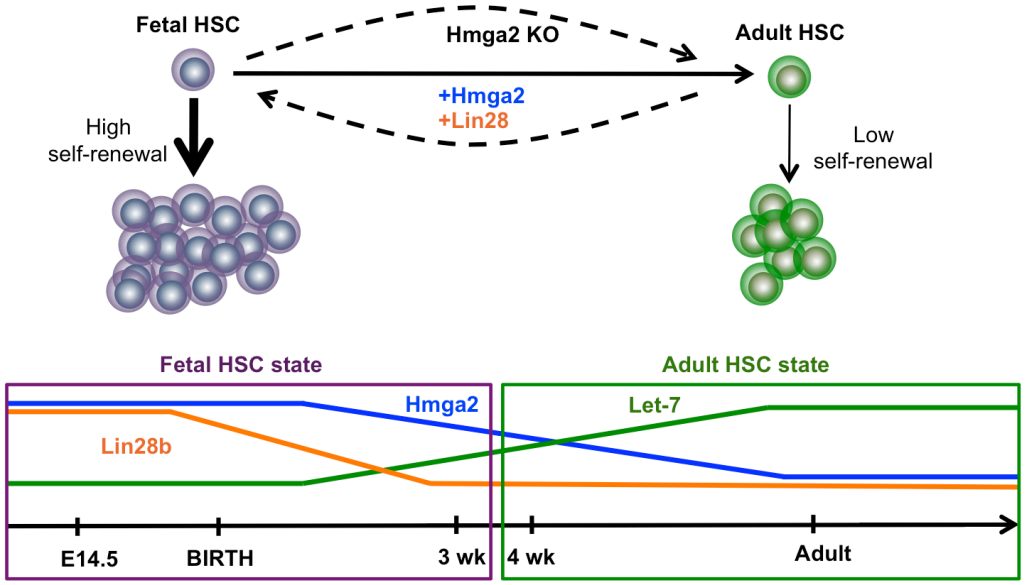

Figure 4.1 Developmental control of HSC self-renewal. The data presented in this thesis support a model whereby developmental changes in HSC self-renewal activity, shown previously to occur between 3 and 4 weeks after birth in the mouse (70), are mediated by the differences in the activity of the Lin28b-let-7-Hmga2 axis. The high self-renewal activity of fetal HSCs can be attained in adult HSCs by ectopic overexpression of Hmga2 or Lin28, and cannot be expressed by *Hmga2*$^{-/-}$ (KO) fetal HSCs. The fetal HSC state is characterized by a high level of expression of Lin28b, which inhibits let-7 miRNAs and thus permits expression of Hmga2.

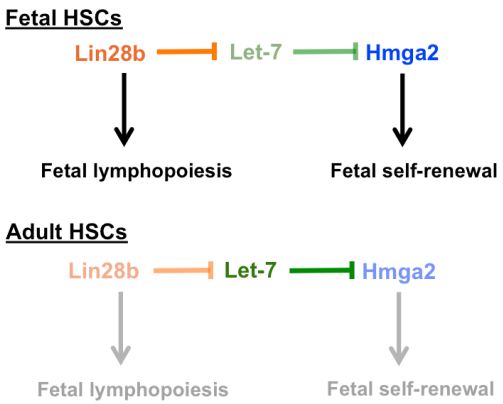

Figure 4.2 Molecular control of fetal HSC properties. Lin28b serves as a master regulator of fetal HSC identity, as evidenced by the activation of a fetal-like self-renewal and lymphopoietic phenotype following its overexpression (140). Lin28b-mediated inhibition let-7 miRNA biogenesis (174), followed by derepression of Hmga2 expression, serves as the mechanism by which Lin28b activates a fetal-like self-renewal. In contrast, fetal lymphopoiesis is activated either directly (as shown) or indirectly (through another let-7 target); however, this property is not activated through Hmga2 depression. Downregulation of Lin28b in adult HSCs leads to a repression of fetal properties in these cells.

References

1. Copley MR, Beer PA, Eaves CJ. Hematopoietic stem cell heterogeneity takes center stage. Cell stem cell. 2012;10(6):690-7. Epub 2012/06/19.
2. Benz C, Copley M, Kent D, Wohrer S, Cores A, Aghaeepour N, et al. Hematopoietic Stem Cell Subtypes Expand Differentially during Development and Display Distinct Lymphopoietic Programs. Cell stem cell. 2012;10(3):273-83.
3. Bowie MB, Kent DG, Copley MR, Eaves CJ. Steel factor responsiveness regulates the high self-renewal phenotype of fetal hematopoietic stem cells. Blood. 2007;109(11):5043-8. Epub 2007/03/01.
4. Kent DG, Copley MR, Benz C, Wohrer S, Dykstra BJ, Ma E, et al. Prospective isolation and molecular characterization of hematopoietic stem cells with durable self-renewal potential. Blood. 2009;113(25):6342-50. Epub 2009/04/21.
5. Szilvassy SJ, Ragland PL, Miller CL, Eaves CJ. The marrow homing efficiency of murine hematopoietic stem cells remains constant during ontogeny. Experimental hematology. 2003;31(4):331-8. Epub 2003/04/15.
6. Cumano A, Godin I. Ontogeny of the hematopoietic system. Annual review of immunology. 2007;25:745-85. Epub 2007/01/05.
7. Medvinsky AL, Samoylina NL, Muller AM, Dzierzak EA. An early pre-liver intraembryonic source of CFU-S in the developing mouse. Nature. 1993;364(6432):64-7. Epub 1993/07/01.
8. Muller AM, Medvinsky A, Strouboulis J, Grosveld F, Dzierzak E. Development of hematopoietic stem cell activity in the mouse embryo. Immunity. 1994;1(4):291-301. Epub 1994/07/01.
9. Medvinsky A, Dzierzak E. Definitive hematopoiesis is autonomously initiated by the AGM region. Cell. 1996;86(6):897-906. Epub 1996/09/20.
10. de Bruijn MF, Speck NA, Peeters MC, Dzierzak E. Definitive hematopoietic stem cells first develop within the major arterial regions of the mouse embryo. The EMBO journal. 2000;19(11):2465-74. Epub 2000/06/03.
11. Gekas C, Dieterlen-Lievre F, Orkin SH, Mikkola HK. The placenta is a niche for hematopoietic stem cells. Developmental cell. 2005;8(3):365-75. Epub 2005/03/02.
12. Rhodes KE, Gekas C, Wang Y, Lux CT, Francis CS, Chan DN, et al. The emergence of hematopoietic stem cells is initiated in the placental vasculature in the absence of circulation. Cell stem cell. 2008;2(3):252-63. Epub 2008/03/29.
13. Kumaravelu P, Hook L, Morrison AM, Ure J, Zhao S, Zuyev S, et al. Quantitative developmental anatomy of definitive haematopoietic stem cells/long-term repopulating units (HSC/RUs): role of the aorta-gonad-mesonephros (AGM) region and the yolk sac in colonisation of the mouse embryonic liver. Development. 2002;129(21):4891-9. Epub 2002/10/25.
14. Houssaint E. Differentiation of the mouse hepatic primordium. II. Extrinsic origin of the haemopoietic cell line. Cell differentiation. 1981;10(5):243-52. Epub 1981/11/01.
15. Johnson GR, Moore MA. Role of stem cell migration in initiation of mouse foetal liver haemopoiesis. Nature. 1975;258(5537):726-8. Epub 1975/12/25.
16. Yoder MC, Hiatt K, Mukherjee P. In vivo repopulating hematopoietic stem cells are present in the murine yolk sac at day 9.0 postcoitus. Proceedings of the National Academy of Sciences of the United States of America. 1997;94(13):6776-80. Epub 1997/06/24.

17. Fleischman RA, Custer RP, Mintz B. Totipotent hematopoietic stem cells: normal self-renewal and differentiation after transplantation between mouse fetuses. Cell. 1982;30(2):351-9. Epub 1982/09/01.
18. Micklem HS, Ford CE, Evans EP, Ogden DA, Papworth DS. Competitive in vivo proliferation of foetal and adult haematopoietic cells in lethally irradiated mice. Journal of cellular physiology. 1972;79(2):293-8. Epub 1972/04/01.
19. Yoder MC. Generation of HSCs in the embryo and assays to detect them. Oncogene. 2004;23(43):7161-3. Epub 2004/09/21.
20. Mikkola HK, Orkin SH. The journey of developing hematopoietic stem cells. Development. 2006;133(19):3733-44. Epub 2006/09/14.
21. Ford CE, Hamerton JL, Barnes DW, Loutit JF. Cytological identification of radiation-chimaeras. Nature. 1956;177(4506):452-4. Epub 1956/03/10.
22. Jacobson LO, Simmons EL, Marks EK, Eldredge JH. Recovery from radiation injury. Science. 1951;113(2940):510-11. Epub 1951/05/04.
23. Doulatov S, Notta F, Laurenti E, Dick JE. Hematopoiesis: a human perspective. Cell stem cell. 2012;10(2):120-36. Epub 2012/02/07.
24. Dykstra B, Kent D, Bowie M, McCaffrey L, Hamilton M, Lyons K, et al. Long-term propagation of distinct hematopoietic differentiation programs in vivo. Cell stem cell. 2007;1(2):218-29. Epub 2008/03/29.
25. Till JE, McCulloch EA. A direct measurement of the radiation sensitivity of normal mouse bone marrow cells. Radiation research. 1961;14:213-22. Epub 1961/02/01.
26. Becker AJ, McCulloch EA, Till JE. Cytological demonstration of the clonal nature of spleen colonies derived from transplanted mouse marrow cells. Nature. 1963;197:452-4. Epub 1963/02/02.
27. Siminovitch L, McCulloch EA, Till JE. The Distribution of Colony-Forming Cells among Spleen Colonies. Journal of cellular physiology. 1963;62:327-36. Epub 1963/12/01.
28. Jones RJ, Collector MI, Barber JP, Vala MS, Fackler MJ, May WS, et al. Characterization of mouse lymphohematopoietic stem cells lacking spleen colony-forming activity. Blood. 1996;88(2):487-91. Epub 1996/07/15.
29. Ploemacher RE, Brons RH. Separation of CFU-S from primitive cells responsible for reconstitution of the bone marrow hemopoietic stem cell compartment following irradiation: evidence for a pre-CFU-S cell. Experimental hematology. 1989;17(3):263-6. Epub 1989/03/01.
30. Ploemacher RE, van der Sluijs JP, Voerman JS, Brons NH. An in vitro limiting-dilution assay of long-term repopulating hematopoietic stem cells in the mouse. Blood. 1989;74(8):2755-63. Epub 1989/12/01.
31. Lemieux ME, Rebel VI, Lansdorp PM, Eaves CJ. Characterization and purification of a primitive hematopoietic cell type in adult mouse marrow capable of lymphomyeloid differentiation in long-term marrow "switch" cultures. Blood. 1995;86(4):1339-47. Epub 1995/08/15.
32. Sutherland HJ, Eaves CJ, Eaves AC, Dragowska W, Lansdorp PM. Characterization and partial purification of human marrow cells capable of initiating long-term hematopoiesis in vitro. Blood. 1989;74(5):1563-70. Epub 1989/10/01.
33. Ploemacher RE, van der Sluijs JP, van Beurden CA, Baert MR, Chan PL. Use of limiting-dilution type long-term marrow cultures in frequency analysis of marrow-repopulating and spleen colony-forming hematopoietic stem cells in the mouse. Blood. 1991;78(10):2527-33. Epub 1991/11/15.

34. Harrison DE. Competitive repopulation: a new assay for long-term stem cell functional capacity. Blood. 1980;55(1):77-81. Epub 1980/01/01.
35. Harrison DE. Evaluating functional abilities of primitive hematopoietic stem cell populations. Curr Top Microbiol Immunol. 1992;177:13-30. Epub 1992/01/01.
36. Szilvassy SJ, Humphries RK, Lansdorp PM, Eaves AC, Eaves CJ. Quantitative assay for totipotent reconstituting hematopoietic stem cells by a competitive repopulation strategy. Proceedings of the National Academy of Sciences of the United States of America. 1990;87(22):8736-40. Epub 1990/11/01.
37. Jordan CT, Lemischka IR. Clonal and systemic analysis of long-term hematopoiesis in the mouse. Genes & development. 1990;4(2):220-32. Epub 1990/02/01.
38. Kiel MJ, Yilmaz OH, Iwashita T, Yilmaz OH, Terhorst C, Morrison SJ. SLAM family receptors distinguish hematopoietic stem and progenitor cells and reveal endothelial niches for stem cells. Cell. 2005;121(7):1109-21. Epub 2005/07/02.
39. Osawa M, Hanada K, Hamada H, Nakauchi H. Long-term lymphohematopoietic reconstitution by a single CD34-low/negative hematopoietic stem cell. Science. 1996;273(5272):242-5. Epub 1996/07/12.
40. Uchida N, Dykstra B, Lyons KJ, Leung FY, Eaves CJ. Different in vivo repopulating activities of purified hematopoietic stem cells before and after being stimulated to divide in vitro with the same kinetics. Experimental hematology. 2003;31(12):1338-47. Epub 2003/12/10.
41. Lu R, Neff NF, Quake SR, Weissman IL. Tracking single hematopoietic stem cells in vivo using high-throughput sequencing in conjunction with viral genetic barcoding. Nature biotechnology. 2011;29(10):928-33. Epub 2011/10/04.
42. Schroeder T. Hematopoietic Stem Cell Heterogeneity: Subtypes, Not Unpredictable Behavior. Cell stem cell. 2010;6(3):203-7.
43. Ding L, Saunders TL, Enikolopov G, Morrison SJ. Endothelial and perivascular cells maintain haematopoietic stem cells. Nature. 2012;481(7382):457-62. Epub 2012/01/28.
44. McKinney-Freeman S, Cahan P, Li H, Lacadie SA, Huang HT, Curran M, et al. The transcriptional landscape of hematopoietic stem cell ontogeny. Cell stem cell. 2012;11(5):701-14. Epub 2012/11/06.
45. Petriv OI, Kuchenbauer F, Delaney AD, Lecault V, White A, Kent D, et al. Comprehensive microRNA expression profiling of the hematopoietic hierarchy. Proceedings of the National Academy of Sciences of the United States of America. 2010;107(35):15443-8. Epub 2010/08/13.
46. Hope KJ, Cellot S, Ting SB, MacRae T, Mayotte N, Iscove NN, et al. An RNAi screen identifies Msi2 and Prox1 as having opposite roles in the regulation of hematopoietic stem cell activity. Cell stem cell. 2010;7(1):101-13. Epub 2010/07/14.
47. Daniel R, Smith JA. Integration site selection by retroviral vectors: molecular mechanism and clinical consequences. Human gene therapy. 2008;19(6):557-68. Epub 2008/06/07.
48. Gerrits A, Dykstra B, Kalmykowa OJ, Klauke K, Verovskaya E, Broekhuis MJ, et al. Cellular barcoding tool for clonal analysis in the hematopoietic system. Blood. 2010;115(13):2610-8. Epub 2010/01/23.
49. Kamel-Reid S, Dick JE. Engraftment of immune-deficient mice with human hematopoietic stem cells. Science. 1988;242(4886):1706-9. Epub 1988/12/23.
50. Wang GP, Berry CC, Malani N, Leboulch P, Fischer A, Hacein-Bey-Abina S, et al. Dynamics of gene-modified progenitor cells analyzed by tracking retroviral integration sites in a human SCID-X1 gene therapy trial. Blood. 2010;115(22):4356-66. Epub 2010/03/17.

51. Cavazzana-Calvo M, Payen E, Negre O, Wang G, Hehir K, Fusil F, et al. Transfusion independence and HMGA2 activation after gene therapy of human beta-thalassaemia. Nature. 2010;467(7313):318-22. Epub 2010/09/17.
52. Cavazzana-Calvo M, Fischer A. Gene therapy for severe combined immunodeficiency: are we there yet? The Journal of clinical investigation. 2007;117(6):1456-65. Epub 2007/06/06.
53. Benveniste P, Frelin C, Janmohamed S, Barbara M, Herrington R, Hyam D, et al. Intermediate-term hematopoietic stem cells with extended but time-limited reconstitution potential. Cell stem cell. 2010;6(1):48-58. Epub 2010/01/16.
54. Spangrude GJ, Heimfeld S, Weissman IL. Purification and characterization of mouse hematopoietic stem cells. Science. 1988;241(4861):58-62. Epub 1988/07/01.
55. Ikuta K, Weissman IL. Evidence that hematopoietic stem cells express mouse c-kit but do not depend on steel factor for their generation. Proceedings of the National Academy of Sciences of the United States of America. 1992;89(4):1502-6. Epub 1992/02/15.
56. Adolfsson J, Borge OJ, Bryder D, Theilgaard-Monch K, Astrand-Grundstrom I, Sitnicka E, et al. Upregulation of Flt3 expression within the bone marrow Lin(-)Sca1(+)c-kit(+) stem cell compartment is accompanied by loss of self-renewal capacity. Immunity. 2001;15(4):659-69. Epub 2001/10/24.
57. Christensen JL, Weissman IL. Flk-2 is a marker in hematopoietic stem cell differentiation: a simple method to isolate long-term stem cells. Proceedings of the National Academy of Sciences of the United States of America. 2001;98(25):14541-6. Epub 2001/11/29.
58. Yilmaz OH, Kiel MJ, Morrison SJ. SLAM family markers are conserved among hematopoietic stem cells from old and reconstituted mice and markedly increase their purity. Blood. 2006;107(3):924-30. Epub 2005/10/13.
59. Wagers AJ, Weissman IL. Differential expression of alpha2 integrin separates long-term and short-term reconstituting Lin-/loThy1.1(lo)c-kit+ Sca-1+ hematopoietic stem cells. Stem Cells. 2006;24(4):1087-94. Epub 2005/12/24.
60. Benveniste P, Cantin C, Hyam D, Iscove NN. Hematopoietic stem cells engraft in mice with absolute efficiency. Nature immunology. 2003;4(7):708-13. Epub 2003/05/27.
61. Pearce DJ, Ridler CM, Simpson C, Bonnet D. Multiparameter analysis of murine bone marrow side population cells. Blood. 2004;103(7):2541-6. Epub 2003/12/03.
62. Wolf NS, Kone A, Priestley GV, Bartelmez SH. In vivo and in vitro characterization of long-term repopulating primitive hematopoietic cells isolated by sequential Hoechst 33342-rhodamine 123 FACS selection. Experimental hematology. 1993;21(5):614-22. Epub 1993/05/01.
63. Bertoncello I, Hodgson GS, Bradley TR. Multiparameter analysis of transplantable hemopoietic stem cells: I. The separation and enrichment of stem cells homing to marrow and spleen on the basis of rhodamine-123 fluorescence. Experimental hematology. 1985;13(10):999-1006. Epub 1985/11/01.
64. Zhou S, Schuetz JD, Bunting KD, Colapietro AM, Sampath J, Morris JJ, et al. The ABC transporter Bcrp1/ABCG2 is expressed in a wide variety of stem cells and is a molecular determinant of the side-population phenotype. Nature medicine. 2001;7(9):1028-34. Epub 2001/09/05.
65. Zhou S, Morris JJ, Barnes Y, Lan L, Schuetz JD, Sorrentino BP. Bcrp1 gene expression is required for normal numbers of side population stem cells in mice, and confers relative protection to mitoxantrone in hematopoietic cells in vivo. Proceedings of the National Academy of Sciences of the United States of America. 2002;99(19):12339-44. Epub 2002/09/10.

66. Uchida N, Leung FY, Eaves CJ. Liver and marrow of adult mdr-1a/1b(-/-) mice show normal generation, function, and multi-tissue trafficking of primitive hematopoietic cells. Experimental hematology. 2002;30(8):862-9. Epub 2002/08/06.
67. Balazs AB, Fabian AJ, Esmon CT, Mulligan RC. Endothelial protein C receptor (CD201) explicitly identifies hematopoietic stem cells in murine bone marrow. Blood. 2006;107(6):2317-21.
68. Kent DG, Dykstra BJ, Cheyne J, Ma E, Eaves CJ. Steel factor coordinately regulates the molecular signature and biologic function of hematopoietic stem cells. Blood. 2008;112(3):560-7. Epub 2008/05/27.
69. Bowie MB, McKnight KD, Kent DG, McCaffrey L, Hoodless PA, Eaves CJ. Hematopoietic stem cells proliferate until after birth and show a reversible phase-specific engraftment defect. The Journal of clinical investigation. 2006;116(10):2808-16. Epub 2006/10/04.
70. Bowie MB, Kent DG, Dykstra B, McKnight KD, McCaffrey L, Hoodless PA, et al. Identification of a new intrinsically timed developmental checkpoint that reprograms key hematopoietic stem cell properties. Proceedings of the National Academy of Sciences of the United States of America. 2007;104(14):5878-82. Epub 2007/03/24.
71. Venezia TA, Merchant AA, Ramos CA, Whitehouse NL, Young AS, Shaw CA, et al. Molecular signatures of proliferation and quiescence in hematopoietic stem cells. Plos Biol. 2004;2(10):1640-51.
72. Kim I, He S, Yilmaz OH, Kiel MJ, Morrison SJ. Enhanced purification of fetal liver hematopoietic stem cells using SLAM family receptors. Blood. 2006;108(2):737-44. Epub 2006/03/30.
73. Noda S, Horiguchi K, Ichikawa H, Miyoshia H. Repopulating activity of ex vivo-expanded murine hematopoietic stem cells resides in the CD48(-)c-Kit(+)Sca-1(+)lineage marker(-) cell population. Stem Cells. 2008;26(3):646-55.
74. Till JE, McCulloch EA, Siminovitch L. A Stochastic Model of Stem Cell Proliferation, Based on the Growth of Spleen Colony-Forming Cells. Proceedings of the National Academy of Sciences of the United States of America. 1964;51:29-36. Epub 1964/01/01.
75. Humphries RK, Eaves AC, Eaves CJ. Self-renewal of hemopoietic stem cells during mixed colony formation in vitro. Proceedings of the National Academy of Sciences of the United States of America. 1981;78(6):3629-33. Epub 1981/06/01.
76. Humphries RK, Jacky PB, Dill FJ, Eaves AC, Eaves CJ. CFU-S in individual erythroid colonies derived in vitro from adult mouse marrow. Nature. 1979;279(5715):718-20. Epub 1979/06/21.
77. Ogawa M, Porter PN, Nakahata T. Renewal and commitment to differentiation of hemopoietic stem cells (an interpretive review). Blood. 1983;61(5):823-9. Epub 1983/05/01.
78. Dick JE, Magli MC, Huszar D, Phillips RA, Bernstein A. Introduction of a selectable gene into primitive stem cells capable of long-term reconstitution of the hemopoietic system of W/Wv mice. Cell. 1985;42(1):71-9. Epub 1985/08/01.
79. Lemischka IR, Raulet DH, Mulligan RC. Developmental potential and dynamic behavior of hematopoietic stem cells. Cell. 1986;45(6):917-27. Epub 1986/06/20.
80. Bryder D, Rossi DJ, Weissman IL. Hematopoietic stem cells: the paradigmatic tissue-specific stem cell. The American journal of pathology. 2006;169(2):338-46. Epub 2006/08/01.

81. Muller-Sieburg CE, Cho RH, Thoman M, Adkins B, Sieburg HB. Deterministic regulation of hematopoietic stem cell self-renewal and differentiation. Blood. 2002;100(4):1302-9. Epub 2002/08/01.
82. Muller-Sieburg C, Sieburg HB, Bernitz JM, Cattarossi G. Stem cell heterogeneity: implications for aging and regenerative medicine. Blood. 2012. Epub 2012/03/13.
83. Dykstra B, Olthof S, Schreuder J, Ritsema M, de Haan G. Clonal analysis reveals multiple functional defects of aged murine hematopoietic stem cells. The Journal of experimental medicine. 2011;208(13):2691-703. Epub 2011/11/24.
84. Sieburg HB, Cho RH, Dykstra B, Uchida N, Eaves CJ, Muller-Sieburg CE. The hematopoietic stem compartment consists of a limited number of discrete stem cell subsets. Blood. 2006;107(6):2311-6. Epub 2005/11/18.
85. Glotzbach JP, Januszyk M, Vial IN, Wong VW, Gelbard A, Kalisky T, et al. An information theoretic, microfluidic-based single cell analysis permits identification of subpopulations among putatively homogeneous stem cells. PloS one. 2011;6(6):e21211. Epub 2011/07/07.
86. Challen GA, Boles NC, Chambers SM, Goodell MA. Distinct hematopoietic stem cell subtypes are differentially regulated by TGF-beta1. Cell stem cell. 2010;6(3):265-78. Epub 2010/03/09.
87. Wang J, Sun Q, Morita Y, Jaing H, Grob A, Lechei A, et al. A Differentiation Checkpoint Limits Hematopoietic Stem Cell Self-Renewal in Response to DNA Damage. Cell. 2012;148(5):1001-14.
88. Broske AM, Vockentanz L, Kharazi S, Huska MR, Mancini E, Scheller M, et al. DNA methylation protects hematopoietic stem cell multipotency from myeloerythroid restriction. Nature genetics. 2009;41(11):1207-15. Epub 2009/10/06.
89. Hodges E, Molaro A, Dos Santos CO, Thekkat P, Song Q, Uren PJ, et al. Directional DNA methylation changes and complex intermediate states accompany lineage specificity in the adult hematopoietic compartment. Molecular cell. 2011;44(1):17-28. Epub 2011/09/20.
90. Ji H, Ehrlich LI, Seita J, Murakami P, Doi A, Lindau P, et al. Comprehensive methylome map of lineage commitment from haematopoietic progenitors. Nature. 2010;467(7313):338-42. Epub 2010/08/20.
91. Trowbridge JJ, Snow JW, Kim J, Orkin SH. DNA methyltransferase 1 is essential for and uniquely regulates hematopoietic stem and progenitor cells. Cell stem cell. 2009;5(4):442-9. Epub 2009/10/03.
92. Challen GA, Sun D, Jeong M, Luo M, Jelinek J, Berg JS, et al. Dnmt3a is essential for hematopoietic stem cell differentiation. Nature genetics. 2012;44(1):23-31. Epub 2011/12/06.
93. Wilson A, Laurenti E, Oser G, van der Wath RC, Blanco-Bose W, Jaworski M, et al. Hematopoietic stem cells reversibly switch from dormancy to self-renewal during homeostasis and repair. Cell. 2008;135(6):1118-29. Epub 2008/12/09.
94. Cheshier SH, Morrison SJ, Liao X, Weissman IL. In vivo proliferation and cell cycle kinetics of long-term self-renewing hematopoietic stem cells. Proceedings of the National Academy of Sciences of the United States of America. 1999;96(6):3120-5. Epub 1999/03/17.
95. Bradford GB, Williams B, Rossi R, Bertoncello I. Quiescence, cycling, and turnover in the primitive hematopoietic stem cell compartment. Experimental hematology. 1997;25(5):445-53. Epub 1997/05/01.
96. Catlin SN, Busque L, Gale RE, Guttorp P, Abkowitz JL. The replication rate of human hematopoietic stem cells in vivo. Blood. 2011;117(17):4460-6. Epub 2011/02/24.

97. Yamazaki S, Iwama A, Takayanagi S, Eto K, Ema H, Nakauchi H. TGF-beta as a candidate bone marrow niche signal to induce hematopoietic stem cell hibernation. Blood. 2009;113(6):1250-6. Epub 2008/10/24.
98. Yamazaki S, Ema H, Karlsson G, Yamaguchi T, Miyoshi H, Shioda S, et al. Nonmyelinating Schwann cells maintain hematopoietic stem cell hibernation in the bone marrow niche. Cell. 2011;147(5):1146-58. Epub 2011/11/29.
99. Miyamoto K, Araki KY, Naka K, Arai F, Takubo K, Yamazaki S, et al. Foxo3a is essential for maintenance of the hematopoietic stem cell pool. Cell stem cell. 2007;1(1):101-12. Epub 2008/03/29.
100. Zou P, Yoshihara H, Hosokawa K, Tai I, Shinmyozu K, Tsukahara F, et al. p57(Kip2) and p27(Kip1) cooperate to maintain hematopoietic stem cell quiescence through interactions with Hsc70. Cell stem cell. 2011;9(3):247-61. Epub 2011/09/03.
101. Takubo K, Goda N, Yamada W, Iriuchishima H, Ikeda E, Kubota Y, et al. Regulation of the HIF-1alpha level is essential for hematopoietic stem cells. Cell stem cell. 2010;7(3):391-402. Epub 2010/09/02.
102. Nakada D, Saunders TL, Morrison SJ. Lkb1 regulates cell cycle and energy metabolism in haematopoietic stem cells. Nature. 2010;468(7324):653-8. Epub 2010/12/03.
103. Hodgson GS, Bradley TR. In vivo kinetic status of hematopoietic stem and progenitor cells as inferred from labeling with bromodeoxyuridine. Experimental hematology. 1984;12(9):683-7. Epub 1984/10/01.
104. Iscove NN, Nawa K. Hematopoietic stem cells expand during serial transplantation in vivo without apparent exhaustion. Current biology : CB. 1997;7(10):805-8. Epub 1997/11/22.
105. Sieburg HB, Rezner BD, Muller-Sieburg CE. Predicting clonal self-renewal and extinction of hematopoietic stem cells. Proceedings of the National Academy of Sciences of the United States of America. 2011;108(11):4370-5. Epub 2011/03/04.
106. Morita Y, Ema H, Nakauchi H. Heterogeneity and hierarchy within the most primitive hematopoietic stem cell compartment. The Journal of experimental medicine. 2010;207(6):1173-82. Epub 2010/04/28.
107. McCulloch EA, Siminovitch L, Till JE. Spleen-Colony Formation in Anemic Mice of Genotype Ww. Science. 1964;144(3620):844-6. Epub 1964/05/15.
108. Sankaran VG, Xu J, Orkin SH. Advances in the understanding of haemoglobin switching. British journal of haematology. 2010;149(2):181-94.
109. McGrath K, Palis J. Ontogeny of erythropoiesis in the mammalian embryo. Curr Top Dev Biol. 2008;82:1-+.
110. DeAlarcon PA, Graeve JLA. Analysis of megakaryocyte ploidy in fetal bone marrow biopsies using a new adaptation of the feulgen technique to measure DNA content and estimate megakaryocyte ploidy from biopsy specimens. Pediatr Res. 1996;39(1):166-70.
111. Graeve JLA, Dealarcon PA. Megakaryocytopoiesis in the Human-Fetus. Arch Dis Child. 1989;64(4):481-4.
112. Ma DC, Sun YH, Chang KZ, Zuo W. Developmental change of megakaryocyte maturation and DNA ploidy in human fetus. Eur J Haematol. 1996;57(2):121-7.
113. Murray NA, Watts TL, Roberts IAG. Endogenous thrombopoietin levels and effect of recombinant human thrombopoietin on megakaryocyte precursors in term and preterm babies. Pediatr Res. 1998;43(1):148-51.
114. Nishihira H, Toyoda Y, Miyazaki H, Kigasawa H, Ohsaki E. Growth of macroscopic human megakaryocyte colonies from cord blood in culture with recombinant human

thrombopoietin (c-mpl ligand) and the effects of gestational age on frequency of colonies. British journal of haematology. 1996;92(1):23-8.
115. Liu ZJ, Italiano J, Ferrer-Marin F, Gutti R, Bailey M, Poterjoy B, et al. Developmental differences in megakaryocytopoiesis are associated with up-regulated TPO signaling through mTOR and elevated GATA-1 levels in neonatal megakaryocytes. Blood. 2011;117(15):4106-17.
116. Becker AJ, McCulloch EA, Siminovitch L, Till JE. The Effect of Differing Demands for Blood Cell Production on DNA Synthesis by Hemopoietic Colony-Forming Cells of Mice. Blood. 1965;26:296-308. Epub 1965/09/01.
117. Rich IN, Kubanek B. Erythroid Colony Formation (Cfue) in Fetal Liver and Adult Bone-Marrow and Spleen from Mouse. Blut. 1976;33(3):171-80.
118. Rich IN, Kubanek B. The Ontogeny of Erythropoiesis in the Mouse Detected by the Erythroid Colony-Forming Technique .2. Transition in Erythropoietin Sensitivity during Development. J Embryol Exp Morph. 1980;58(Aug):143-55.
119. Fleming WH, Alpern EJ, Uchida N, Ikuta K, Spangrude GJ, Weissman IL. Functional heterogeneity is associated with the cell cycle status of murine hematopoietic stem cells. The Journal of cell biology. 1993;122(4):897-902. Epub 1993/08/01.
120. Morrison SJ, Hemmati HD, Wandycz AM, Weissman IL. The purification and characterization of fetal liver hematopoietic stem cells. Proceedings of the National Academy of Sciences of the United States of America. 1995;92(22):10302-6. Epub 1995/10/24.
121. Rebel VI, Miller CL, Thornbury GR, Dragowska WH, Eaves CJ, Lansdorp PM. A comparison of long-term repopulating hematopoietic stem cells in fetal liver and adult bone marrow from the mouse. Experimental hematology. 1996;24(5):638-48. Epub 1996/04/01.
122. Rebel VI, Miller CL, Eaves CJ, Lansdorp PM. The repopulation potential of fetal liver hematopoietic stem cells in mice exceeds that of their liver adult bone marrow counterparts. Blood. 1996;87(8):3500-7. Epub 1996/04/15.
123. Pawliuk R, Eaves C, Humphries RK. Evidence of both ontogeny and transplant dose-regulated expansion of hematopoietic stem cells in vivo. Blood. 1996;88(8):2852-8. Epub 1996/10/15.
124. Hayakawa K, Hardy RR, Herzenberg LA, Herzenberg LA. Progenitors for Ly-1 B-Cells Are Distinct from Progenitors for Other B-Cells. Journal of Experimental Medicine. 1985;161(6):1554-68.
125. Kikuchi K, Kondo M. Developmental switch of mouse hematopoietic stem cells from fetal to adult type occurs in bone marrow after birth. Proceedings of the National Academy of Sciences of the United States of America. 2006;103(47):17852-7. Epub 2006/11/09.
126. Havran WL, Allison JP. Developmentally Ordered Appearance of Thymocytes Expressing Different T-Cell Antigen Receptors. Nature. 1988;335(6189):443-5.
127. Ikuta K, Kina T, MacNeil I, Uchida N, Peault B, Chien YH, et al. A developmental switch in thymic lymphocyte maturation potential occurs at the level of hematopoietic stem cells. Cell. 1990;62(5):863-74. Epub 1990/09/07.
128. Geissler EN, Mcfarland EC, Russell ES. Analysis of Pleiotropism at the Dominant White-Spotting (W) Locus of the House Mouse - a Description of 10 New W-Alleles. Genetics. 1981;97(2):337-61.
129. Miller CL, Rebel VI, Lemieux ME, Helgason CD, Lansdorp PM, Eaves CJ. Studies of W mutant mice provide evidence for alternate mechanisms capable of activating hematopoietic stem cells. Experimental hematology. 1996;24(2):185-94.

130. Huang E, Nocka K, Beier DR, Chu TY, Buck J, Lahm HW, et al. The Hematopoietic Growth Factor-Kl Is Encoded by the Si-Locus and Is the Ligand of the C-Kit Receptor, the Gene-Product of the W-Locus. Cell. 1990;63(1):225-33.
131. Ashman LK. The biology of stem cell factor and its receptor C-kit. Int J Biochem Cell B. 1999;31(10):1037-51.
132. Miller CL, Rebel VI, Helgason CD, Lansdorp PM, Eaves CJ. Impaired steel factor responsiveness differentially affects the detection and long-term maintenance of fetal liver hematopoietic stem cells in vivo. Blood. 1997;89(4):1214-23.
133. Audet J, Miller CL, Eaves CJ, Piret JM. Common and distinct features of cytokine effects on hematopoietic stem and progenitor cells revealed by dose-response surface analysis. Biotechnology and bioengineering. 2002;80(4):393-404. Epub 2002/09/27.
134. Zandstra PW, Conneally E, Petzer AL, Piret JM, Eaves CJ. Cytokine manipulation of primitive human hematopoietic cell self-renewal. Proceedings of the National Academy of Sciences of the United States of America. 1997;94(9):4698-703. Epub 1997/04/29.
135. Park IK, Qian D, Kiel M, Becker MW, Pihalja M, Weissman IL, et al. Bmi-1 is required for maintenance of adult self-renewing haematopoietic stem cells. Nature. 2003;423(6937):302-5. Epub 2003/04/26.
136. Hock H, Hamblen MJ, Rooke HM, Schindler JW, Saleque S, Fujiwara Y, et al. Gfi-1 restricts proliferation and preserves functional integrity of haematopoietic stem cells. Nature. 2004;431(7011):1002-7. Epub 2004/10/01.
137. Hock H, Meade E, Medeiros S, Schindler JW, Valk PJ, Fujiwara Y, et al. Tel/Etv6 is an essential and selective regulator of adult hematopoietic stem cell survival. Genes & development. 2004;18(19):2336-41. Epub 2004/09/17.
138. Kim I, Saunders TL, Morrison SJ. Sox17 dependence distinguishes the transcriptional regulation of fetal from adult hematopoietic stem cells. Cell. 2007;130(3):470-83. Epub 2007/07/28.
139. He S, Kim I, Lim MS, Morrison SJ. Sox17 expression confers self-renewal potential and fetal stem cell characteristics upon adult hematopoietic progenitors. Genes & development. 2011;25(15):1613-27. Epub 2011/08/11.
140. Yuan J, Nguyen CK, Liu X, Kanellopoulou C, Muljo SA. Lin28b Reprograms Adult Bone Marrow Hematopoietic Progenitors to Mediate Fetal-like Lymphopoiesis. Science. 2012. Epub 2012/02/22.
141. Gutti RK, Sallmon H, Liu ZJ, Ferrer-Marin F, Cantor A, Bailey M, et al. Developmental Differences In the Let-7b/IMP-1/IGF-II Axis contribute to the High Proliferative Rate of Neonatal Megakaryocyte progenitors. Blood. 2010;116(21):674-.
142. Ye M, Zhang H, Amabile G, Yang H, Staber PB, Zhang P, et al. C/EBPa controls acquisition and maintenance of adult haematopoietic stem cell quiescence. Nature cell biology. 2013. Epub 2013/03/19.
143. Gothert JR, Gustin SE, Hall MA, Green AR, Gottgens B, Izon DJ, et al. In vivo fate-tracing studies using the Scl stem cell enhancer: embryonic hematopoietic stem cells significantly contribute to adult hematopoiesis. Blood. 2005;105(7):2724-32.
144. Samokhvalov IM, Samokhvalova NI, Nishikawa S. Cell tracing shows the contribution of the yolk sac to adult haematopoiesis. Nature. 2007;446(7139):1056-61.
145. Arai F, Hirao A, Suda T. Regulation of hematopoietic stem cells by the niche. Trends Cardiovas Med. 2005;15(2):75-9.

146. Reinhart BJ, Slack FJ, Basson M, Pasquinelli AE, Bettinger JC, Rougvie AE, et al. The 21-nucleotide let-7 RNA regulates developmental timing in Caenorhabditis elegans. Nature. 2000;403(6772):901-6.
147. Grosshans H, Johnson T, Reinert KL, Gerstein M, Slack FJ. The temporal patterning MicroRNA let-7 regulates several transcription factors at the larval to adult transition in C-elegans. Developmental cell. 2005;8(3):321-30.
148. Abrahante JE, Daul AL, Li M, Volk ML, Tennessen JM, Miller EA, et al. The Caenorhabditis elegans hunchback-like gene lin-57/hbl-1 controls developmental time and is regulated by microRNAs. Developmental cell. 2003;4(5):625-37.
149. Lin SY, Johnson SM, Abraham M, Vella MC, Pasquinelli A, Gamberi C, et al. The C-elegans hunchback homolog, hbl-1, controls temporal patterning and is a probable microRNA target. Developmental cell. 2003;4(5):639-50.
150. Abney ER, Bartlett PP, Raff MC. Astrocytes, Ependymal Cells, and Oligodendrocytes Develop on Schedule in Dissociated Cell-Cultures of Embryonic Rat-Brain. Dev Biol. 1981;83(2):301-10.
151. Hart IK, Richardson WD, Heldin CH, Westermark B, Raff MC. Pdgf Receptors on Cells of the Oligodendrocyte-Type-2 Astrocyte (O-2a) Cell Lineage. Development. 1989;105(3):595-603.
152. Durand B, Fero ML, Roberts JM, Raff MC. p27(Kip1) alters the response of cells to mitogen and is part of a cell-intrinsic timer that arrests the cell cycle and initiates differentiation. Current Biology. 1998;8(8):431-40.
153. Ito T, Tajima F, Ogawa M. Developmental changes of CD34 expression by murine hematopoietic stem cells. Experimental hematology. 2000;28(11):1269-73.
154. Sato T, Laver JH, Ogawa M. Reversible expression of CD34 by murine hematopoietic stem cells. Blood. 1999;94(8):2548-54.
155. Randall TD, Lund FE, Howard MC, Weissman IL. Expression of murine CD38 defines a population of long-term reconstituting hematopoietic stem cells. Blood. 1996;87(10):4057-67.
156. Tajima F, Deguchi T, Laver JH, Zeng HQ, Ogawa M. Reciprocal expression of CD38 and CD34 by adult murine hematopoietic stem cells. Blood. 2001;97(9):2618-24.
157. Chen CZ, Li M, de Graaf D, Monti S, Gottgens B, Sanchez MJ, et al. Identification of endoglin as a functional marker that defines long-term repopulating hematopoietic stem cells. Proceedings of the National Academy of Sciences of the United States of America. 2002;99(24):15468-73. Epub 2002/11/20.
158. Zhang CC, Lodish HF. Murine hematopoietic stem cells change their surface phenotype during ex vivo expansion. Blood. 2005;105(11):4314-20.
159. Uchida N, Dykstra B, Lyons K, Leung F, Kristiansen M, Eaves C. ABC transporter activities of murine hematopoietic stem cells vary according to their developmental and activation status. Blood. 2004;103(12):4487-95.
160. Goodell MA, Brose K, Paradis G, Conner AS, Mulligan RC. Isolation and functional properties of murine hematopoietic stem cells that are replicating in vivo. Journal of Experimental Medicine. 1996;183(4):1797-806.
161. Moore T, Huang S, Terstappen LWMM, Bennett M, Kumar V. Expression of Cd43 on Murine and Human Pluripotent Hematopoietic Stem-Cells. Journal of Immunology. 1994;153(11):4978-87.
162. Iwasaki H, Arai F, Kubota Y, Suda T. Expression of endothelial protein C receptor confines hematopoietic stem cell in murine fetal liver. Blood. 2007;110(11):379A-80A.

163. Dzierzak E, Speck NA. Of lineage and legacy: the development of mammalian hematopoietic stem cells. Nature immunology. 2008;9(2):129-36. Epub 2008/01/22.
164. Ema H, Nakauchi H. Expansion of hematopoietic stem cells in the developing liver of a mouse embryo. Blood. 2000;95(7):2284-8. Epub 2000/03/25.
165. Dzierzak E, Medvinsky A. The discovery of a source of adult hematopoietic cells in the embryo. Development. 2008;135(14):2343-6. Epub 2008/06/24.
166. Phillips RL, Ernst RE, Brunk B, Ivanova N, Mahan MA, Deanehan JK, et al. The genetic program of hematopoietic stem cells. Science. 2000;288(5471):1635-40.
167. Oh IH, Lau A, Eaves CJ. During ontogeny primitive (CD34(+)CD38(-)) hematopoietic cells show altered expression of a subset of genes associated with early cytokine and differentiation responses of their adult counterparts. Blood. 2000;96(13):4160-8.
168. Pineault N, Helgason CD, Lawrence HJ, Humphries RK. Differential expression of Hox, Meis1, and Pbx1 genes in primitive cells throughout murine hematopoietic ontogeny. Experimental hematology. 2002;30(1):49-57.
169. Kiel MJ, Iwashita T, Yilmaz OH, Morrison SJ. Spatial differences in hematopoiesis but not in stem cells indicate a lack of regional patterning in definitive hematopoietic stem cells. Dev Biol. 2005;283(1):29-39.
170. Gentleman RC, Carey VJ, Bates DM, Bolstad B, Dettling M, Dudoit S, et al. Bioconductor: open software development for computational biology and bioinformatics. Genome Biol. 2004;5(10).
171. Kent D, Copley M, Benz C, Dykstra B, Bowie M, Eaves C. Regulation of hematopoietic stem cells by the steel factor/KIT signaling pathway. Clinical cancer research : an official journal of the American Association for Cancer Research. 2008;14(7):1926-30. Epub 2008/04/03.
172. Robertson N, Oveisi-Fordorei M, Zuyderduyn SD, Varhol RJ, Fjell C, Marra M, et al. DiscoverySpace: an interactive data analysis application. Genome Biol. 2007;8(1).
173. Randall TD, Weissman IL. Phenotypic and functional changes induced at the clonal level in hematopoietic stem cells after 5-fluorouracil treatment. Blood. 1997;89(10):3596-606.
174. Viswanathan SR, Daley GQ, Gregory RI. Selective blockade of microRNA processing by Lin28. Science. 2008;320(5872):97-100. Epub 2008/02/23.
175. Piskounova E, Viswanathan SR, Janas M, LaPierre RJ, Daley GQ, Sliz P, et al. Determinants of microRNA processing inhibition by the developmentally regulated RNA-binding protein Lin28. The Journal of biological chemistry. 2008;283(31):21310-4. Epub 2008/06/14.
176. Piskounova E, Polytarchou C, Thornton JE, LaPierre RJ, Pothoulakis C, Hagan JP, et al. Lin28A and Lin28B inhibit let-7 microRNA biogenesis by distinct mechanisms. Cell. 2011;147(5):1066-79. Epub 2011/11/29.
177. Reeves R, Nissen MS. The A.T-DNA-binding domain of mammalian high mobility group I chromosomal proteins. A novel peptide motif for recognizing DNA structure. The Journal of biological chemistry. 1990;265(15):8573-82. Epub 1990/05/25.
178. Rommel B, Rogalla P, Jox A, Kalle CV, Kazmierczak B, Wolf J, et al. HMGI-C, a member of the high mobility group family of proteins, is expressed in hematopoietic stem cells and in leukemic cells. Leukemia & lymphoma. 1997;26(5-6):603-7. Epub 1997/08/01.
179. Anand A, Chada K. In vivo modulation of Hmgic reduces obesity. Nature genetics. 2000;24(4):377-80. Epub 2000/03/31.

180. Chieffi P, Battista S, Barchi M, Di Agostino S, Pierantoni GM, Fedele M, et al. HMGA1 and HMGA2 protein expression in mouse spermatogenesis. Oncogene. 2002;21(22):3644-50. Epub 2002/05/29.
181. Di Agostino S, Fedele M, Chieffi P, Fusco A, Rossi P, Geremia R, et al. Phosphorylation of high-mobility group protein A2 by Nek2 kinase during the first meiotic division in mouse spermatocytes. Molecular biology of the cell. 2004;15(3):1224-32. Epub 2003/12/12.
182. Zhou X, Benson KF, Ashar HR, Chada K. Mutation responsible for the mouse pygmy phenotype in the developmentally regulated factor HMGI-C. Nature. 1995;376(6543):771-4. Epub 1995/08/31.
183. Nishino J, Kim I, Chada K, Morrison SJ. Hmga2 promotes neural stem cell self-renewal in young but not old mice by reducing p16Ink4a and p19Arf Expression. Cell. 2008;135(2):227-39. Epub 2008/10/30.
184. Fusco A, Fedele M. Roles of HMGA proteins in cancer. Nature reviews Cancer. 2007;7(12):899-910. Epub 2007/11/16.
185. Odero MD, Grand FH, Iqbal S, Ross F, Roman JP, Vizmanos JL, et al. Disruption and aberrant expression of HMGA2 as a consequence of diverse chromosomal translocations in myeloid malignancies. Leukemia : official journal of the Leukemia Society of America, Leukemia Research Fund, UK. 2005;19(2):245-52. Epub 2004/12/25.
186. Mayr C, Hemann MT, Bartel DP. Disrupting the pairing between let-7 and Hmga2 enhances oncogenic transformation. Science. 2007;315(5818):1576-9. Epub 2007/02/27.
187. Lee YS, Dutta A. The tumor suppressor microRNA let-7 represses the HMGA2 oncogene. Genes & development. 2007;21(9):1025-30. Epub 2007/04/18.
188. Hayes GD, Ruvkun G. Misexpression of the Caenorhabditis elegans miRNA let-7 is sufficient to drive developmental programs. Cold Spring Harbor symposia on quantitative biology. 2006;71:21-7. Epub 2007/03/27.
189. Zhang CC, Lodish HF. Insulin-like growth factor 2 expressed in a novel fetal liver cell population is a growth factor for hematopoietic stem cells. Blood. 2004;103(7):2513-21. Epub 2003/11/01.
190. Zhang CC, Kaba M, Ge G, Xie K, Tong W, Hug C, et al. Angiopoietin-like proteins stimulate ex vivo expansion of hematopoietic stem cells. Nature medicine. 2006;12(2):240-5. Epub 2006/01/24.
191. Lansdorp PM, Dragowska W, Mayani H. Ontogeny-related changes in proliferative potential of human hematopoietic cells. The Journal of experimental medicine. 1993;178(3):787-91. Epub 1993/09/01.
192. Harrison DE, Zhong RK, Jordan CT, Lemischka IR, Astle CM. Relative to adult marrow, fetal liver repopulates nearly five times more effectively long-term than short-term. Experimental hematology. 1997;25(4):293-7. Epub 1997/04/01.
193. Moss EG, Lee RC, Ambros V. The cold shock domain protein LIN-28 controls developmental timing in C. elegans and is regulated by the lin-4 RNA. Cell. 1997;88(5):637-46. Epub 1997/03/07.
194. Viswanathan SR, Daley GQ. Lin28: A microRNA regulator with a macro role. Cell. 2010;140(4):445-9. Epub 2010/02/25.
195. Xiang X, Benson KF, Chada K. Mini-mouse: disruption of the pygmy locus in a transgenic insertional mutant. Science. 1990;247(4945):967-9. Epub 1990/02/23.
196. Challita PM, Skelton D, el-Khoueiry A, Yu XJ, Weinberg K, Kohn DB. Multiple modifications in cis elements of the long terminal repeat of retroviral vectors lead to increased

expression and decreased DNA methylation in embryonic carcinoma cells. Journal of virology. 1995;69(2):748-55. Epub 1995/02/01.
197. Carbonaro DA, Jin X, Petersen D, Wang X, Dorey F, Kil KS, et al. In vivo transduction by intravenous injection of a lentiviral vector expressing human ADA into neonatal ADA gene knockout mice: a novel form of enzyme replacement therapy for ADA deficiency. Molecular therapy : the journal of the American Society of Gene Therapy. 2006;13(6):1110-20. Epub 2006/05/03.
198. Imren S, Fabry ME, Westerman KA, Pawliuk R, Tang P, Rosten PM, et al. High-level beta-globin expression and preferred intragenic integration after lentiviral transduction of human cord blood stem cells. Journal of Clinical Investigation. 2004;114(7):953-62.
199. Boggs DR. The Total Marrow Mass of the Mouse - a Simplified Method of Measurement. Am J Hematol. 1984;16(3):277-86.
200. Hu YF, Smyth GK. ELDA: Extreme limiting dilution analysis for comparing depleted and enriched populations in stem cell and other assays. J Immunol Methods. 2009;347(1-2):70-8.
201. Bussing I, Slack FJ, Grosshans H. let-7 microRNAs in development, stem cells and cancer. Trends in molecular medicine. 2008;14(9):400-9. Epub 2008/08/05.
202. Brants JR, Ayoubi TA, Chada K, Marchal K, Van de Ven WJ, Petit MM. Differential regulation of the insulin-like growth factor II mRNA-binding protein genes by architectural transcription factor HMGA2. FEBS letters. 2004;569(1-3):277-83. Epub 2004/07/01.
203. Cleynen I, Brants JR, Peeters K, Deckers R, Debiec-Rychter M, Sciot R, et al. HMGA2 regulates transcription of the Imp2 gene via an intronic regulatory element in cooperation with nuclear factor-kappaB. Molecular cancer research : MCR. 2007;5(4):363-72. Epub 2007/04/12.
204. Li Z, Gilbert JA, Zhang Y, Zhang M, Qiu Q, Ramanujan K, et al. An HMGA2-IGF2BP2 Axis Regulates Myoblast Proliferation and Myogenesis. Developmental cell. 2012. Epub 2012/11/28.
205. Ikeda K, Mason PJ, Bessler M. 3'UTR-truncated Hmga2 cDNA causes MPN-like hematopoiesis by conferring a clonal growth advantage at the level of HSC in mice. Blood. 2011;117(22):5860-9. Epub 2011/04/05.
206. Toledano H, D'Alterio C, Czech B, Levine E, Jones DL. The let-7-Imp axis regulates ageing of the Drosophila testis stem-cell niche. Nature. 2012;485(7400):605-10. Epub 2012/06/05.
207. Christiansen J, Kolte AM, Hansen T, Nielsen FC. IGF2 mRNA-binding protein 2: biological function and putative role in type 2 diabetes. Journal of molecular endocrinology. 2009;43(5):187-95. Epub 2009/05/12.
208. Dai N, Rapley J, Angel M, Yanik MF, Blower MD, Avruch J. mTOR phosphorylates IMP2 to promote IGF2 mRNA translation by internal ribosomal entry. Genes & development. 2011;25(11):1159-72. Epub 2011/05/18.
209. Tybl E, Shi FD, Kessler SM, Tierling S, Walter J, Bohle RM, et al. Overexpression of the IGF2-mRNA binding protein p62 in transgenic mice induces a steatotic phenotype. Journal of hepatology. 2011;54(5):994-1001. Epub 2010/12/15.
210. Maki RG. Small is beautiful: insulin-like growth factors and their role in growth, development, and cancer. Journal of clinical oncology : official journal of the American Society of Clinical Oncology. 2010;28(33):4985-95. Epub 2010/10/27.
211. Inoue N, Izui-Sarumaru T, Murakami Y, Endo Y, Nishimura JI, Kurokawa K, et al. Molecular basis of clonal expansion of hematopoiesis in 2 patients with paroxysmal nocturnal hemoglobinuria (PNH). Blood. 2006;108(13):4232-6.

212. Murakami Y, Inoue N, Shichishima T, Ohta R, Noji H, Maeda Y, et al. Deregulated expression of HMGA2 is implicated in clonal expansion of PIGA deficient cells in paroxysmal nocturnal haemoglobinuria. British journal of haematology. 2012;156(3):383-7. Epub 2011/10/25.
213. Mochizuki-Kashio M, Mishima Y, Miyagi S, Negishi M, Saraya A, Konuma T, et al. Dependency on the polycomb gene Ezh2 distinguishes fetal from adult hematopoietic stem cells. Blood. 2011;118(25):6553-61. Epub 2011/11/02.
214. Benson KF, Chada K. Mini-mouse: phenotypic characterization of a transgenic insertional mutant allelic to pygmy. Genetical research. 1994;64(1):27-33. Epub 1994/08/01.
215. Lynch SA, Foulds N, Thuresson AC, Collins AL, Anneren G, Hedberg BO, et al. The 12q14 microdeletion syndrome: six new cases confirming the role of HMGA2 in growth. Eur J Hum Genet. 2011;19(5):534-9.
216. Mari F, Hermanns P, Giovannucci-Uzielli ML, Galluzzi F, Scott D, Lee B, et al. Refinement of the 12q14 microdeletion syndrome: primordial dwarfism and developmental delay with or without osteopoikilosis. Eur J Hum Genet. 2009;17(9):1141-7.
217. Weedon MN, Lettre G, Freathy RM, Lindgren CM, Voight BF, Perry JRB, et al. A common variant of HMGA2 is associated with adult and childhood height in the general population. Nature genetics. 2007;39(10):1245-50.
218. Lin SC, Lin CR, Gukovsky I, Lusis AJ, Sawchenko PE, Rosenfeld MG. Molecular basis of the little mouse phenotype and implications for cell type-specific growth. Nature. 1993;364(6434):208-13. Epub 1993/07/15.
219. Li S, Crenshaw EB, 3rd, Rawson EJ, Simmons DM, Swanson LW, Rosenfeld MG. Dwarf locus mutants lacking three pituitary cell types result from mutations in the POU-domain gene pit-1. Nature. 1990;347(6293):528-33. Epub 1990/10/11.
220. Sinha YN, Wolff GL, Baxter SR, Domon OE. Serum and pituitary concentrations of growth hormone and prolactin in pygmy mice. Proc Soc Exp Biol Med. 1979;162(1):221-3. Epub 1979/10/01.
221. Nissley SP, Knazek RA, Wolff GL. Somatomedin activity in sera of genetically small mice. Hormone and metabolic research = Hormon- und Stoffwechselforschung = Hormones et metabolisme. 1980;12(4):158-64. Epub 1980/04/01.
222. Hyun S. Body size regulation and insulin-like growth factor signaling. Cellular and molecular life sciences : CMLS. 2013. Epub 2013/03/20.
223. Liu JP, Baker J, Perkins AS, Robertson EJ, Efstratiadis A. Mice carrying null mutations of the genes encoding insulin-like growth factor I (Igf-1) and type 1 IGF receptor (Igf1r). Cell. 1993;75(1):59-72. Epub 1993/10/08.
224. Lupu F, Terwilliger JD, Lee K, Segre GV, Efstratiadis A. Roles of growth hormone and insulin-like growth factor 1 in mouse postnatal growth. Dev Biol. 2001;229(1):141-62. Epub 2001/01/03.
225. Baker J, Liu JP, Robertson EJ, Efstratiadis A. Role of insulin-like growth factors in embryonic and postnatal growth. Cell. 1993;75(1):73-82. Epub 1993/10/08.
226. Efstratiadis A. Genetics of mouse growth. The International journal of developmental biology. 1998;42(7):955-76. Epub 1998/12/16.
227. Kruger GM, Mosher JT, Bixby S, Joseph N, Iwashita T, Morrison SJ. Neural crest stem cells persist in the adult gut but undergo changes in self-renewal, neuronal subtype potential, and factor responsiveness. Neuron. 2002;35(4):657-69. Epub 2002/08/27.

228. Schofiel.R. A Comparative Study of Repopulating Potential of Grafts from Various Haemopoietic Sources - Cfu Repopulation. Cell Tissue Kinet. 1970;3(2):119-&.
229. Scotting PJ, Walker DA, Perilongo G. Childhood solid tumours: a developmental disorder. Nature reviews Cancer. 2005;5(6):481-8. Epub 2005/05/21.
230. Roberts KG, Mullighan CG. How new advances in genetic analysis are influencing the understanding and treatment of childhood acute leukemia. Curr Opin Pediatr. 2011;23(1):34-40.
231. Speck NA, Gilliland DG. Core-binding factors in haematopoiesis and leukaemia. Nature reviews Cancer. 2002;2(7):502-13. Epub 2002/07/03.
232. Schindler JW, Van Buren D, Foudi A, Krejci O, Qin J, Orkin SH, et al. TEL-AML1 corrupts hematopoietic stem cells to persist in the bone marrow and initiate leukemia. Cell stem cell. 2009;5(1):43-53. Epub 2009/07/03.
233. Romano AA, Allanson JE, Dahlgren J, Gelb BD, Hall B, Pierpont ME, et al. Noonan Syndrome: Clinical Features, Diagnosis, and Management Guidelines. Pediatrics. 2010;126(4):746-59.
234. Matsuda K, Shimada A, Yoshida N, Ogawa A, Watanabe A, Yajima S, et al. Spontaneous improvement of hematologic abnormalities in patients having juvenile myelomonocytic leukemia with specific RAS mutations. Blood. 2007;109(12):5477-80. Epub 2007/03/03.
235. Gamis AS, Smith FO. Transient myeloproliferative disorder in children with Down syndrome: clarity to this enigmatic disorder. British journal of haematology. 2012;159(3):277-87. Epub 2012/09/13.
236. Viswanathan SR, Powers JT, Einhorn W, Hoshida Y, Ng TL, Toffanin S, et al. Lin28 promotes transformation and is associated with advanced human malignancies. Nature genetics. 2009;41(7):843-U109.
237. Boyerinas B, Park SM, Hau A, Murmann AE, Peter ME. The role of let-7 in cell differentiation and cancer. Endocrine-related cancer. 2010;17(1):F19-36. Epub 2009/09/26.
238. Li Z, Zhang Y, Ramanujan K, Ma Y, Kirsch DG, Glass DJ. Oncogenic NRAS, required for pathogenesis of embryonic rhabdomyosarcoma, relies upon the HMGA2-IGF2BP2 pathway. Cancer research. 2013. Epub 2013/03/29.
239. Zhu H, Shyh-Chang N, Segre AV, Shinoda G, Shah SP, Einhorn WS, et al. The Lin28/let-7 axis regulates glucose metabolism. Cell. 2011;147(1):81-94. Epub 2011/10/04.
240. McCarty MF. Metformin may antagonize Lin28 and/or Lin28B activity, thereby boosting let-7 levels and antagonizing cancer progression. Medical hypotheses. 2012;78(2):262-9. Epub 2011/12/02.
241. Copelan EA. Hematopoietic stem-cell transplantation. The New England journal of medicine. 2006;354(17):1813-26. Epub 2006/04/28.
242. Takizawa H, Schanz U, Manz MG. Ex vivo expansion of hematopoietic stem cells: mission accomplished? Swiss medical weekly. 2011;141:w13316. Epub 2012/01/19.
243. Kardel MD, Eaves CJ. Modeling human hematopoietic cell development from pluripotent stem cells. Experimental hematology. 2012;40(8):601-11. Epub 2012/04/19.
244. Broxmeyer HE, Cooper S, Hass DM, Hathaway JK, Stehman FB, Hangoc G. Experimental basis of cord blood transplantation. Bone marrow transplantation. 2009;44(10):627-33. Epub 2009/10/06.
245. Deshayes S, Morris MC, Divita G, Heitz F. Cell-penetrating peptides: tools for intracellular delivery of therapeutics. Cellular and molecular life sciences : CMLS. 2005;62(16):1839-49. Epub 2005/06/22.

246. Obad S, dos Santos CO, Petri A, Heidenblad M, Broom O, Ruse C, et al. Silencing of microRNA families by seed-targeting tiny LNAs. Nature genetics. 2011;43(4):371-8. Epub 2011/03/23.
247. Varelas X, Wrana JL. Coordinating developmental signaling: novel roles for the Hippo pathway. Trends in cell biology. 2012;22(2):88-96. Epub 2011/12/14.
248. Jansson L, Larsson J. Normal hematopoietic stem cell function in mice with enforced expression of the Hippo signaling effector YAP1. PloS one. 2012;7(2):e32013. Epub 2012/03/01.

Appendices

Appendix A Supplementary data

A.1 Affymetrix transcript analysis of adult BM relative to fetal liver Lin$^-$Sca1$^+$c-Kit$^+$ (LSK) cells using a cut-off FDR of <0.2

ID	Log fold-change	Expression	t	P value	FDR
14955_H19	-3.528622187	6.874239254	-13.72730271	1.27E-06	0.008926494
380669_Lin28b	-3.297511428	6.110080929	-8.290977691	4.64E-05	0.051234381
70458_2610318N02Rik	-3.284560623	6.559000911	-7.264430963	0.000114174	0.070474852
319765_Igf2bp2	-3.015974577	7.254572268	-9.556601136	1.72E-05	0.038017084
20592_Kdm5d	-2.894103861	6.943095796	-12.77909736	2.14E-06	0.010641837
26908_Eif2s3y	-2.886446242	4.921866267	-4.849318279	0.001487281	0.16150691
751545_Mir505	-2.748756798	5.607148336	-6.549114527	0.000227212	0.077051311
71994_Cnn3	-2.60945993	3.889515097	-13.61784387	1.35E-06	0.008926494
56431_Dstn	-2.590739242	7.919423241	-6.295559689	0.000293899	0.084549029
26900_Ddx3y	-2.559150015	6.192158316	-6.824522388	0.000173212	0.073253882
16852_Lgals1	-2.392192688	9.09322589	-6.2829164	0.000297753	0.084549029
245595_Zfp711	-2.242123079	5.17298233	-5.311991838	0.000858964	0.13550498
140488_Igf2bp3	-2.231176024	6.766507207	-6.337286318	0.000281569	0.084549029
20529_Slc31a1	-2.107030164	7.019892965	-7.006479567	0.000145431	0.070474852
140486_Igf2bp1	-2.049522133	7.157979115	-8.989806452	2.64E-05	0.039079784
66311_Cenpw	-2.021833661	7.123157294	-4.696471714	0.001794993	0.174720193
20454_St3gal5	-2.008423647	7.059787838	-6.320905031	0.00028634	0.084549029
387181_Mir186	-1.891096893	4.127643256	-5.924763049	0.000434082	0.105222512
50706_Postn	-1.880413368	6.511872206	-10.54064718	8.59E-06	0.028223996
15364_Hmga2	-1.790425037	8.423152353	-7.630444904	8.19E-05	0.062620042
18576_Pde3b	-1.779901891	6.774828371	-5.575050949	0.000636968	0.121890502
16826_Ldb2	-1.777512314	6.846865249	-8.768995696	3.15E-05	0.039079784
53611_Vti1a	-1.741524521	6.449802887	-4.901394266	0.001396053	0.159092696
240168_Rasgrp3	-1.73346438	6.183799477	-5.711629751	0.000547348	0.114522451
18597_Pdha1	-1.721589578	8.701434994	-4.77318119	0.001632643	0.168883473
11799_Birc5	-1.704433765	8.437299541	-5.465313322	0.000720776	0.126464331
68205_Urm1	-1.693059125	6.934628688	-5.712026193	0.000547109	0.114522451
20620_Plk2	-1.691329345	8.106843914	-7.642827015	8.10E-05	0.062620042
56309_Mycbp	-1.683790841	6.47982469	-5.238842982	0.000934988	0.13893162
71085_Arhgap19	-1.677763279	6.698367193	-4.469114853	0.002389394	0.197576506
380686_Cnrip1	-1.631116227	6.748632192	-5.214057526	0.000962406	0.13893162
20646_Snrpn	-1.625060807	6.425884964	-4.742033116	0.00169654	0.170967255

67531_5730408K05Rik	-1.613648534	7.498391919	-5.214195379	0.000962251	0.13893162
72440_5930416I19Rik	-1.604073501	7.876170404	-6.451499483	0.000250658	0.081677637
80884_Maged2	-1.600013476	6.412335687	-5.251543102	0.000921274	0.13893162
67849_Cdca5	-1.57645652	7.525420478	-4.452581227	0.002440342	0.199615975
66468_Ska1	-1.567441137	6.233709139	-5.941147716	0.000426514	0.10466453
433638_I830077J02Rik	-1.559027978	6.819553941	-5.031662555	0.001193629	0.151869452
18392_Orc1	-1.548082817	5.577767355	-4.4677066	0.002393688	0.197576506
12428_Ccna2	-1.506779893	8.698044545	-4.621642445	0.001970536	0.18563199
70021_Nt5dc2	-1.490480295	8.129094973	-4.656981666	0.001885398	0.179769693
17161_Maoa	-1.489325706	6.742757784	-5.432320567	0.0007483	0.127127929
11605_Gla	-1.480167093	7.063047242	-5.447041354	0.000735879	0.126464331
66701_Spryd4	-1.46202613	6.507222187	-4.693350042	0.001801964	0.174720193
12443_Ccnd1	-1.452336379	7.90311207	-5.405028546	0.000771947	0.12894106
12649_Chek1	-1.445523481	7.834612946	-5.091642482	0.001111465	0.149512701
52696_Zwint	-1.442839631	7.60661048	-6.064519857	0.000374011	0.097351133
224171_C330027C09Rik	-1.440106123	7.446556542	-5.484685736	0.000705136	0.126464331
58246_Slc35b4	-1.422430799	6.714120104	-6.265456202	0.000303167	0.084739188
16162_Il12rb2	-1.412617777	7.151077325	-4.910658163	0.001380477	0.159092696
104884_Tdp1	-1.388917719	6.589192916	-5.97075198	0.000413209	0.103966552
59126_Nek6	-1.35597564	7.222784772	-7.785105477	7.15E-05	0.059179681
72502_Cwf19l1	-1.351484062	7.029655404	-5.855280972	0.000467868	0.107472511
66074_Tmem167	-1.347654539	5.594480339	-4.440527261	0.002478233	0.19982632
72155_Cenpn	-1.332460306	7.194952167	-4.76012954	0.00165909	0.169489188
19659_Rbp1	-1.3281763	9.545932281	-4.565282826	0.002115143	0.19312238
14086_Fscn1	-1.314352584	6.665469793	-6.544035083	0.00022837	0.077051311
27214_Dbf4	-1.313432299	7.958091892	-5.449602589	0.000733741	0.126464331
16002_Igf2	-1.313268373	6.985511698	-5.171551321	0.001011511	0.142792162
69716_Trip13	-1.296986978	7.672553071	-6.378041307	0.000270078	0.084549029
66664_Tmem41a	-1.29050643	7.127090983	-4.898666942	0.001400675	0.159092696
67381_Med4	-1.286821241	7.276892943	-4.873298479	0.001444484	0.16150691
67529_Fgfr1op2	-1.278802196	8.959585141	-4.484238274	0.002343807	0.197103867
30954_Siva1	-1.278782176	9.184095685	-6.285651747	0.000296914	0.084549029
20810_Srm	-1.269062134	7.97300349	-4.92540558	0.001356073	0.158346425
68979_Nol11	-1.254471603	7.07368407	-5.349456272	0.000822686	0.13370568
19946_Rpl30	-1.25149809	9.307519137	-4.463530085	0.002406473	0.197658919
68033_Cox19	-1.244286004	6.532818447	-4.67528743	0.001842886	0.177820593
27053_Asns	-1.225386523	7.380603896	-4.430837464	0.002509157	0.19982632
13436_Dnmt3b	-1.22389002	8.24653725	-6.542560097	0.000228708	0.077051311
20250_Scd2	-1.208661231	7.594784552	-4.949779037	0.001316772	0.158346425
66071_Ethe1	-1.194573303	7.397734793	-5.129410289	0.00106293	0.145709416
223691_Eif3l	-1.18777133	9.12123925	-4.925603635	0.001355749	0.158346425
67164_Lipt2	-1.174453402	6.816334455	-4.946293037	0.001322316	0.158346425
72542_Pgam5	-1.173085835	6.497444671	-4.468669624	0.002390751	0.197576506

170676_Peg10	-1.169539748	6.286550725	-4.735062066	0.001711213	0.170967255
54366_Ctnnal1	-1.168856984	7.664585909	-4.899531419	0.001399208	0.159092696
16648_Kpna3	-1.16496785	8.192404819	-4.467103664	0.002395529	0.197576506
22137_Ttk	-1.164669875	7.820112138	-5.561708975	0.000646558	0.121890502
12798_Cnn2	-1.144564216	7.723026823	-6.288888454	0.000295926	0.084549029
68981_Snrpa1	-1.142291856	9.234363695	-4.843239201	0.001498349	0.16150691
74359_4931414P19Rik	-1.140302952	5.21649639	-5.850303062	0.000470398	0.107472511
108011_Ap4e1	-1.139650217	6.369468105	-5.367913509	0.000805437	0.13341396
66448_Mrpl20	-1.133067958	6.550198637	-4.560560666	0.002127776	0.19312238
20425_Shmt1	-1.12776491	6.773255563	-5.028696823	0.001197862	0.151869452
67071_Rps6ka6	-1.124366201	7.083970369	-4.758343668	0.001662745	0.169489188
217837_Itpk1	-1.123812461	7.043127046	-5.697587546	0.000555886	0.115097342
14225_Fkbp1a	-1.123547002	8.963141047	-5.658904584	0.000580178	0.11767548
14083_Ptk2	-1.121394184	7.419246757	-6.290461797	0.000295446	0.084549029
16414_Itgb2	-1.109519079	6.742897067	-5.824102205	0.000483968	0.108683861
20595_Smn1	-1.108603419	7.981136468	-5.067076956	0.001144339	0.150197422
68971_1500001M20Rik	-1.104323114	8.404070967	-5.050965192	0.001166481	0.151543359
20610_Sumo3	-1.087893801	8.222533363	-4.98525436	0.001261787	0.157739216
74340_Ahcyl2	-1.080896129	7.844754829	-4.42643717	0.002523339	0.19982632
12534_Cdk1	-1.077018261	8.103195125	-4.994283309	0.001248198	0.157028087
503550_Klri1	-1.076335018	5.564186794	-6.253465668	0.000306949	0.084739188
27374_Prmt5	-1.076063562	8.468133393	-4.651665194	0.001897945	0.179769693
21991_Tpi1	-1.070660243	9.239369348	-5.325877977	0.000845316	0.13441875
110279_Bcr	-1.057904111	7.181442251	-4.489394241	0.002328483	0.197103867
13496_Arid3a	-1.042634957	6.708516449	-4.861336663	0.00146566	0.16150691
192173_Fam195b	-1.036702037	7.627508	-6.056689494	0.000377121	0.097351133
54198_Snx3	-1.036688837	7.820864717	-5.063976303	0.001148564	0.150197422
19075_Prim1	-1.028360391	8.475220269	-4.485974593	0.002338634	0.197103867
24135_Zfp68	-1.02552873	8.211130379	-4.749318967	0.001681352	0.170511416
97541_Qars	-1.008386427	7.929951202	-5.783304983	0.000505967	0.110517656
12144_Blm	-1.007689084	7.519225145	-4.888752358	0.001417621	0.160102536
20135_Rrm2	-1.007131067	7.933365878	-4.958324141	0.001303291	0.158346425
67103_Ptgr1	-1.007018797	7.79769996	-4.603715028	0.002015327	0.188068756
27052_Aoah	-1.002622134	6.134837337	-5.274849132	0.000896679	0.138164999
100043385_Gm16494	-0.987245342	8.305735566	-5.231126038	0.000943431	0.13893162
28000_Prpf19	-0.985455019	8.047918906	-4.720046208	0.001743292	0.171541707
56444_Actr10	-0.982352097	7.142018912	-5.448559841	0.00073461	0.126464331
107701_Sf3b4	-0.96969486	7.029371849	-5.350907399	0.000821315	0.13370568
214580_Pstk	-0.955721615	7.232764079	-5.275482771	0.00089602	0.138164999
21787_Tfg	-0.955525795	8.889106073	-4.541664381	0.002179158	0.194238212
80907_Lactb	-0.936178013	6.620835306	-4.482120252	0.002350134	0.197103867
69639_Exosc8	-0.933581938	9.15858673	-5.337470592	0.000834105	0.13370568
14221_Fjx1	-0.928458861	5.184320994	-5.08182834	0.001124472	0.149512701

231571_Rpap2	-0.921789796	7.064562365	-4.549101202	0.002158776	0.193288245
73674_Wdr75	-0.898624937	8.334419929	-4.924687488	0.00135725	0.158346425
28030_Gfm1	-0.881431748	7.311208861	-5.081628838	0.001124738	0.149512701
66694_Uqcrfs1	-0.875976381	8.004808163	-4.527214807	0.002219363	0.195195921
101861_Ints4	-0.86679589	7.941335206	-4.427790987	0.002518966	0.19982632
70024_Mcm10	-0.85733098	7.451671622	-4.515598481	0.002252272	0.196352703
50497_Hspa14	-0.833943678	8.787784673	-4.577488284	0.00208287	0.191672221
64652_Nisch	-0.816577013	8.378667047	-4.560917054	0.00212682	0.19312238
12442_Ccnb2	-0.766914767	9.42244299	-4.484891549	0.00234186	0.197103867
16998_Ltbp3	0.789908299	7.79156372	4.488591613	0.002330861	0.197103867
103841_Cuedc1	0.853401022	6.665947924	4.430563355	0.002510038	0.19982632
52668_Ifi27l1	0.887406703	9.237724532	4.655195633	0.001889603	0.179769693
99633_Lphn2	0.893699492	7.097769206	4.69575449	0.001796592	0.174720193
77577_Spns3	0.903578709	6.498567981	4.812706054	0.001555328	0.16532222
140795_P2ry14	0.917558379	7.809859356	4.782727804	0.00161359	0.168883473
20975_Synj2	0.929149457	7.452988564	4.510902535	0.002265727	0.196533248
78896_1500015O10Rik	0.935475216	6.120103026	5.034347556	0.001189812	0.151869452
21825_Thbs1	0.937060381	6.708825621	4.72676712	0.001728853	0.170967255
229323_Gpr171	0.938104624	8.401776738	4.841707571	0.001501152	0.16150691
106878_2010002N04Rik	0.940502935	6.287925116	4.781985577	0.001615063	0.168883473
12767_Cxcr4	0.966802835	8.860292415	5.142210579	0.001047014	0.144524272
104418_Dgkz	0.973416217	8.062675017	4.522207265	0.002233485	0.195572573
74276_Cldnd2	0.981695212	6.149969811	4.535632586	0.002195843	0.194851698
72433_Rab38	0.99811607	8.659164072	5.212143103	0.00096456	0.13893162
320405_Cadps2	1.023244051	6.605785477	4.951208187	0.001314507	0.158346425
53625_B3gnt2	1.042883	8.121591636	4.727156867	0.00172802	0.170967255
320554_Tcp11l1	1.046166102	6.554103994	5.205124852	0.000972503	0.139067979
239985_Arid1b	1.054178672	8.084766324	5.452668084	0.000731191	0.126464331
14739_S1pr2	1.059852587	7.98923655	5.494194484	0.000697597	0.126464331
12333_Capn1	1.071851192	7.298308213	4.732626686	0.001716372	0.170967255
257635_Sdsl	1.072211938	6.750374309	5.761442886	0.00051821	0.11196147
57869_Adck2	1.077373508	6.470617223	5.613443736	0.000610238	0.120096058
15953_Ifi47	1.080777013	7.657815752	6.189157548	0.000328145	0.089349906
215900_Fam26f	1.081618621	7.039495477	4.446400521	0.002459691	0.19982632
11852_Rhob	1.097137676	6.073708261	5.819045458	0.000486636	0.108683861
619289_Rfx8	1.100288288	7.294753227	5.444469956	0.000738032	0.126464331
17754_Mtap1a	1.125572202	7.167844038	4.858288441	0.001471111	0.16150691
71790_Anxa9	1.129401611	6.052293115	5.17037031	0.001012914	0.142792162
13134_Dach1	1.150988908	7.79412843	5.51245684	0.000683366	0.125770959
73998_Herc3	1.162077111	6.377473816	4.769621209	0.00163981	0.168883473
16439_Itpr2	1.171066611	7.774379802	5.027515225	0.001199552	0.151869452
11443_Chrnb1	1.183881683	6.623127308	4.93542237	0.001339768	0.158346425
17532_Mras	1.184376049	6.84027655	5.406412453	0.000770728	0.12894106

235028_Zfp426	1.192423289	6.166320826	4.595630863	0.002035887	0.189099678
27278_Clnk	1.230109978	8.985103188	4.932780022	0.001344048	0.158346425
236604_Pisd-ps1	1.233111627	9.296441778	5.291334063	0.000879719	0.137686464
15040_H2-T23	1.242721342	9.244154802	6.334239291	0.000282449	0.084549029
57390_Psors1c2	1.24315167	8.307109848	5.078975733	0.001128284	0.149512701
18793_Plaur	1.265574264	7.164606933	7.098742209	0.00013327	0.070474852
18669_Abcb1b	1.268063476	7.354139775	5.234370483	0.000939871	0.13893162
19271_Ptprj	1.268430055	7.621480842	4.651109476	0.001899262	0.179769693
17988_Ndrg1	1.284222571	8.297514953	7.215312025	0.000119496	0.070474852
246728_Oas2	1.325364099	7.253168724	4.769629507	0.001639794	0.168883473
69632_Arhgef12	1.343196251	7.473429171	4.837197374	0.00150944	0.16150691
14281_Fos	1.345250888	9.421883804	5.263544422	0.000908517	0.138912267
18631_Pex11a	1.345458307	6.14854601	4.531399908	0.002207635	0.195027424
13982_Esr1	1.35078091	7.219050632	4.614328204	0.001988678	0.186457278
58203_Zbp1	1.355262697	6.833591724	6.780185585	0.000180846	0.073562543
22035_Tnfsf10	1.373581472	7.082309383	6.120039471	0.000352756	0.094753076
381232_5830416P10Rik	1.379743074	7.051248205	5.948854172	0.000423006	0.10466453
100217446_Snord47	1.385687091	9.107048521	5.587949301	0.000627846	0.121890502
12517_Cd72	1.392011851	7.417735068	5.532664579	0.000667991	0.124090286
545622_Ptpn3	1.424228149	6.466699121	7.920566349	6.35E-05	0.054889168
18027_Nfia	1.437404224	6.954335239	5.568742161	0.000641483	0.121890502
231507_Plac8	1.439430529	10.02174906	7.006964842	0.000145364	0.070474852
320560_Dennd5b	1.443281635	6.423998817	5.869172318	0.000460887	0.107472511
13518_Dst	1.444805627	7.456520145	5.339917359	0.00083176	0.13370568
637515_Nlrp1b	1.446423384	6.184770382	5.162870736	0.001021875	0.143040864
13417_Dnahc8	1.486888445	7.550004923	6.773549072	0.00018202	0.073562543
23795_Agr2	1.487236963	7.790348363	5.143614724	0.001045284	0.144524272
20750_Spp1	1.504119761	6.989799467	6.080037205	0.000367931	0.097351133
71720_Osbpl3	1.521193306	7.261267372	8.597166195	3.61E-05	0.042206957
17907_Mylpf	1.522989262	5.70647931	6.967922304	0.000150875	0.070474852
24000_Ptpn21	1.523724797	6.402094864	7.559728665	8.73E-05	0.06423295
19367_Rad9	1.531026601	6.649147535	4.441904244	0.002473872	0.19982632
15959_Ifit3	1.548213966	6.388031705	4.936093213	0.001338683	0.158346425
15064_Mr1	1.550694408	6.031645557	4.428685354	0.002516082	0.19982632
384009_Glipr2	1.556492071	7.059494327	7.134470947	0.000128869	0.070474852
16764_Aff3	1.558487774	7.55906324	5.556950195	0.000650017	0.121890502
108052_Slc14a1	1.562431711	8.140744635	5.714372934	0.000545697	0.114522451
110454_Ly6a	1.593130597	7.303880366	4.550378388	0.002155297	0.193288245
100302594_Snord14e	1.595332558	10.21596443	4.956740546	0.001305778	0.158346425
13482_Dpp4	1.599972562	8.017426159	5.216914379	0.000959201	0.13893162
14964_H2-D1	1.608182428	9.089861022	7.127137709	0.000129759	0.070474852
11668_Aldh1a1	1.628825594	8.189179323	8.841360014	2.97E-05	0.039079784
69069_1810011H11Rik	1.630685504	7.159953868	4.859140543	0.001469585	0.16150691

110557_H2-Q6	1.633369916	8.422684076	9.23953647	2.18E-05	0.039079784
11555_Adrb2	1.653209556	6.673142044	6.711583158	0.000193407	0.073929716
59010_Sqrdl	1.67217849	6.458062396	6.756679353	0.000185044	0.073562543
234311_Ddx60	1.693661189	7.420016796	6.579359254	0.000220451	0.077051311
50778_Rgs1	1.704210128	9.21181105	5.873431529	0.00045877	0.107472511
107607_Nod1	1.706817202	6.491295228	7.090791318	0.000134272	0.070474852
63953_Dusp10	1.707645779	5.722897163	4.83618407	0.001511309	0.16150691
387160_Mir142	1.720989781	6.018456015	7.003457821	0.00014585	0.070474852
668139_Gm8995	1.722917438	9.20762147	5.907230778	0.000442345	0.105933531
12580_Cdkn2c	1.744190708	6.656234904	8.074361509	5.57E-05	0.052692782
226101_Myof	1.757490963	7.763687717	4.579928629	0.002076482	0.191672221
14972_H2-K1	1.779713807	9.175335927	7.077295574	0.000135992	0.070474852
66569_Gdpd1	1.806859946	6.892284159	6.854343249	0.000168279	0.07271499
71653_4930506M07Rik	1.810784155	6.523945181	5.786300594	0.000504315	0.110517656
207839_Galnt6	1.824357142	6.417263541	8.872663437	2.90E-05	0.039079784
22359_Vldlr	1.824961189	7.692352744	8.121236545	5.35E-05	0.052692782
20684_Sp100	1.875601599	8.567234505	6.886550005	0.000163127	0.072055122
14282_Fosb	1.913507768	9.291425728	7.426401306	9.84E-05	0.069862826
74519_Cyp2j9	1.917229946	7.278095386	7.02849737	0.00014242	0.070474852
72685_Dnajc6	1.92528052	7.594993042	6.651776968	0.000205153	0.076077981
11910_Atf3	1.940742834	6.778648692	4.78381731	0.001611431	0.168883473
239853_Gpr128	1.990128392	8.042025522	5.09062294	0.001112808	0.149512701
100303751_Snora31	2.008787971	8.974826901	5.623875493	0.000603191	0.119896285
15039_H2-T22	2.027026277	7.880555653	6.043114611	0.000382582	0.097494554
234577_Cpne2	2.042683368	8.453633797	6.644273698	0.000206682	0.076077981
14961_H2-Ab1	2.05063121	7.489785763	7.98905066	5.99E-05	0.0540992
26367_Ceacam2	2.097245694	6.3450126	4.488121644	0.002332255	0.197103867
14998_H2-DMa	2.134648433	8.037772447	6.893044345	0.00016211	0.072055122
18667_Pgr	2.17414261	6.520298229	6.577970236	0.000220757	0.077051311
69895_Snhg8	2.176479358	6.852767547	6.487527485	0.000241705	0.080072945
12362_Casp1	2.2472904	7.501008652	4.850725591	0.001484731	0.16150691
240327_Gm4951	2.248997771	6.439258867	7.301618146	0.000110321	0.070474852
13040_Ctss	2.304593883	7.377532421	6.713635236	0.000193017	0.073929716
14913_Guca1a	2.321556395	6.249627985	4.507989202	0.002274118	0.196533248
56490_Zbtb20	2.353088046	8.088543341	4.921651717	0.00136224	0.158346425
11639_Ak4	2.393998409	5.864614412	10.13436764	1.14E-05	0.028223996
11658_Alcam	2.398754695	8.264635893	9.207213542	2.24E-05	0.039079784
99899_Ifi44	2.401882074	7.431529712	8.212496057	4.95E-05	0.051826772
436493_H2-Gs10	2.48533868	7.879804011	6.97405123	0.000149995	0.070474852
53603_Tslp	2.494968967	6.434181795	4.550986925	0.002153641	0.193288245
17063_Muc13	2.543126518	10.0039245	10.30797475	1.01E-05	0.028223996
93694_Clec2d	2.596829297	7.44643297	10.18145645	1.10E-05	0.028223996
16177_Il1r1	2.704227375	7.220499679	5.677066182	0.00056863	0.116522197

56744_Pf4	2.746300187	8.022438383	5.631312357	0.000598222	0.119896285
70086_Cysltr2	2.879409817	6.960670774	6.957001385	0.000152459	0.070474852
59310_Myl10	3.342445832	8.917121818	8.904505896	2.83E-05	0.039079784
21673_Dntt	4.52417173	7.514739086	17.68186767	1.97E-07	0.003913054

A.2 LDA data used for quantification of HSC numbers in 6 week post-transplant primary recipients of transduced-HSCs

	Control-transduced transplanted		Hmga2-transduced transplanted		Lin28-transduced transplanted	
Proportion of 1° BM transplanted (%)	Transplanted mice	Positive mice*	Transplanted mice	Positive mice*	Transplanted mice	Positive mice*
7.7	12	12	12	12	12	12
0.75	8	4	8	8	8	8
0.20	4	2	4	4	3	3
0.094	8	1	8	6	8	3
0.050	4	0	4	4	4	1
0.023	4	0	4	0	4	0
0.013	4	0	4	0	4	1

*A mouse was considered positive for a lentivirus-transduced HSC if 16 weeks post-transplant the peripheral blood contained >1% YFP^+ cells overall and >1% YFP^+ GM-lineage cells.

A.3 LDA data used for quantification of HSC numbers in 8-12 month post-transplant secondary recipient mice that received the highest dose of primary mouse BM

	Control-transduced transplanted			Hmga2-transduced transplanted			
Proportion of 2° BM transplanted (%)	Transplanted mice	Positive mice*	HSCs/mouse (95% C.I.)**	Transplanted mice	Positive mice*	HSCs/mouse (95% C.I.)**	P-value
0.33	4	4		4	4		
0.25	4	1		4	4		
0.056	4	0		4	4		
0.050	4	0	310 (140-680)	4	3	5700 (3000-11000)	$3.3x10^{-9}$
0.010	8	0		7	3		
0.0067	4	1		4	0		
0.0056	4	0		4	4		

*A mouse was considered positive for a lentivirus-transduced HSC if 16 weeks post-transplant the peripheral blood contained >1% YFP^+ cells overall and >1% YFP^+ GM-lineage cells.
**HSC number per mouse and P-value of comparison was determined by ELDA (http://bioinf.wehi.edu.au/software/elda/index.html).

A.4 LDA of adult BM from Hmga2 KO and WT mice to determine HSC frequency and absolute number

Genotype	Number of cells transplanted	Transplanted mice	Positive mice*	HSC frequency (1/) (95% C.I.)**	Cells per tissue per mouse***	HSCs per mouse (95% C.I.)
Hmga2$^{+/+}$	$1.0x10^5$	4	4	67000 (176451-25441)	$2.4x10^8$	3600 (1400-9400)
	$2.0x10^4$	5	0			
	$4.0x10^3$	4	0			
Hmga2$^{-/-}$	$1.0x10^5$	4	3	75883 (211196-27265)	$7.2x10^7$	950 (340-2600)
	$2.0x10^4$	4	1			
	$4.0x10^3$	4	0			

*A mouse was considered positive for an HSC if 16 weeks post-transplant the peripheral blood contained >1% donor-derived cells overall and >1% donor-derived GM-lineage cells.
**HSC number per mouse and P-value of comparison was determined by ELDA (http://bioinf.wehi.edu.au/software/elda/index.html).
***See Fig. 3b. Cell number per mouse was calculated by assuming 2 femora and 2 tibiae are equivalent to 25% of the total BM.

A.5 LDA of E14.5 FL from Hmga2 KO and WT littermates to determine HSC frequency and absolute number

Genotype	Number of cells transplanted	Transplanted mice	Positive mice*	HSC frequency (1/) (95% C.I.)**	Cells per liver per embryo***	HSCs per embryo (95% C.I.)
$Hmga2^{+/+}$	$1.7x10^5$	12	12	35853 (61333-20959)	$1.6x10^7$	450 (260-760)
	$8.5x10^4$	8	7			
	$3.5x10^4$	4	2			
	$1.7x10^4$	8	3			
	$6.8x10^3$	4	0			
	$3.4x10^3$	4	2			
$Hmga2^{-/-}$	$1.7x10^5$	13	11	46895 (78554-27996)	$1.9x10^7$	405 (240-680)
	$8.5x10^4$	8	7			
	$3.5x10^4$	4	1			
	$1.7x10^4$	6	5			
	$6.8x10^3$	4	0			
	$3.4x10^3$	4	4			

*A mouse was considered positive for an HSC if 16 weeks post-transplant the peripheral blood contained >1% donor-derived cells overall and >1% donor-derived GM-lineage cells.
**HSC frequencies were determined by ELDA (http://bioinf.wehi.edu.au/software/elda/index.html).
***See Fig. 3b.

A.6 LDA data used for quantification of HSC numbers in 6-week post-transplant primary recipients of Hmga2 KO or WT E14.5 FL cells

	Hmga2$^{+/+}$ transplanted		*Hmga2*$^{-/-}$ transplanted	
Proportion of 1° BM transplanted (%)	Transplanted mice	Positive mice*	Transplanted mice	Positive mice*
2.5	14	14	14	8
0.50	4	4	4	4
0.25	10	8	10	3
0.10	9	5	10	1
0.050	4	1	4	0
0.033	3	0	3	0
0.017	3	2	3	0

*A mouse was considered positive for an HSC if 16 weeks post-transplant the peripheral blood contained >1% donor-derived cells overall and >1% donor-derived GM-lineage cells.

A.7 Affymetrix transcript analysis of Hmga2 KO relative to WT fetal liver LSK cells using a cut-off FDR of <0.3

ID	Log fold-change	Expression	t	P value	FDR
15364_Hmga2	6.751	7.888	30.051	4.415E-08	0.001
319765_Igf2bp2	7.115	7.395	13.952	5.350E-06	0.053
215335_Slc36a1	-3.247	5.763	-11.864	1.447E-05	0.070
67466_Pdcl	2.580	7.267	11.551	1.703E-05	0.070
14339_Aktip	4.598	6.295	11.496	1.753E-05	0.070
503550_Klri1	3.196	5.505	10.907	2.413E-05	0.080
53970_Rfx5	2.484	5.705	10.467	3.097E-05	0.088
19274_Ptprm	-3.581	7.245	-9.381	5.975E-05	0.148
67596_5830405N20Rik	-2.559	7.316	-8.931	8.007E-05	0.161
625098_Slc38a6	2.946	6.812	8.915	8.093E-05	0.161
69926_Dnahc17	3.231	8.137	8.759	8.986E-05	0.162
13139_Dgka	-3.839	7.219	-8.368	1.177E-04	0.195
18634_Pex7	-2.179	8.219	-7.607	2.051E-04	0.292
269401_Znf512b	3.363	7.723	7.602	2.060E-04	0.292
215494_C85492	1.572	5.788	7.263	2.679E-04	0.299
14470_Rabac1	1.818	7.483	7.225	2.761E-04	0.299
98303_D630023F18Rik	-3.350	6.841	-7.172	2.881E-04	0.299
11480_Acvr2a	2.171	8.446	7.159	2.911E-04	0.299
66679_Rae1	2.577	9.456	6.977	3.372E-04	0.299
70454_Cenpl	3.246	5.736	6.929	3.508E-04	0.299
18751_Prkcb	-3.471	5.770	-6.895	3.607E-04	0.299
18007_Neo1	2.334	8.516	6.839	3.777E-04	0.299
232408_Klrb1f	2.797	5.360	6.819	3.841E-04	0.299
210172_Zfp526	4.868	5.600	6.787	3.945E-04	0.299
246707_Emilin2	-1.833	7.415	-6.760	4.034E-04	0.299
56388_Cyp3a25	2.673	4.426	6.719	4.174E-04	0.299
94346_Tmem40	1.627	7.898	6.708	4.214E-04	0.299
235339_Dlat	-2.981	7.594	-6.682	4.309E-04	0.299
217830_9030617O03Rik	2.503	6.017	6.663	4.377E-04	0.299

Appendix B Supplementary materials and methods

B.1 List of populations and phenotypes used for analysis and sorting

Population(s)	Designation	Phenotype
Hematopoietic stem cells	ESLAM	$EPCR^{+}CD45^{+}CD48^{-}CD150^{+}$
Hematopoietic stem and progenitors	LSK	$Lin^{-}Sca1^{+}c\text{-}Kit^{+}$
Common myeloid progenitors	CMP	$Lin^{-}Sca1^{-}c\text{-}Kit^{+}CD34^{+}CD16/32^{lo}$
Granulocyte/monocyte progenitors	GMP	$Lin^{-}Sca1^{-}c\text{-}Kit^{+}CD34^{+}CD16/32^{hi}$
Megakaryocyte/erythroid progenitors	MEP	$Lin^{-}Sca1^{-}c\text{-}Kit^{+}CD34^{-}CD16/32^{-}$
Common lymphoid progenitors	CLP	$Lin^{-}Sca1^{lo}\text{-}c\text{-}Ki^{t+}CD127^{+}$
Granulocytes/monocytes	GM	$Lyg6g^{+}Mac1^{+}$
B lymphocytes	B	$B220^{+}$ or $CD19^{+}$
T lymphocytes	T	$CD3\varepsilon^{+}$ or $CD5^{+}$
B-2 lymphocytes	B2	$CD19^{+}B220^{+}CD5^{-}$
B-1a lymphocytes	B1a	$CD19^{+}B220^{-}CD5^{+}$
B-1b lymphocytes	B1b	$CD19^{+}B220^{-}CD5^{-}$
Follicular zone B2 splenocytes	Fo B	$CD19^{+}B220^{+}CD23^{+}CD1d^{-}$
Marginal zone B2 splenocytes	MZ B	$CD19^{+}B220^{+}CD23^{-}CD1d^{+}$

B.2 List of antibodies used for FACS

Antigen	Clone	Fluorochrome(s)
CD45(LCA)	104	FITC/AF700
CD45.1	A20	FITC/PECy7/APC/AF700
CD45.2	104	FITC/APCCy7/AF700
CD201 (EPCR)	EPCR1560	PE
CD150	TC15-12F12.2	PECy7/biotin
CD48	HM48-1	APC
CD4	GK1.5	FITC/biotin
CD8α	53-6.7	FITC/biotin
Gr1	RB6-8C5	FITC/biotin/PE
CD19	eBio1D3	FITC/biotin/PE
B220	RA3/6B2	FITC/biotin/PE
CD5	53-7.3	53-7.3
Sca1	E13-161.7	E13-161.7
c-Kit	2B8	APC
CD11b (Mac1)	M1/70	FITC/biotin/PE
CD43	S7	FITC
CD41	FITC	MWReg30

B.3 List of primers used for qRT-PCR transcript measurements

Gene symbol	Sense (5' to 3')	Antisense (5' to 3')
Gapdh	AACTTTGGCATTGTGGAAGG	ATGCAGGGATGATGTTCTGG
Hmga2	GGTGCCACAGAAGCGAGGAC	GGGCTCACAGGTTGGCTCTT
Igf2bp1	GGCTCAGTACGGTACAGTGGA	ACCACAGCTGTCTCACTTTCAG
Igf2bp2	GGGAAAATCATGGAAGTTGACTA	CGGGATGTTCCGAATCTG
Igf2bp3	AAACAGCTTTCTCGCTTTGC	TCCGCACTTTAGCATCTGGT
Lin28b	GAGTCCAGGATGATTCCAAGA	TGCTCTGACAGTAATGGCACTT
Slc31a1	GGGATCCAGTTCTGAGAGGA	GAAAAAGATGAGATTCAGTGGAAAA
Slc36a1	GCGGACAACTTTAAGCAGGT	TTGTTGTTGCAGTTGGTGGT
Pdcl	TAGGCGAGCGTCCTTTGTT	ATCATCCAGGGTTGTCATGG
Rfx5	CTGAAGCGGTCCTTCAGTTC	GGGCTCTTTCATCCTCTTCAG
Aktip	TCCTGATGGCGACTGTCC	TATGGTTCCGCCTCCACTT
Klri1	ACACAAAAACCTGGGCAGAG	TGAAGAATCCACCCATCCAT
Ccnd1	CGCCCTCCGTATCTTACTTCA	TCGCACTTCTGCTCCTCACAG
Ccnd2	GGCCAAGATCACCCACACT	ATGCTGCTCTTGACGGAACT
Ccnd3	CGAAACCACGCCCCTGAC	GACCAGCACCTCCCACTCC
Cdkn2c	GAACTGCGCTGCAGGTTAT	TCAAATTGGGATTAGCACCTC
Cdkn1a	GTACTTCCTCTGCCCTGCTG	TCTGCGCTTGGAGTGATAGA
Cdkn1b	GGTTAGCGGAGCAGTGTCCA	GGCCCTTTTGTTTTGCGAAG
Jak2	TGGGAATGTGTGTGCTAAAAA	TTTGATGAAAGGTGGGTTCC
Stat3	GGCACCTTGGATTGAGAGTC	ACTCTTGCAGGAATCGGCTA
Stat5a	GTTCGCGAAGCCAACAAT	TTCTCCGTGTCCTGTGTGAT
Sh2b3	CAACACACACAAGGCTGTCA	CCTGTGCACAAGAACTACATCTG

Cdh2	GCGCCATCATCATCGCTATCCTT	GCCGTTTCATCCATACCACAAA
Inpp5d	TCCCACTAGTTGTTGAACTTTACCTT	GGCCTGGGGAGAGCTGTT
Lyl1	GACCCTTCAGCATCTTCCCTAACA	AGCCACCTTCTGGGGTTGGT
Hmga2	AGCCACCTTCTGGGGTTGGT	GGGCTCACAGGTTGGCTCTT
Psap	ACTGTGGGGCCGTGAAGC	GTCGCAAGGAAGGGATTTCG
Pld3	GCTGAGGAACCGGAAGCTGT	GGGAAAGGGGTGGTCCTGAG
Rhob	GGGGCACGCAGAGTGGTT	GCAACAGTAGTGGCTTGCTGGTT
Vwf	GGCGAGGATGGAGTTCGACA	TGACAGGGCTGATGGTCTGG
Chd4	GCTGCCAGAGATCCCAAACG	TTGCCCTTAAGAGCTGGACAA
Smarcc1	TGGGAGAGCCCGGACACG	TTGGTAGGAGCATCTGCATGAAC
Smarcc2	TCTTCAGCCGAAGCCTCCAC	CCCTTCTCAGGGAAGTTCAGCA
Tubb5	CAGCTGGACCGAATCTCTGTGT	GGACCTGAGCGAACGGAGTC
Eif1a	CCGCTGCGTTTTGGTCACTA	TCGGTTCTGGCCTGGTTCTC
Hdac3	TCAACGTGGGTGATGACTGC	GCAGAGATGCGCCTGTGTA
Trim27	GAAGAGACGGCGGGCACA	GCTGCTCAAACTCCCAGACAA
Prnp	TCCAATTTAGGAGAGCCAAGCA	GCCGACATCAGTCCACATAGTCA
Mlx	TGTGTCTTCAGCTGGATTGAGGA	GGACACCGATCACAATCTCTCG
Car3	TGGCTAAGGAGTGGGGCTAC	GTCCCCTTTGGCAATTGGAT
Cul4a	GGAGAACATTTGACAGCAATTCTACA	GTGAGGTCGGGCACCCTGT
Plp1	TCAGTCTATTGCCTTCCCTAGCAA	GCATTCCATGGGAGAACACCA